INVESTIGATION OF WELDABILITY
OF HOT-WORK TOOL STEELS

N. A. SINCLAIR
J. G. MACIORA
R. P. SOPHER

GENERAL DYNAMICS CORPORATION
ELECTRIC BOAT DIVISION

DECEMBER 1961

AERONAUTICAL SYSTEMS DIVISION

NOTICES

NOTICES

When Government drawings, specifications, or other data are used for any purpose other than in connection with a definitely related Government procurement operation, the United States Government thereby incurs no responsibility nor any obligation whatsoever; and the fact that the Government may have formulated, furnished, or in any way supplied the said drawings, specifications, or other data, is not to be regarded by implication or otherwise as in any manner licensing the holder or any other person or corporation, or conveying any rights or permission to manufacture, use, or sell any patented invention that may in any way be related thereto.

Qualified requesters may obtain copies of this report from the Armed Services Technical Information Agency, (ASTIA), Arlington Hall Station, Arlington 12, Virginia.

This report has been released to the Office of Technical Services, U. S. Department of Commerce, Washington 25, D. C., for sale to the general public.

Copies of ASD Technical Reports and Technical Notes should not be returned to the Aeronautical Systems Division unless return is required by security considerations, contractual obligations, or notice on a specific document.

INVESTIGATION OF WELDABILITY
OF HOT-WORK TOOL STEELS

N. A. SINCLAIR
J. G. MACIORA
R. P. SOPHER

GENERAL DYNAMICS CORPORATION
ELECTRIC BOAT DIVISION

DECEMBER 1961

FOREWORD

This report was prepared by the Research and Development
Department of Electric Boat Division of the General Dynamics
Corporation under USAF Contract No. AF 33(616)-6519. The contract
was initiated under Project No. 7381 "Materials Application",
Task No. 73810, "Exploratory Design and Prototype Development".
The work was administered under the direction of the Directorate
of Materials and Processes, Deputy for Aeronautical Systems Division,
with Lt. Colonel E. M. Kennedy and Mr. P. Hendricks acting as project
engineers.

This report covers work conducted from April 3, 1959 to
March 31, 1961.

ABSTRACT

The weldability of six hot-work tool steels was investigated to develop optimum welding procedures. Welds were made in sheet and plate with the inert-gas tungsten-arc and inert-gas consumable electrode processes under various welding conditions.

Variations in preheat, postheat, and energy input were found to have statistically significant, but practically unimportant, effects on mechanical properties after hardening and tempering.

Most mechanical-test failures were initiated in the welds whether or not defects were present. The weld metal retained its heterogeneous microstructure after hardening and tempering even when previously subject to annealing-type heat treatments.

Lehigh-restraint-test studies indicated that hot and cold cracking can occur. Low-temperature cracking can be prevented by increasing the preheat temperature.

Large-radius Charpy-impact specimens were found to be more satisfactory than the V-notched specimens for these steels.

The high-temperature weld tensile strength at $1000^\circ F$ was 190,000 psi for an H-11 steel; it was reduced to 156,000 after holding at $1000^\circ F$ for 24 hours.

Small-scale pressure vessels were tested both dynamically and statically. Sheet-bulge tests were tested dynamically. One out of four vessels, and three out of five bulge specimens failed at relatively high strengths.

PUBLICATION REVIEW

This report has been reviewed and is approved.

FOR THE COMMANDER:

I. PERLMUTTER
Chief, Physical Metallurgy Branch
Metals and Ceramics Laboratory
Directorate of Materials and Processes

TABLE OF CONTENTS

LIST OF FIGURES

LIST OF FIGURES

LIST OF TABLES

LIST OF TABLES
(Continued)

viii

INTRODUCTION

Hot-work tool steels are among the most promising materials for use in aircraft and missiles. High tensile strengths in the range of 250,000 to 300,000 psi give these materials a favorable strength-to-weight ratio. These steels also possess good high temperature properties when tempered in the range of 1000 F. Warpage is reduced since these steels are air hardening. In addition the material can be obtained readily in a wide variety of forms.

The hot-work tool steels are being considered for structural members where weight reduction and strength are both necessary, and for rocket-motor cases where strength at elevated temperatures may be required.

The tool steels have not been seriously considered for exterior skin of aircraft because they lack adequate corrosion resistance. The corrosion resistance problem is receiving attention, however, and for temperatures above 375 F an aluminized silicone enamel is employed. Special non-embrittling plating and vapor deposition methods are also employed.

Welded structural members must withstand rapidly applied loads at temperatures as low as -65 F, while rocket cases must withstand explosive loading (particularly when solid fuels are used) under biaxial loading conditions. The weld metal may contain defects which are the equivalent of a notch. These conditions are conducive to producing brittle fractures. One of the problems is to learn how to weld these materials and maintain strength, ductility, and resistance to brittle fracture of the welded assemblies.

The main objective of this program was to determine the effects of welding parameters of preheat, postheat, and energy input on the mechanical properties of sheet and plate weldments after hardening and tempering for six different hot-work tool steels. It was also necessary to develop procedures for welding these steels. Both inert-gas tungsten electrode (TIG) and inert-gas consumable electrode (MIG) welding processes were used in this investigation. These air-melted steels were welded in the annealed condition with filler wire from the same heat of steel. After welding they were hardened and tempered and evaluated by tensile, bend, and impact tests. Restraint tests, chemical analyses, and metallographic examinations were also performed on the weldments. The type of cracking and the effects of preheat on the restraint cracking behavior of the six steels were determined. High temperature properties of weldments were determined at 400, 600, and 1000 F. Micro-examination of weldment microstructures in the as-welded condition was conducted to determine the effects of welding conditions on microstructure before hardening and tempering.

The influence of welding parameters on mechanical properties of welded joints was studied in detail for an H-11 type steel. This information was then used to select the welding parameters for the other tool steels studied in the program.

LITERATURE SURVEY

General Status of the Field

The aircraft and missile industries are searching for materials which have good hot-strength and high strength-to-weight ratios. Aluminum has a good strength-to-weight ratio but lacks adequate high temperature properties. The low alloy steels, such as AISI 4340 and AISI 4130, have been used to a great extent. Increased strength of these steels is achieved by lowering the tempering temperature, thereby limiting their high temperature range. Titanium exhibits a superior strength-to-weight ratio but fabrication is still considered a problem. The high temperature limit of titanium alloys is below that of the hot-work tool steels. Other materials under consideration for aircraft and missile applications are the refractory metals, modified 12 percent chromium steels, and austenitic stainless steels.

Some of the most promising materials for current use in aircraft are the chromium-alloy hot-work-tool steels. A high strength-to-weight ratio is combined with good hot strength, ease of fabrication, and favorable cost and availability.

In an effort to reduce the weight of airborne structures, safety factors have been reduced to the order of 1.1[1]. Therefore, the mechanical properties of the weld metal, heat-affected zone, and base metal, must be as uniform as possible. It is not difficult to achieve strength in a weld equal to that of the base material, but it is difficult to obtain uniform ductility in a weldment even when a heat treatment follows the welding operation.

Welding

The weldability of hot-work tool steels is considered good if proper techniques are used. These steels are generally preheated, welded in the annealed condition, and stress-relieved (or postheated).

The inert-gas tungsten-arc welding process (TIG) is most often used for welding thin plate and sheet materials. The inert-gas consumable-electrode process (MIG) is used for welding thicker sections. The submerged-arc and metal-arc coated-electrode

---

[1] Reference 1

2

processes have been used also for welding thicker plates. In the submerged-arc process the flux contains some of the alloying elements, and it has been discovered that their effect is dependent upon the welding voltage. Several commercial coated electrodes have been used to weld some of the hot-work tool steels.[1]

It is generally recommended that the weld filler-wire be of the same composition as the base material in order to produce uniform mechanical properties. Good results have been reported, however, with wire containing slightly less carbon than the base material.[2]

Although it is believed that the hot-work tool steels are susceptible to hydrogen embrittlement, it is likely that the heat treatments following welding drive off all hydrogen in the material.

Many variables of the welding procedure directly influence the microstructure and properties of weldments that are not heat-treated after welding. Since weldments of hot-work tool steels are heat-treated, effects of weld variables may not be so pronounced. Nevertheless, the microstructure prior to heat-treatment may influence the final heat-treated microstructure and resultant mechanical properties.

Preheat

Rapid cooling during weld metal solidification raises the fracture-transition temperature of both the weld metal and base plate in the as-welded conditions[3]. Therefore, a preheat is beneficial because it reduces the cooling rate. Of course, preheat does not have the effect of reducing residual stresses as does postheating.

Postheat

For steels which are to be heat-treated after welding, a postheat (usually above 1000 F) serves as a stress relief operation to prevent fracturing from rough handling prior to heat-treating. The postheat temperature is important since it will affect the final heat-treat microstructure.

Energy Input

It has been reported that variations in voltage, amperage, and travel speed can be considered as one variable, the energy input. Higher energy input was reported to result in weaker but

---

1   Reference 2
2   Reference 3
3   Reference 4

3

more ductile welds in the as-welded condition[1]. Higher energy input also reduces the weld cooling rate somewhat.

Heat-Treatment

As the hot-work tool steels are austenitized at higher temperatures more carbides are dissolved in the austenite (which results in greater hardness); however, the grain size is increased and there is a tendency to retain more austenite upon quenching. It is apparent that there is an optimum austenitizing temperature which gives the required strength and hardness. These steels are hardened by air cooling or an oil quench; air cooling is preferred since it results in less distortion.

The hot-work tool steels are susceptible to decarburization; therefore, heating should be done in a slightly reducing atmosphere or a salt bath.

Tempering is done at temperatures around 1000 F where secondary hardening occurs. Two and sometimes three tempering cycles are employed to eliminate the embrittling effects of martensite transformed from retained austenite. These steels contain small amounts of retained austenite in the as-quenched condition, most of which are transformed to untempered martensite after the first tempering operation. These small amounts of untempered martensite are brittle and must be tempered by a second tempering operation. For steels in which the transformation is quite sluggish a third temper or a deep freeze operation may be advisable.

Evaluation Tests for Weldments

The chromium-alloy hot-work tool steels, as well as most crystalline materials, may fracture in either a ductile or a brittle manner. In evaluating the effects of welding procedure on mechanical properties, it is necessary to determine if the resistance to fracture of the weld region is equal to that of the base metal with respect to both ductile and brittle behavior. The extent to which the weld region and base metal can be compared depends upon the selection of the proper weldment evaluation tests.

Unnotched specimens are used to determine ultimate strength, yield strength, and ductility which predicts the resistance of metals to ductile fracture. The tendency of a metal to fracture in a brittle manner is determined by notched specimens.

Mechanical Properties

Published transverse and longitudinal tensile properties of H-11 steel sheet and plate were reviewed. The specimens were austenitized at 1850 F, air cooled, and double tempered at various

---

1 Reference 5

temperatures. As the tensile strength decreased, the ductility increased. A compromise between good strength and ductility was achieved at tempering temperatures of 1000 to 1050 F. The strength and ductility were lower for the sheet material. Ductility was greatly reduced when the material was tested transverse to the major rolling direction.

DESCRIPTION OF PROJECT

This section discusses the materials, equipment, and procedures used in this program for welding, heat treating, and testing.

Materials

Six different hot-work tool steels were investigated in this program; their compositions are given in Table 1. Most of the steels are of modified H-11, H-12, and H-13 compositions. All further reference in this report to a steel as a specific type (i.e., H-11, Type No. 3) should be understood to mean the modified composition given in Table 1. The weld filler wires were of the same composition and from the same heat as the corresponding base metals.

A maximum limit of 0.012 percent phosphorous and sulfur was requested to reduce the likelihood of weld cracking. Some of the steel producers could not meet this requirement in an air-melted steel, therefore the limints were increased to 0.015 percent. Composition limits specified upon purchase of the steel and actual compositions of weld wire and weld metal determined by spectrographic and analytical analyses are given in Table 1. It is evident that the limits for phosphorous and sulfur, as well as some other elements, were exceeded for some steels. Carbon content of the weld wires was generally within the specified limits, indicating that decarburization did not occur during drawing. The loss of carbon during the welding process was greater for plate welded by the MIG process than for sheet welded by the TIG process.

Base metal was ordered in 0.090 ± 0.009-inch thick sheet and 0.500 ± 0.040-inch thick plate in a hot-rolled, annealed and pickled condition. Decarburization limits for sheet were a hardness variation of two points Rockwell "c" or equivalent and a maximum decarburization depth of 0.003 inch. For plate, the decarburization limits were three points Rockwell "c" and 0.02-inch maximum depth.

TABLE 1. CHEMICAL COMPOSITION OF WELD WIRE AND WELD METAL FOR AIR-MELTED STEELS

Steel No., Symbol & Class	Composition	C	Mn	P	S	Si	Cr	Mo	V	Other
1 (P)	Specified[a]	0.37 to 0.43	0.45 to 0.65	0.015 max.	0.015 max.	0.90 to 1.10 (b)	3.00 to 3.50 (b)	2.30 to 2.70 (b)	0.23 to 0.43 (b)	---
	Actual[c]	0.35	0.43	0.016	0.008	---	---	---	---	---
	WM Plate [d]	0.31	0.54	0.012	0.009	---	---	---	---	---
	WM Sheet [e]	0.35	0.56	0.008	0.009	---	---	---	---	---
2 (A) H-11	Specified	0.37 to 0.43	0.20 to 0.50	0.015 max.	0.015 max.	0.80 to 1.10	4.75 to 5.50	1.30 to 1.50	0.35 to 0.55	---
	Actual	0.41	0.35	0.018	0.007	---	---	---	---	---
	WM Plate	0.36	0.39	0.009	0.006	---	---	---	---	---
	WM Sheet	0.38	0.36	0.011	0.004	---	---	---	---	---
3 (V) H-11	Specified	0.37 to 0.43	0.20 to 0.40	0.015 max.	0.015 max.	0.80 to 1.00	4.75 to 5.25	1.20 to 1.40	0.40 to 0.60	---
	Actual	0.39	0.35	0.10	0.006	0.89	4.79	1.36	0.32	---
	WM Plate	0.37	0.28	0.015	0.005	---	---	---	---	---
	WM Sheet	0.37	0.33	0.015	0.005	---	---	---	---	---
4 (C) H-12	Specified	0.37 to 0.43	0.22 to 0.43	0.015 max.	0.015 max.	0.83 to 1.23	4.73 to 5.25	1.25 to 1.45	0.15 to 0.33	1.0 to 1.75 (W)
	Actual	0.36	0.31	0.015	0.018	---	---	---	---	---
	WM Plate	0.32	0.36	0.009	0.020	---	---	---	---	---
	WM Sheet	0.32	0.36	0.012	0.023	---	---	---	---	---

TABLE 1. CHEMICAL COMPOSITION OF WELD WIRE AND WELD METAL FOR AIR-MELTED STEELS
(Continued)

Steel No. Symbol & Class	Composition	C	Mn	P	S	Si	Cr	Mo	V	Other
5(J) H-13	Specified	0.47 to 0.53	0.30 to 0.50	0.015 max.	0.015 max.	0.90 to 1.10	4.75 to 5.25	1.30 to 1.50	0.90 to 1.10	1.40 to 1.60 (Ni)
	Actual	0.49	0.27	0.020	0.005	----	----	----	----	----
	WM Plate	0.43	0.29	0.016	0.006	----	----	----	----	----
	WM Sheet	0.47	0.29	0.011	0.007	----	----	----	----	----
6(M) H-13	Specified	0.37 to 0.43	0.20 to 0.40	0.015 max.	0.015 max.	0.90 to 1.10	4.75 to 5.25	0.90 to 1.10	0.90 to 1.10	----
	Actual	0.45	0.20	0.024	0.005	----	----	----	----	----
	WM Plate	0.040	0.30	0.018	0.006	----	----	----	----	----
	WM Sheet	0.045	0.30	0.012	0.010	----	----	----	----	----

(a) Weld wire composition specified upon purchase.
(b) Composition was not measured for these elements.
(c) Actual measured weld-wire composition.
(d) Actual measured weld-metal composition in plate welded with the MIG process.
(e) Actual measured weld-metal composition in sheet welded with the TIG process.

7

Heat Treatment

All steels were hardened at an austenitizing temperature of 1850 ± 25 F, still-air cooled to room temperature, and double tempered at 1050 ± 10 F for two plus two hours. All post-weld heat treatments and hardening and tempering operations were conducted in an argon atmosphere, except for the pressure vessel specimens which were hardened and tempered in dissociated ammonia (in a larger furnace). Decarburization of the pressure vessels and bulge test specimens was not appreciable. The surfaces of the other test specimens were finish ground, thereby eliminating all traces of decarburization.

Welding

Welding Processes and Equipment

The automatic inert-gas-shielded, tungsten-arc welding process (TIG) was used to prepare the butt weldments for all the 0.090-inch sheet material. A 300-amp d-c (straight polarity) rectifier-type arc-welding machine with an open-circuit voltage of 80 volts was used. The arc was started on a starting tab by the retract method. A 3/32-inch diameter, two percent thoriated-tungsten electrode was used. The electrode was ground with a double taper to permit greater current density and minimize loss of tungsten into the weld deposit.

The automatic inert-gas-shielded consumable-electrode (MIG) welding process was used to prepare the 0.500-inch butt and Lehigh restraint plate weldments. A 750-amp constant-voltage-type welding machine with a maximum open-circuit voltage of 50 volts was used.

Joint Design

A single-bevel, 60-degree, included-angle, V-joint, 0.040-inch ± 0.010-inch land, and 0.060-inch root opening was used for the 0.090-inch sheet. Starting and run-off tabs were welded to both ends of the one-foot-long specimen prior to the welding operation. The 0.060-inch root opening was used to permit the use of a relatively low energy heat input, yet one that could be varied for parameter variation studies.

A double-bevel, 45-degree, included-angle, V-joint design was used for the 0.500-inch plate material. An 0.045-inch root opening and a 0.060-inch ± 0.010-inch land were used. Starting and run-off tabs were used for plate welds also.

All joints were machined parallel to the predominant rolling direction of the sheet and plate, the only exception being the pressure vessels, whose longitudinal weld was transverse to the rolling direction.

8

Welding Fixtures

Sheet Weldments - The sheet welding was accomplished on a flat-plate welding fixture. This fixture was then mounted on a variable speed, motor-driven carriage which traversed the specimen under the tungsten-arc torch. An automatic filler-wire feeder was used, as shown in Figure 1.

A copper back-up bar, with an 1/8-inch radius groove and 0.040-inch diameter holes spaced at one-inch intervals along the length, was used to direct the purging gas on the underside of the weld joint. This copper back-up bar was placed in a groove in the flat-plate fixture with the surface flush with the top of the fixture.

Electrical strip-heaters were used to maintain the desired preheat and interpass temperatures. The required temperature was maintained by a temperature-deviation on-off controller.

The sheet specimens were held in place by heavy-duty quick-acting clamps.

The welding of the longitudinal seam of a pressure vessel with the TIG equipment is shown in Figure 1.

Plate Weldments - The plate weldments were prepared on the welding fixture described above with the exception that the MIG welding head traveled on a side-beam carriage and the fixture remained stationary. A copper back-up bar was shaped to fit the underside groove of the weld joint and to eliminate copper pick-up in the weld metal. This back-up bar was also placed in the groove of the flat-plate fixture and was flush with the top of the fixture. Electrical strip-heaters and an on-off controller were used to maintain the desired preheat and interpass temperatures.

The Lehigh restraint tests were conducted in the same manner with the exception that no copper back-up bar was used. The MIG equipment is shown in Figure 2.

Cleaning Studies

Cleanliness is one of the most important factors in achieving a sound quality weldment. Items which contributed to the soundness of the weld deposit were the cleanliness of the weld filler wires, base metals, and shielding gases, as well as methods of cleaning between passes.

Filler Wire - The most successful method of obtaining quality-grade welding filler wire was to purchase level-wound spooled weld with a bright finish. The filler wire was packaged in a hermetically

9

FIGURE 1 WELDING LONGITUDINAL SEAM OF PRESSURE VESSEL WITH THE AUTOMATIC TIG WELDING PROCESS
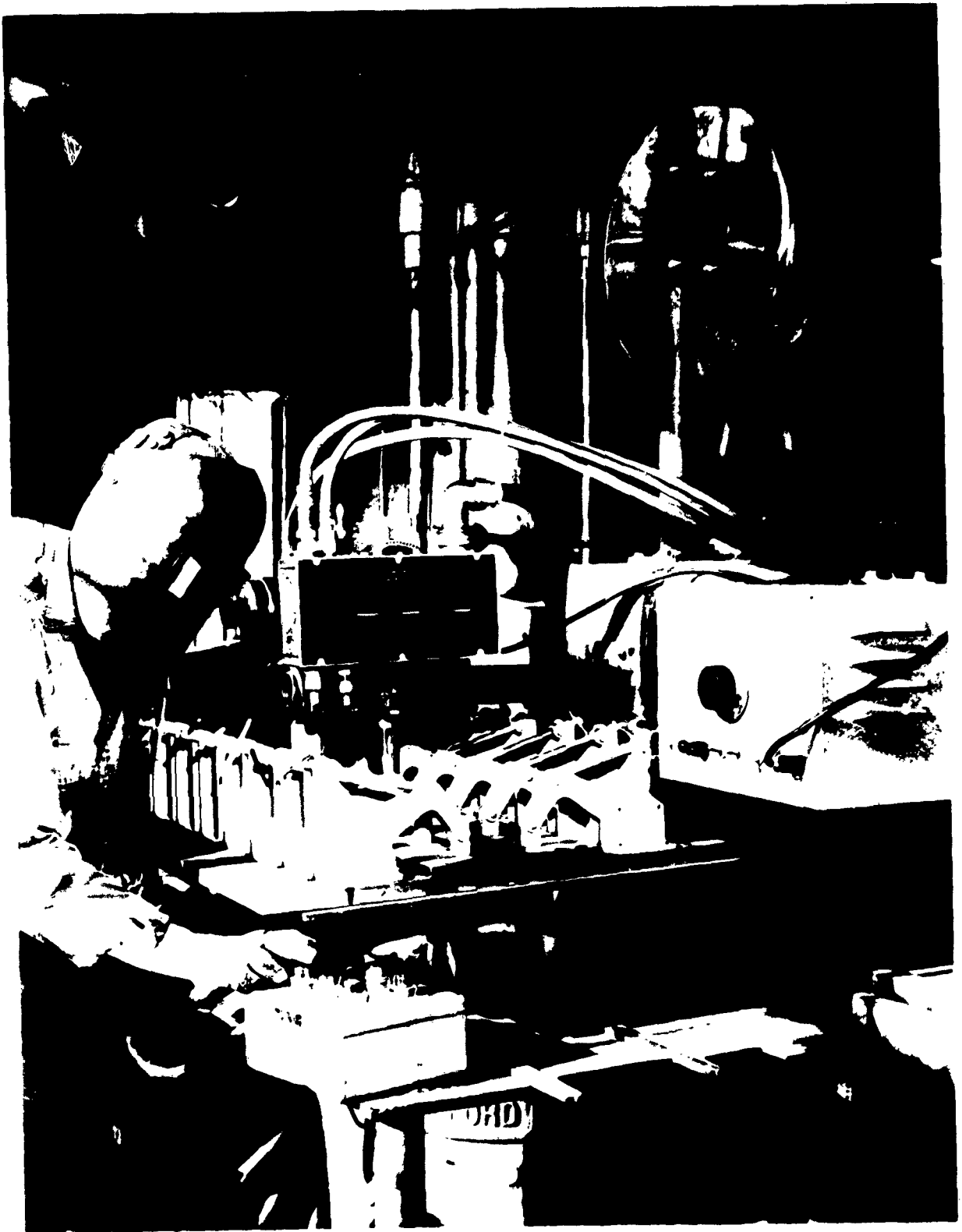
FIGURE 2 INERT-GAS CONSUMABLE-ELECTRODE WEI DING PROCESS

sealed container containing a desiccant. Copper flashing was not permitted because foreign material could be entrapped underneath the copper flash. Oxidation of the wire occurred in a few instances when the vendor neglected the desiccant and/or improperly sealed the packaging container. In these cases, the wire was recleaned in the laboratory prior to use.

Sheet and Plate Material - The as-received sheet and plate materials were machined to the required joint geometry. Prior to welding, the top and bottom surfaces of the specimens were hand-ground to remove any mill oxide for a minimum distance of one inch from the beveled joint, and washed with 1-1-1 trichloroethane solvent to remove any traces of oil or oxide prior to the welding operation.

The possibility of oxide formation during preheating above 550 F was reduced by allowing only a short time between setting up the sheet specimens and the actual welding operation. However, in the heav-er 0.500-inch thick specimens, the surface was protected by inert-gas during the preheat operation since a longer time was required to obtain temperatures above 550 F.

Multipass Welding - A cleaning operation was required between passes in multipass welding. Unless a trailing shield was used in addition to torch shielding, an oxide scale formed which was removed by a forceful hand or power brushing operation for the 0.090-inch sheet material. The oxide-scale on the 0.500-inch thick plate was completely removed by hand-grinding between passes.

Shielding and Purging Gases

Both argon and helium, and a combination of the two gases, were used in initial studies for shielding the arc during TIG welding of the sheet material. Consistent penetration and arc-stability were obtained with 100 percent argon gas in the previously described joint geometry. The purging gas was 100 percent argon.

Pure helium was used with the TIG automatic process for welding 0.500-inch plate. The helium gas did not produce any apparent porosity upon radiographic examination, using a two per-cent penetrameter sensitivity, and good arc stability was obtained. Special tests were conducted with the helium gas to insure that the gas was free of moisture. Helium was best suited for this applica-tion since maximum penetration was desired.

The shielding gases used with the MIG process on the 0.500-inch plate were: argon + 1% oxygen, 100% argon, and 100% helium. The best cleanliness, arc stability, and penetration resulted from the use of argon + 1% oxygen gas. Argon + 2% oxygen gas was not used because of the possible detrimental loss of alloying elements.

In all the welding processes used (manual TIG, automatic TIG, and the automatic MIG) the rate of flow of the shielding and purging gases had to be carefully controlled to minimize gas turbulence and possible aspiration of air into the arc-column.

Inspection Methods

Welds were closely inspected as the welding progressed. Visual inspection was used during the progress of welding. The weldments were partially ground to remove the weld-bead reinforcement before being radiographed. Radiographs of the 0.090-inch sheet weldments were satisfactory with a two-percent penetrameter sensitivity. However, the radiographs of the 0.500-inch weldments were not satisfactory at this sensitivity, since fine porosity, which was later found to reduce the mechanical properties (ductility) of the materials, was not detected. To increase the radiographic sensitivity the weld-bead reinforcement was removed from all sheet and plate weldments and the penetrameter sensitivity increased to one percent. Upon meeting the radiography requirements, the weldments were machined for the mechanical-properties tests.

Welding Procedures

Automatic-TIG Sheet Weldments - The initial procedures for sheet weldments were developed on H-11 steel No. 3. The arc voltage, welding current, wire-feed rate, and travel speed were varied to give three conditions of energy input. These welding procedures were used for the remaining five steels with slight modifications in welding current, filler-wire feed rate, and travel speed. Satisfactory weld-face build-up and penetration were obtained in all test plates. No transverse cracks were experienced using the copper back-up bar on the backside of the weld, since the penetration was controlled so that the weld metal did not touch the back-up bar. The welding conditions are given in Table 2.

TABLE 2. TYPICAL CONDITIONS FOR AUTOMATIC TIG
WELDING OF 0.090-INCH SHEET WELDMENTS

Condition	Low Energy Input, 6550 joules/in	Medium Energy Input, 7900 joules/in	High Energy Input, 10,100 joules/in
Preheat and Interpass Temp., $^{\circ}F$	400;600;800	400;600;800	400;600;800
Arc Voltage, V.	10.0	10.0	10.0
Arc Current, amp, DCSP	120	115	135
Filler-Wire Dia., in.	0.046	0.046	0.046
Wire Feed Rate, ipm	21	21	32

13

TABLE 2. TYPICAL CONDITIONS FOR AUTOMATIC TIG
WELDING OF 0.090-INCH SHEET WELDMENTS
(Cont'd.)

Condition	Low Energy Input, 6550 joules/in	Medium Energy Input, 7900 joules/in	High Energy Input, 10,100 joules/in
Work Travel Speed, ipm	11	8-3/4	8
Shielding Gas	Argon	Argon	Argon
Purging Gas	Argon	Argon	Argon
Torch Shield Gas Flow, cu ft/hr	10	10	10
Purging Gas Flow, cu ft/hr	10	10	10
Tungsten Electrode, Dia., in.	3/32	3/32	3/32
Number of Passes	2	2	1

Single- and double-pass sequences were used in developing the
welding procedures initially with H-11 steel No. 3. All the
weldments in the other five steels were prepared with the double-
pass sequence. Full penetration and satisfactory underbead contour
with a minimum energy input was obtained in the first pass.
Filler wire was used in both passes. For the second pass, suffi-
cient filler-metal was provided to obtain the desired weld-face
bead contour.

Manual-TIG Sheet Weldments - Steel No. 2 was developed for only
the manual TIG welding procedure. The procedure consisted of two
passes on one side. The welding conditions are given in Table 3.
The lower energy input was used on the first pass to control the
amount of weld penetration. The higher energy input was used in
the second pass to provide sufficient heat to melt the filler wire
and obtain the weld-face contour.

TABLE 3. WELDING CONDITIONS FOR MANUAL TIG
WELDING OF SHEET (0.090-in.) WELDMENTS

Condition	Pass No. 1	Pass No. 2
Preheat and Interpass Temp., °F	400	400
Arc Voltage, V.	10.0	12.0
Arc Current, amp, DCSP	103	115
Filler Wire Dia., in.	0.062	0.062
Travel Speed, ipm (approximate)	8	7-1/2
Shielding Gas	Argon	Argon
Purging Gas	Argon	Argon
Torch Shield Gas Flow, cu ft/hr	10	10
Purging Gas Flow, cu ft/hr	10	10
Tungsten Electrode Dia., in.	3/32	3/32
Cup Size	No. 6	No. 6
Energy Input, joules/in.	7,700	11,000

14

Automatic-MIG Plate Weldments - The initial procedures for plate weldments were developed also on steel No. 3. The procedures were developed using single and double-passes per side with appropriate energy inputs. These welding procedures had to be modified for each steel to obtain the best arc stability. After a high incidence of porosity was found in welded plate of steel No. 3, a trailing shield was used for the other steels to help reduce heavy oxidization of each weld pass. The welding conditions are given in Table 4.

TABLE 4.   TYPICAL WELDING CONDITIONS FOR AUTOMATIC
MIG 0.500-INCH PLATE WELDMENTS

Condition	40,600 joules/in	50,000 joules/in
Preheat and Interpass Temp., °F	400;800	400;800
Arc Voltage, V.	29.0	29.0
Arc Current, amp, DCRP	350	330
Filler Wire Dia., in.	0.062	0.062
Wire Feed Rate, ft pm	17-1/2	15
Travel Speed, ipm	15	11.5
Shielding Gas	Argon + 1% O_2	Argon + 1% O_2
Trailing Gas	Argon	Argon
Torch Shield Gas Flow, cu ft/hr	50	50
Trailing Shield Gas Flow, cu ft/hr	50	50
Number of Passes, per side	2	1

Single- and double-pass per side weldments were made initially in plate of steel No. 3. The remaining five steel plate weldments were made with a double-pass per side.

Automatic-TIG Plate Weldments - Steel No. 2 was the only steel for which the plate was welded with the automatic TIG process. The two-pass per side procedure was used. The welding conditions are given in Table 5.

TABLE 5.   WELDING CONDITIONS FOR AUTOMATIC
TIG 0.500-INCH PLATE WELDMENTS

Conditions	Energy Input, 51,000 joules/in
Preheat and Interpass Temp., °F	400;800
Arc Voltage, V.	14.0
Arc Current, amp, DCSP	304
Filler Wire Dia., in.	0.062
Wire Feed Rate, ipm	20-30
Travel Speed, ipm	5

TABLE 5. WELDING CONDITIONS FOR AUTOMATIC
TIG 0.500-INCH PLATE WELDMENTS

(cont'd.)

	Energy Input, 51,000 joules/in
Shielding Gas	Helium
Purging Gas	Argon
Torch Shield Gas Flow, cu ft/hr	20
Purging Gas Flow, cu ft/hr	10
Tungsten Electrode Dia., in.	1/8

Bulge Specimens and Pressure Vessels - The bulge specimens were welded with the double-pass sequence. The first pass was manually TIG welded and the second pass was welded by the automatic TIG process. An energy input of approximately 7900 joules per inch was used for both passes. It was necessary to use manual TIG welding for the first pass because the root-opening was machined wider than required, and the automatic welding process would not permit bridging the gap as easily as the manual TIG welding process. The preheat temperature used was 400 F. The other conditions are given in Table 2.

The girth and boss welds of the pressure vessel were tacked every 90 degrees by the manual TIG process and filler wire, as described under tack welding. The manual TIG process was used for these girth and boss joints with an energy input of 7700 joules per inch which is slightly below the medium energy level of 7900 joules per inch given in Table 2. Other conditions are listed in Table 2. For the girth welds, a three-pass sequence, quartering every 180 degrees, was used. The boss welds were made using a two-pass sequence, quartering every 180 degrees. The manual TIG process and the quartering 180-degree sequence were used to minimize any possible distortion during welding since elaborate fixturing was not used during the welding operation.

Lehigh Restraint Tests - The modified Lehigh restraint tests were welded with the MIG process. Only one pass at any energy input of 40,600 joules/inch was made in each test specimen. The other welding conditions are given in Table 4, automatic MIG 0.50-inch welding conditions.

Tack Welding - No tack-welding was permitted in the flat-sheet or plate weldments. Previous experience with other low-alloy steels has shown that tack welds may be a source of porosity and cracks. Since tack welds are usually made with a lower preheat, rapid cooling of the weld area and the high shrinkage stresses induce cracks and porosity. In the small-diameter pressure vessels, tacking was used only in the circumferential and boss welds. This tacking operation consisted of using a preheat of 500 F, producing large

16

and frequent tacks with the addition of filler metal to overcome the high shrinkage-stresses, and minimizing the possibility of cracks by a slower cooling rate.

Weld Repair - Weld repairs were made on some of the bulge specimens and pressure-vessel weldments of steel No. 2. These weldments were previously postheat-treated at 1350 F for two hours or at 1700 F for 1/2 hour, then air cooled and tempered at 1350 F for two hours after the initial welding operation. In order to eliminate micro-cracks in the repair welds, a preheat of 450-550 F was used. Immediately upon the completion of the repair weld, the preheated bulge plate or pressure vessel was placed in the argon-atmosphere furnace at 1350 F for two hours and air cooled. The weld repair was then radiographed and examined. If the radiographs were satisfactory, the test weldments were postheated at 1700 F, air cooled, then heated at 1350 F for two hours and air cooled (postheat condition No. 2). The weldments were then hardened and double-tempered.

Welding Characteristics

Automatic-TIG Sheet Weldments - Table 6 presents an evaluation of the welding characteristics of sheet weldments welded by the TIG-automatic process.

TABLE 6. WELDABILITY CHARACTERISTICS OF HOT-WORK TOOL STEEL SHEET MATERIAL (Automatic TIG Process-Argon Shielding Gas)

Steel	Class of Steel	Arc Stability	Weld Metal Fluidity	Sensitivity to Machine Settings	Bead Contour
1	----	Very Good	Very Good	Small	Small Crown
2	H-11 Mod.	Good	Good	Small	Small Crown
3	H-11 Mod.	Very Good	Very Good	Small	Small Crown
4	H-12 Mod.	Fair	Fair	Small	Small Crown
5	H-13 Mod.	Fair	Fair	Small	Small Crown
6	H-13 Mod.	Fair	Fair	Large	Flat

Steel No. 6 required the largest energy-input (increase of 10%) to maintain a stable arc.

The arc length was approximately 1/8 inch; spatter was no problem. The sensitivity (voltage, amperage, and arc gap) to machine-settings for steels No. 1 through 5 was small; steel No. 6, however, was quite sensitive. The largest energy input (increase of 10%) was required for steel No. 6. The bead contour for steels No. 1 through 5 was a small crown; steel No. 6 had a flat crown. The use of the trailing shield minimized the formation of oxide scale.

17

<u>Automatic-MIG Plate Weldments</u> - The mechanical-property tests of steel No. 3 revealed fine porosity in the weld deposit that was not detected by radiography using a two-percent penetrameter sensitivity. To improve detection of this porosity, the sensitivity was increased to one percent.

During the plate-welding of the other five steels, scattered moderate porosity (1/8" dia.) was experienced. To overcome this porosity, test weldments were made in which the arc-voltage was varied at one-volt intervals. Radiography and macro-sectioning of the test plates showed that porosity increased if the arc-voltage deviation varied more than ± 1/2 volt. This was the maximum variation that could be tolerated for best arc characteristics and minimum porosity without the aspiration of air into the arc column. Weldments of steel No. 1 could not be prepared with an absence of porosity. The porosity in this steel was reduced from gross to scattered quantities.

The welding characteristics of the various filler wires were observed during MIG welding of 0.500-inch plate and the results are listed in Table 7.

TABLE 7. WELDABILITY CHARACTERISTICS OF HOT-WORK TOOL STEEL PLATE MATERIAL (Automatic MIG Process - Argon and 1% Oxygen Shielding Gas)

Steel	Class of Steel	Arc Stability	Weld Metal Fluidity	Spatter	Optimum Voltage Setting*
1	----	Very Good	Good	Very Good	30**
2	H-11 Mod.	Good	Very Good	Good	32
3	H-11 Mod.	Good	Very Good	Good	30
4	H-12 Mod.	Good	Fair	Good	33
5	H-13 Mod.	Good	Fair	Good	32
6	H-13 Mod.	Good	Fair	Good	31

* Most suitable voltage with amperage adjusted to give best arc stability.
** Additional experiments required.

The arc stability was good for all the steels but did not reach the excellent rating of some of the alloy-steel filler-wires used on other projects in the laboratory. The arc-length used for all the steels was 3/8 inch. The sensitivity to machine settings for all steels was especially great with respect to the voltage. The amperage settings could be varied ± 10 amps without any appreciable effect. The bead contour of the MIG weld deposits for all the steels had a slight crown. The cup height, bottom of cup to the bottom of the groove, for the first pass was 7/8 inch. The distance from the contact tube to the bottom of the groove was

18

1-1/8 inches for the first pass. The cup height for the second pass was 5/8 inch with a contact tube-to-work distance of 7/8 inch.

Mechanical Testing

The mechanical test specimens were taken from plate and sheet weldments one-foot long by eight-inches wide. Two weldments were required to evaluate each welding condition under investigation. Two longitudinal-weld bend test specimens were taken from one sheet weldment while two transverse-weld tensile specimens and one transverse-notch longitudinal-weld tensile specimen were taken from the other sheet weldment. Two transverse-weld tensile specimens and two transverse-weld bend specimens were taken from one plate weldment while Charpy impact specimens were taken from the other.

Tensile

Transverse-weld tensile tests whose dimensions are given in Table 8 were used to evaluate both sheet and plate weldments.

TABLE 8. DIMENSIONS OF TEST SPECIMENS

Type of Test	Thickness, in.	Length, in.	Width of Test Section, in.	Width of Grip, in.
Tensile				
Plate	.375 ± .010	6-3/4	.500 ± .010[a]	1.25
Sheet	.070 ± .010	7-3/4	.500 ± .010	0.750
Bend				
Plate	.470 ± .010	6-3/4	2 ± .015	-----
Sheet	.070 ± .010	6	2 ± .015	-----

(a) Some specimens were reduced from .5 to .25 inch width because of gripping difficulties.

The sheet tensile specimens were held in self-aligning K-grips, while the plate specimens were held in heavy-duty jaws. The extensometer was removed soon after the 0.2 percent strain-offset proportional limit (or yield strength) was achieved. Total elongation of the weld and adjacent base metal was measured over 1/2-, 1-, and 2-inch gage lengths. The gage lengths were placed symmetrical to the weld center line.

A special pin-loaded longitudinal-weld tensile specimen containing a single transverse-notch across the weld, heat-affected zone, and base metal was used also to evaluate the sheet weldments. The notch-fracture strength was obtained and the source of fracture initiation (whether the weld metal, heat-affected zone, or base

19

metal) was determined by observation of the fracture face. A drawing of the specimen is given in Figure 3.

High-temperature tensile tests were performed on welded sheet specimens of H-11 steel No. 2 at 400, 800, and 1000 F. Some of the specimens were held at the test temperature, under no load, for a period of 24 hours prior to testing to determine whether detrimental structural changes would occur. The load was applied through self-aligning K-grips. Deflection was measured by means of a deflectometer which recorded the cross-head travel to provide a load-deflection curve. Since cross-head deflection was measured, the active gage length was the distance between the grips modified to an equivalent length to take into account the lesser amount of strain occurring in the wider sections of the specimen. An equivalent gage length of 4.5 inches was used in determining the yield strength; the procedure for determining the equivalent gage length is given in the Appendix.

Two thermocouple wires were attached to each high-temperature test specimen, one inch above and one inch below the mid-point of the specimen length, to record the temperatures. Maximum temperature variation along the specimen was ± 20 F at 400 F and ± 10 F at 800 and 1000 F.

Bend

The longitudinal-weld bend tests were performed on sheet specimens, whose dimensions are given in Table 8. The weld was parallel to the direction of the bending stresses. The load from a hydraulic jack was applied by a three-point loading die. The bottom half of the die contained two supports located 2-1/4 inches apart, each support having a fixed radius of 1/2 inch. The top-half loading dies were of progressively smaller radii (in 1/16-inch increments) thus increasing the bend angle until fracture occurred. The radius of the die at which fracture occurred was noted. From the fracture radius and the specimen thickness, a nominal percent elongation of the outer fiber of the bend specimen was determined.

Transverse-weld plate-bend tests were performed with the weld perpendicular to the direction of the bending stresses. Four-point loading was employed to insure a constant bending moment across the weld metal, HAZ, and base metal between the inside rolls spaced two inches apart. The minimum bending radius was measured after fracture by matching the fracture faces as closely as possible.

Charpy Impact

V-notch Charpy impact specimens were used initially for H-11 steel No. 3. A modified Charpy specimen having a 1/2-inch radius

20
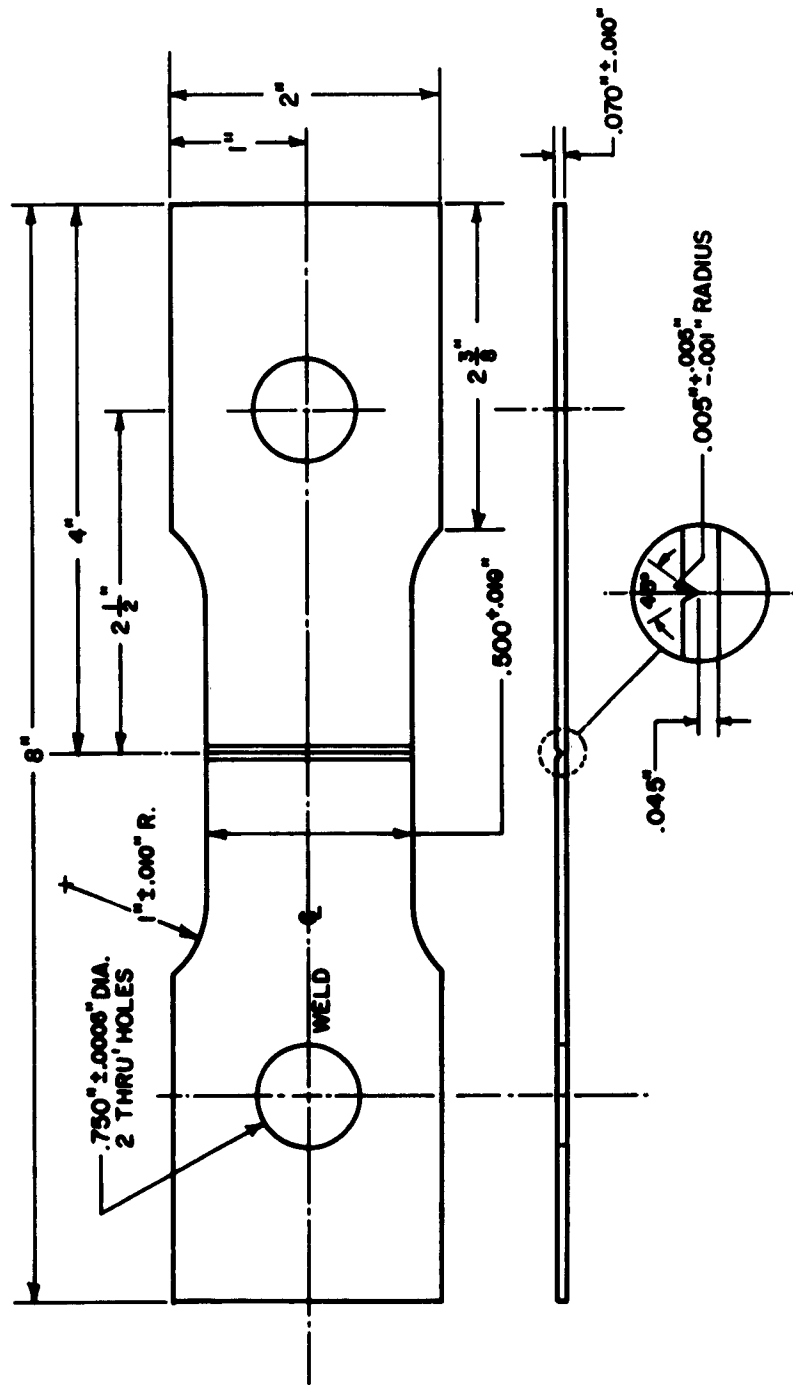
FIGURE 3 LONGITUDINAL WELD, TRANSVERSE NOTCH, TENSILE SPECIMEN

notch was used subsequently for H-11 steel No. 2 to provide more discrimination in the results. The other dimensions of the large-radius Charpy specimens were the same as the standard Charpy specimens.

Bulge Tests

Special impulse-bulge tests were performed to evaluate the resistance of welded sheets to rapidly applied biaxial stresses.

In this test, a 430-pound weight was dropped 23 feet onto a piston to load hydraulically an eight-inch diameter surface of a welded-sheet disc. A photograph and a drawing of the machine are shown in Figures 4 and 5, respectively. The hydraulic fluid was glycerin. The specimen received an initial preload of about 2000 psi before the weight was dropped in order to increase the loading capacity of the machine.

The specimen was about one foot in outside diameter with a ten-inch diameter bolt-hole pitch-circle. The four-inch long weld in the center of the specimen was ground and polished flush with the unground surfaces of the sheet.

A Baldwin SR-4 rosette strain gage, type AR7-2, of a 1/4-inch gage length was mounted in the center of the specimen (with respect to the bolt hole circle), and static and dynamic strains were recorded on a Consolidated Electrodynamics Model 5-119 recorder having a frequency response of 5000 cps. Paper speed was 160 ips, cylinder-pressure variation with time was photographed from an oscilloscope screen.

Pressure Vessels

Small welded pressure vessels were tested under static and dynamic conditions as a final evaluation of the welding procedures and parameters developed earlier in the program.

Four vessels were made of 0.090-inch thick sheet of H-11 steel No. 2. The cylinders were 11-1/2 inches long by 6-1/8 inch inside diameter and were fabricated with a longitudinal weld perpendicular to the rolling direction. They were capped with deep-drawn hemispherical heads (having a cylindrical section of one-inch length at the ends) welded circumferentially to the cylinder. The two dynamically tested vessels were capped only at one end. The other end was left open, fitted into the cylinder of the drop-weight test machine and sealed by an "O" ring. Hydraulic jacks held the vessels in place. The two statically-tested vessels were capped at both ends, one head containing a welded boss shaped to prevent an abrupt change in the thickness of the vessel.

Each vessel was stress relieved at 1350 F for two hours and

A. Weight

B. Piston Rod

. Specimen Location
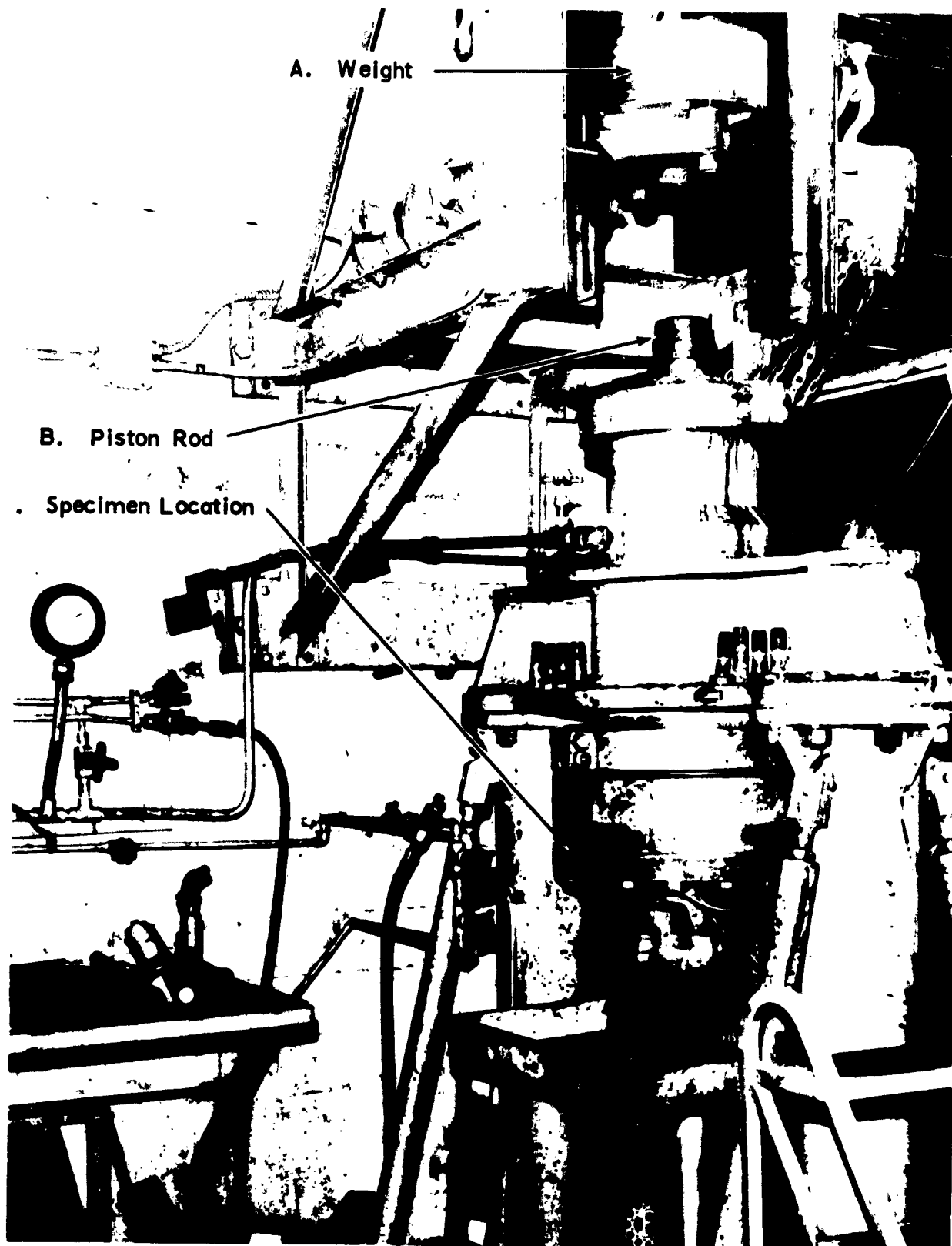
Figure 4 Bulge Test Machine
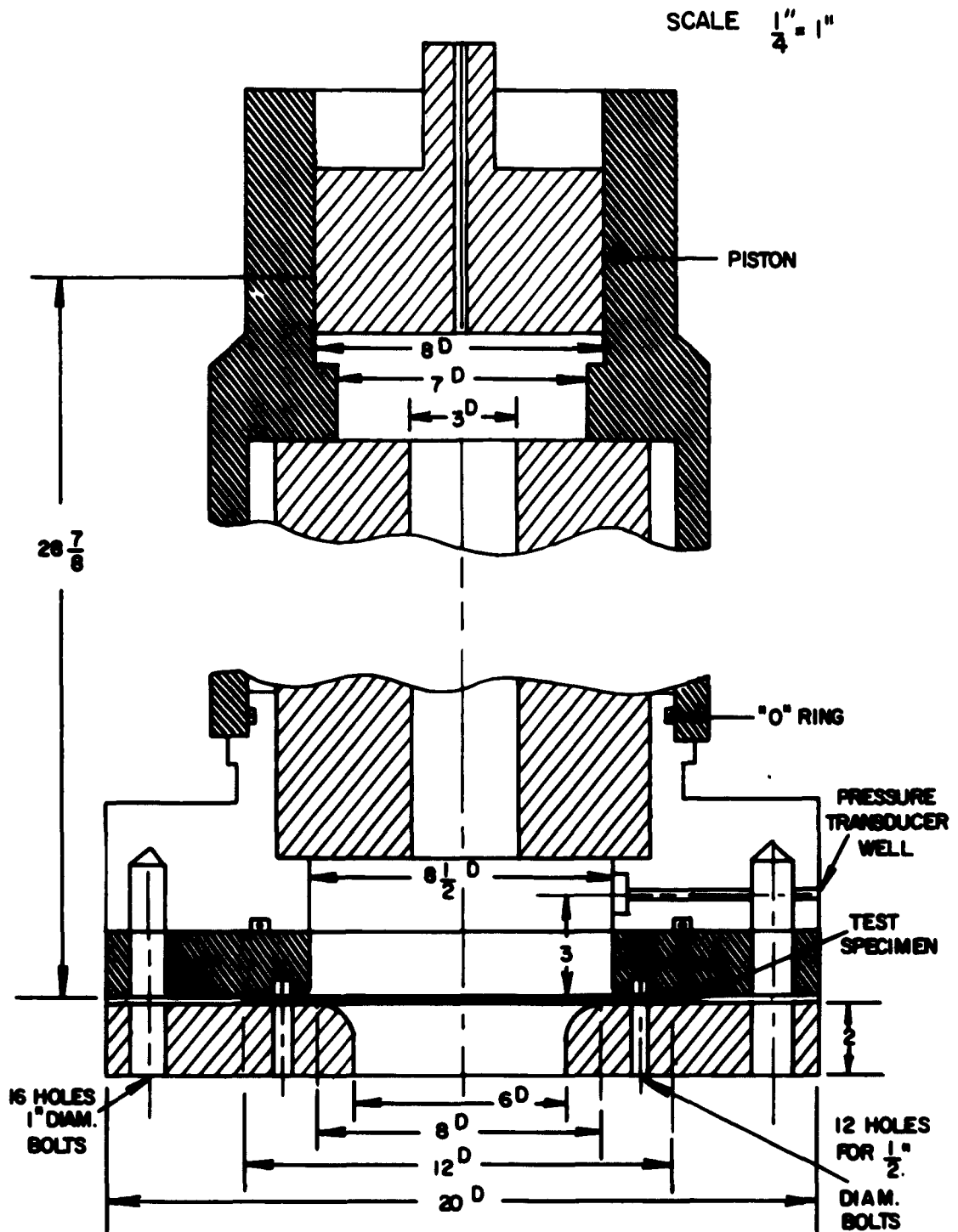
FIGURE 5.   BULGE TEST   MACHINE   SECTIONAL   VIEW

24

radiographed upon completion of each weld. The dynamically tested
vessels containing one circumferential and one longitudinal weld
were stress relieved twice, while the static vessels were stress
relieved four times except where repair welds were required. In
those cases, each repair weld was stress relieved immediately
following welding as discussed previously. Each weld was ground
inside and outside so that the reinforcement blended smoothly with
the rest of the vessel. Only the circumferential boss-weld was
not ground inside, as it was the final closure-weld.

Circumferential strains were measured at the mid-length loca-
tion of the cylinder at the longitudinal weld and at the base-metal
90 degrees away from the weld. Baldwin SR4 (No. N FAB-50-12) strain
gages of 1/2-inch gage length were used. Data were recorded with
the same equipment used for the bulge tests.

Restraint Tests

Lehigh restraint test specimens were made, as shown in
Figure 6, in 1/2-inch plate to determine the cracking susceptibility
of the filler metals. The standard Lehigh-specimen weld-joint
geometry was modified to approximate more closely the geometry of
the actual test weldments used in this program. The amount of
restraint was decreased by increasing the length of the saw cuts
along the sides of the specimen. Cracking was determined by
radiographic inspection and, when necessary, by macroscopic
examination.

In those cases where cracking occurred, the welding procedures
were adjusted in an attempt to eliminate cracking.

Single-pass welds were made in the 0.5-inch plate specimens
by the MIG process with a shielding gas of argon plus one percent
oxygen. The plates were cleaned with a power-wire brush and 1-1-1
trichloroethane solvent. The welds were allowed to cool to room
temperature immediately after welding and were then stress relieved
at 1350 F for two hours. The stress-relief treatment was used to
reduce the possibility of the cracks extending during aging at
room temperature before they could be inspected.

RESULTS AND DISCUSSION

Restraint Tests

The results of the restraint tests are given in Table 9.
Increasing the preheat temperature reduces the cracking-
susceptibility of welds deposited in these steels under restraint.
The H-12 steel No. 4 filler wire was the most crack sensitive
while the other steel filler wires had about the same crack
susceptibility under restraint. A welding wire of slightly lower
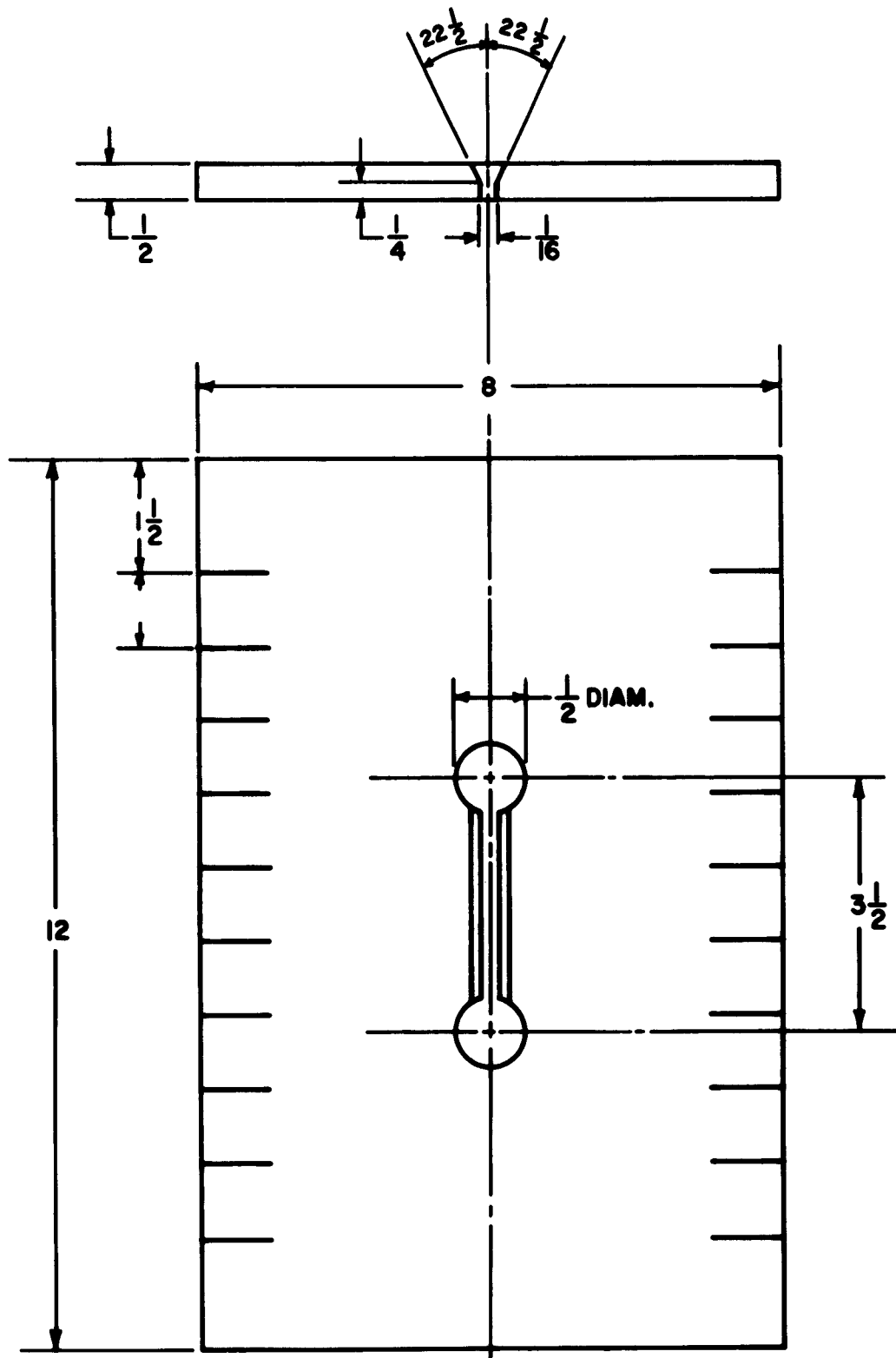
FIGURE 5; RESTRAINT TEST DESIGN

TABLE 9. LEHIGH RESTRAINT TEST RESULTS

Steel No. and Type (modified)	Specimen No.	Saw Cuts	Preheat, °F	Cracks	Detected by
1, no specific type	1	None	600	Yes	Radiography
	2	None	800	No	(a)
	3(b)	None	800	Yes	Micro-examination
2, H-11	1	None	600	Yes	Radiography
	2	None	700	Yes	Radiography
	3	None	700	No	-----
	4	None	800	No	-----
3, H-11	1	None	400	Yes	Radiography
	2	None	500	Yes	Radiography
	3	None	600	Yes	Macro-examination
	4(c)	None	600	Yes	Macro-examination
	5	None	700	No	--------
	6	None	800	No	--------
4, H-12	1	None	700	Yes	Macro-examination
	2	None	800	Yes	Macro-examination
	3	1-inch	800	No	-----
5, H-13	1	None	600	Yes	Radiography
	2	None	800	No	-----
6, H-13	1	None	600	Yes	Radiography
	2	None	800	No	-----

(a) Specimens in which no cracks were found were inspected by both radiography and macro-examination. All specimens were radiographed.

(b) This specimen received a special isothermal postheat at 1350 for ten hours to determine the nature of cracking.

(c) A special weld wire of 0.35 percent carbon was used.

carbon content (0.35 percent) did not affect the results of specimen No. 4 of H-11 steel No. 3 at a 600 F preheat.

Specimen No. 3 of steel No. 1 was not cooled from the 800 F preheat temperature but was postheated immediately to 1350 F and held for ten hours to provide isothermal transformation of the austenite. A crack occurred in the center of the weld cross-section as shown in Figure 7a. Since the center of the weld was the last to solidify and since suddenly applied quenching stresses were absent, it was reasoned that high-temperature shrinkage-cracking had occurred.

Since cracking could be eliminated by increasing the preheat, it was evident that shrinkage stresses from solidification were not responsible alone for the cracking, but that the cracking also occurred at lower temperatures. With lower preheats, less ductile weld microstructures were produced as a result of the more rapid cooling rate. Metallographic observation of the weld-metal microstructures revealed that the preheat of 400 F resulted in a much lighter dendritic pattern and a more acicular structure than the 800 F preheat.

The effect of reducing the preheat temperature from 800 F to 400 F in these restraint tests was to increase the theoretical cooling rate more than 15 times at the center line of the weld metal at 1000 F. Theoretical cooling rates for these restraint tests as a function of preheat temperature and plate thickness are given in Table 10.

TABLE 10. THEORETICAL COOLING RATES AT 1000 F AT CENTER OF A WELD IN THE LEHIGH RESTRAINT TESTS

Preheat Temperature, F	Energy Input, BTU/in.	Cooling Rate, F/sec. Plate Thickness,	
		0.50 in.	0.090 in.
400	41.8	3.43	.112
500	41.8	1.98	.064
600	41.8	1.02	.033
700	41.9	.426	.013
800	43.5	.222	.006

In general, it was found that most of the cracks initiated at the root where penetration was incomplete (purposely, to cause a high stress concentration notch), and that the cracks propagated upward through the center of the weld along the center line of the symmetrical weld structure pattern. The crack pattern of Figure 7b, however, indicates that cracking may have initiated in the center of the weld as well as at the root, and that the crack which was initiated at the center intersected the one from the root.
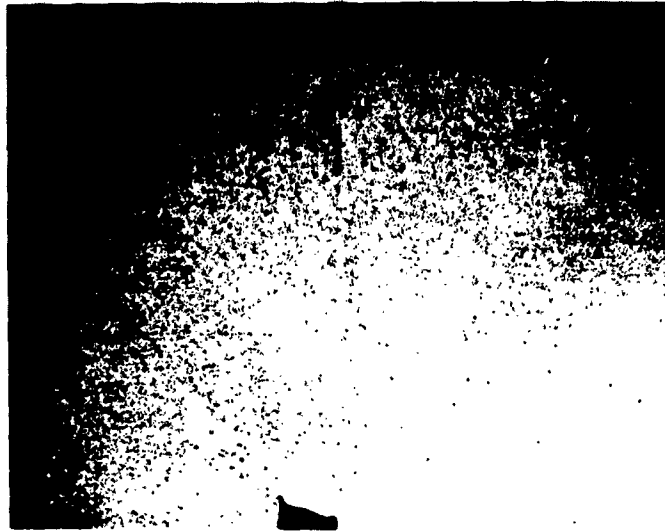
6X   Etchant: 5% Nital   R3188

a)   Crack in Steel No. 1 Specimen No. 3 Held Isothermally
          at 1350 F for 10 Hours (preheat 600 F)

6X   Etchant: Vilella's   R2086

b)   Crack in Steel No. 1 Specimen No. 3 (preheat 600 F)

FIGURE 7.   CRACKS IN LEHIGH RESTRAINT SPECIMENS

29

It is concluded that both high and low temperature cracking occurred but that the low temperature cracking occurred more readily. The results of the study were not verified by statistically reliable quantities since only comparative results were desired.

Variation of Weld Parameters Study (H-11 Steel No. 3)

Effects of Energy Input, Preheat, and Postheat

The effects of these weld parameters on mechanical properties after hardening and tempering were evaluated for sheet welds in steel No. 3, made by the TIG welding process. The investigation was carried out in accordance with statistical principles of the analysis of variance in order to obtain the greatest amount of information from the tests. A similar welding-parameter study was performed for 0.5-inch plate in which the MIG welding process was used.

A pilot investigation using only energy-input Level Y, shown in Table 11, was made to evaluate the effects of a 200 F preheat temperature which permitted almost total transformation to martensite before the postheat treatment. This preheat has recently been adopted by some industrial fabricators of hot-work tool steels. The greatest energy input condition Y was used with the low preheat to insure complete penetration of the joint.

The symbol-notation system used in this report for the various welding parameters is given in Table 11. For example, welding condition V-AlX indicates the use of a 400 F preheat, a postheat at 1350 F for two hours, followed by an air cool and an energy-input of 7900 joules per inch for each of two passes using a 1/32-inch diameter filler wire. The prefix V denotes the use of steel No. 3 of Table 1. For preheat condition A, the weldment was cooled to 400 F from welding before the postheat treatment. For preheat condition B the weldment was cooled to 600 F (above the Ms) following welding and held isothermally for 24 hours to obtain isothermal transformation to bainite. For the preheat condition C, the weld was not allowed to cool below the Ms temperature before postheat treating. The remainder of the table is self-explanatory.

All specimens were hardened and double tempered after postheat treating.

Metallographic Studies

An examination of microstructures of the as-welded specimens (before hardening) was made and the results are outlined in Table 12.

TABLE 11. WELD PARAMETER CONDITIONS. Symbol in parentheses is a notation system to denote that condition.

Sheet Specimens

Preheat	Postheat	Energy Input
400 F (A)	1350 F, for two hours, air cool to room temperature (1)	7900 joules per inch, two passes, 1/32-in.* wire (X)
600 F (B) (24-hr. hold)	1700 F, air cool to room temperature and temper 1350 F (2)	10,100 joules per inch, one pass, .045-in. wire (Y)
800 F (C)	1700 F, slow cool to 1350 F, hold for two hours and air cool (3')[a]	6550 joules per inch, two passes, .045-in. wire (Z)
None (D)	1350 F for long time, cool to room temperature (4)	
200 F (H)		

Plate Specimens

Preheat	Postheat	Energy Input
400 F (E)	1350 F, air cool to room temperature (1)	50,000 joules per inch, two passes, 1/16-in. wire (V)
800 F (F)	1700 F, air cool to room temperature and temper 1350 F (2)	40,600 joules per inch, four passes, 1/16-in. wire (W)
800 F (G) (allow subsequent cool to 150 F		51,000 joules per inch, four passes, 1/16-in. wire (U)

[a] The presence of a "prime" symbol above the postheat designation (i.e., V-A3'X) indicates that the specimens were full annealed and rehardened. The full anneal then becomes the significant postheat treatment. The full annealing treatment was: 1600 F for 1/2 hour, slow cool to 1000 F, and air cool.

Material Prefix Designation

P - Steel No. 1	C - Steel No. 4
A - Steel No. 2	J - Steel No. 5
V - Steel No. 3	M - Steel No 6

* Note: A .045-inch wire was used with this energy input for the other five steels (other than Steel No. 3).

31

TABLE 12. WELDMENT MICROSTRUCTURES AS POSTHEAT TREATED (UNHARDENED)

Weldment Condition and No.	Weld Metal					HAZ					Base Metal		
	1	2	3	4	5	1	2	3	4	5	2	3	4
H1 Y 60		X		H		X							
B1 X 50		X		L	L					X			X
Y 75		X		L	L					X			X
Z 65		X		L	VL	X							X
A1 X 48		X		H	L	X				X			X
Y 56		X		L		X				VL			X
X 63		X		VL	VL	X							X
C1 X 42				H	H		X			H			X
Y 70		X		VL	X	X	VL			H			X
Z 71		X		L	L	X	L			H			X
H2 Y 61	X	X		L			X				X		
B2 X 51	X	X		H		X	X				X		
Y 74	X	X		L		X	X				X		
Z 67		X		L	VL		X				X		
A2 X 4	X	X		H		X	X				X		
Y 73		X		VL			X				X		
Z 76	L	X		VL		L	X				X		
C2 X 44	X	X		H		X					X		
Y 69	X	X		L		X	X				X		
Z 77	X	X		L	VL	X	X				X		
H3 Y 62		X	X	L			X				X		
B3 X 52		X	L		H			VL		H	X	X	
Y 59		X					X			L	X		
Z 64		X				X	X				X		
A3 X 49	X	X	H	H		X		H			X		
Y 57		X			L		X			VL	X		
Z 66		X		H			X			X	X		
C3 X 46		X	L	H	X			H			X		
Y 68		X	H	H	X			H			X		
Z 72		X	H	H	X			H			X		

Legend

L - Light amount
H - Heavy amount
X - Present, i.e., moderate amount
V - Very, i.e., VL = very light

TABLE 12 (Continued)

Code to Microstructures

Microstructure Designation	Weld Metal	HAZ	Base Metal
1	Acicular Pattern	Acicular Pattern	--------------
2	Tempered or Annealed Structure	Tempered or Annealed Structure	Tempered or Annealed Structure
3	Intergranular Carbide Precipitate	Intergranular Carbide Precipitate	Grain Boundary Discernible
4	Extent of Delineation of the Dendrite Pattern	Spheroidite (or fine pearlite), Segregated about Grain Boundaries Leaving a Ferrite Core	Spheroidite Structure
5	Untempered Martensitic Structure	Untempered Martensitic Structure	--------------

The 200 F preheat (preheat H) resulted in nearly total transformation to martensite, while the 400 F preheat (preheat A) permitted only approximately 20 percent transformation to martensite. Preheat B at 600 F, in which the specimen was held at 600 F for 24 hours, accomplished the formation of bainite, while the 800 F preheat (C) maintained the weld metal in an austenitic state.

Preheats B and H, combined with postheat 1, resulted in a process-annealed structure (or highly tempered bainite) and martensite, respectively. Traces of a very fine white constituent (probably untempered martensite, but possibly ferrite) were found in the B1 treatments.

Preheats A and C combined with postheat 1 resulted in a structure of untempered and tempered martensite. The two-hour isothermal hold at 1350 F, which was adequate as a process anneal, was inadequate to wholly transform the austenite isothermally to pearlite; hence, the austenite remaining after the two-hour hold transformed to martensite upon cooling to room temperature. This type of treatment in which the weld is not permitted to cool below the Ms temperature before postheating at 1350 F for a short time was reported as being widely used in the First Quarterly Progress Report. The resulting untempered martensite present after postheat treating might be considered as conducive to cracking.

Postheat treatments 2 and 3 both involved heating to 1700 F above the A temperature; hence, the resulting microstructures were influenced by the preheats except possibly as affected by grain size. Such an effect on grain size was not observed, although grain size was usually not discernible. All specimens receiving postheat 2 resulted in a fairly homogeneous acicular structure, free from intergranular precipitates or white constituents. The microstructures of specimens receiving postheat 3 were not as uniform as those of postheat 2 since the treatment was more difficult to control. They were characterized by large HAZ grains (No. 3 ASTM grain size maximum) and a high degree of carbon segregation. The C3 combination resulted in fine-line type of carbide segregation and untempered martensite in the center of the very coarse dendrites, indicating incomplete transformation of the austenite with postheat treatment 3.

Macrostructures and microstructures of as-welded weldments No. 60 (V-H1Y), No. 61 (V-H2Y), and No. 62 (V-H3Y) which had received a 200 F preheat are shown in Figures 8 through 11, indicating that a predominantly homogeneous and tempered microstructure results from this preheat. Microstructures for weldments No. 66 (V-A2Z) and No. 52 (V-B3X) are shown in Figures 12 and 13. Figure 13 shows patches of untempered martensite (white) in the center of regions of high chemical segregation.

34
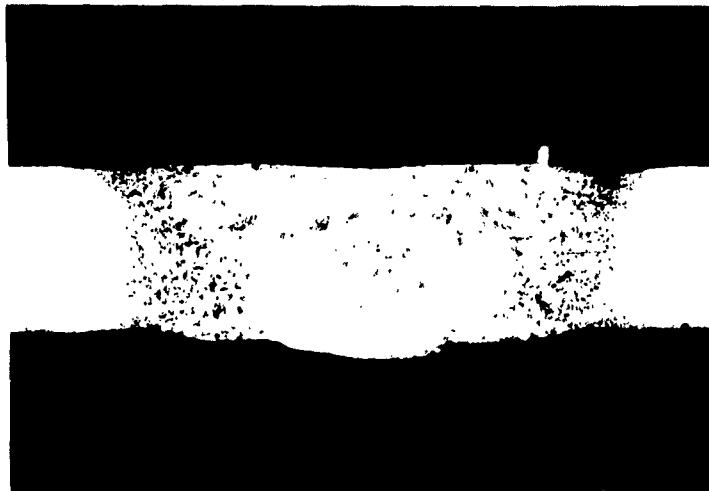
10X   Etchant: 2% Nital   R3063

(a) Cross Section View

600X   Etchant: 2% Nital   R3129

(b) Heat Affected Zone

FIGURE 8.   PHOTOMICROGRAPHS OF WELDMENT CONDITIONS V-H1Y
             (Weldment No. 60).
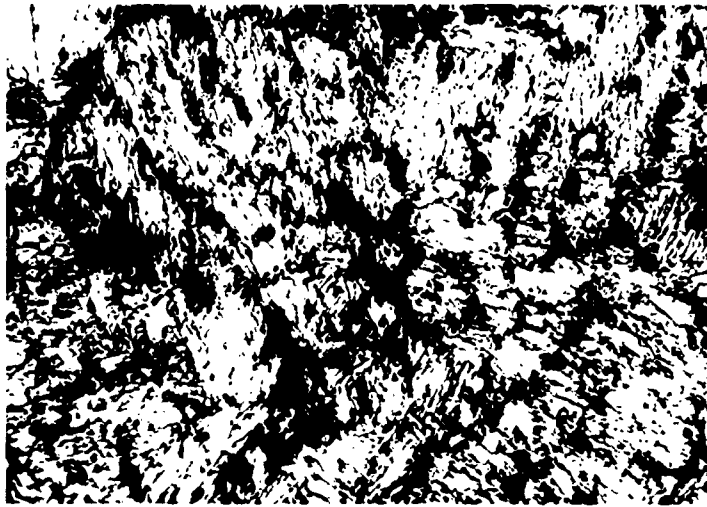
600X   Etchant: 2% Nital   R3130

(a)   Weld Metal Structure of Weldment Condition V-H1Y
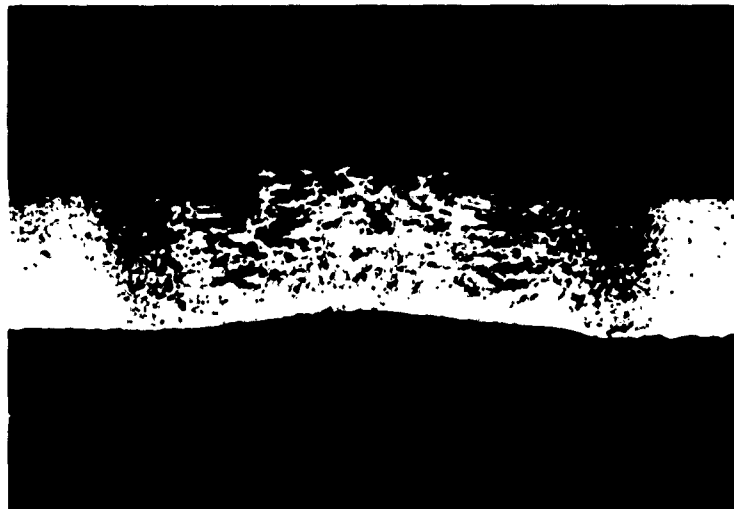
10X   Etchant: 2% Nital   R3062

(b)   Cross Section View of Weldment Condition V-H2Y

FIGURE 9.   PHOTOMICROGRAPHS OF WELDMENT CONDITIONS
            V-H1Y (Weldment No. 60) AND V-H2Y
            (Weldment No. 61)
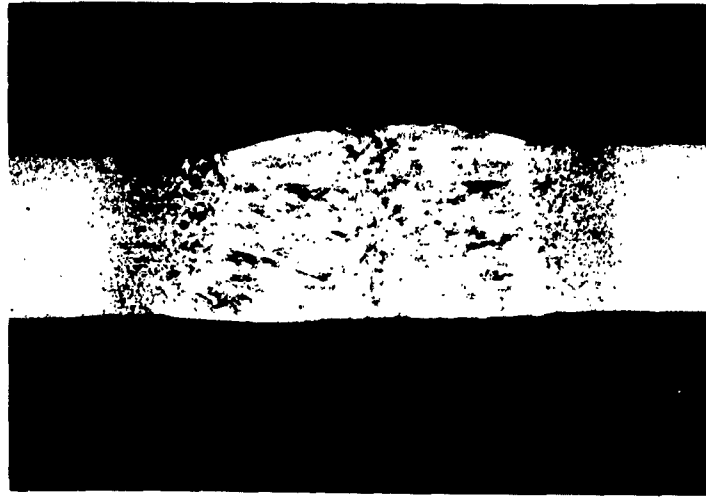
10X   Etchant: 2% Nital   R3061

(a)   Cross Section View of Weldment

600X   Etchant: 2% Nital   R3064

(b)   Base Metal Structure

FIGURE 10. PHOTOMICROGRAPHS OF WELDMENT CONDITION V-H3Y
(Weldment No. 62)
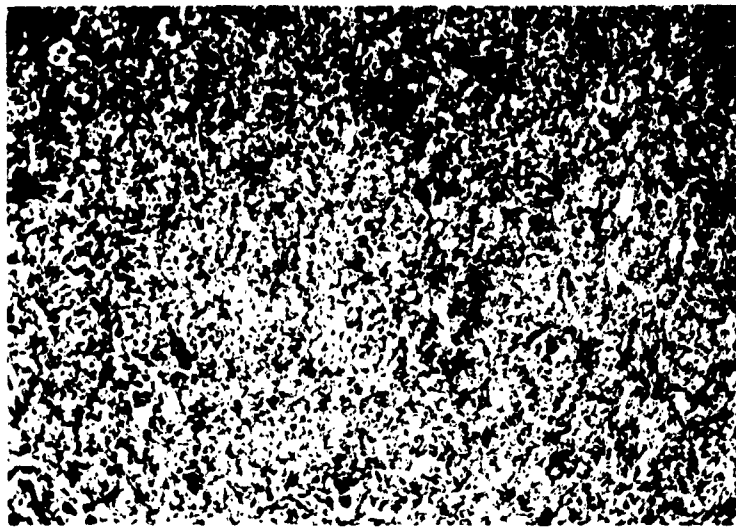
600X   Etchant: 2% Nital   R3066

(a) Heat-affected zone structure
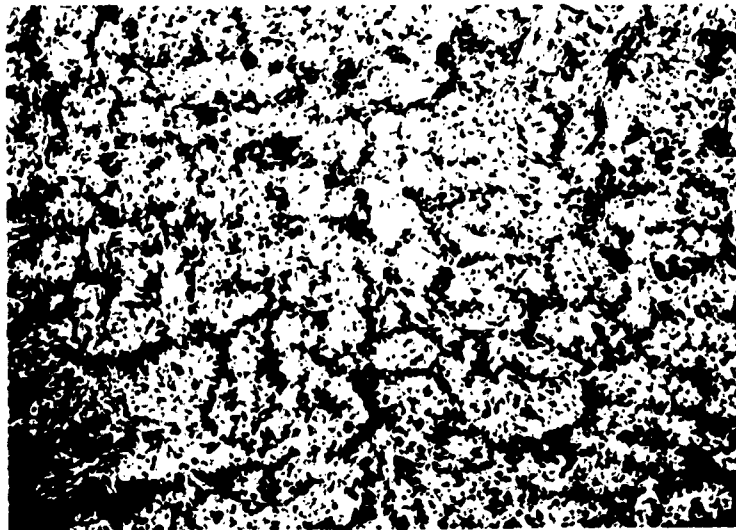
600X   Etchant: 2% Nital   R3065

(b) Weld metal structure

FIGURE 11. PHOTOMICROGRAPHS OF WELDMENT
           CONDITION V-H3Y (Weldment No. 62)
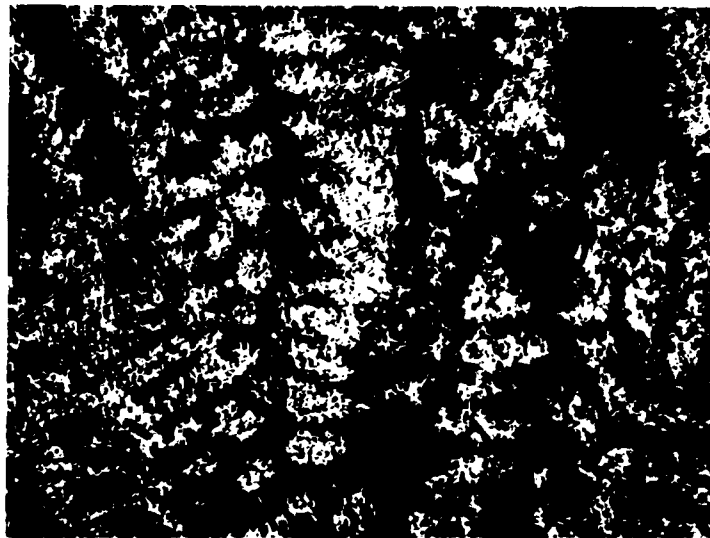
600X   Etchant: 2% Nital   R3132

(a)   Weld-Metal Structure
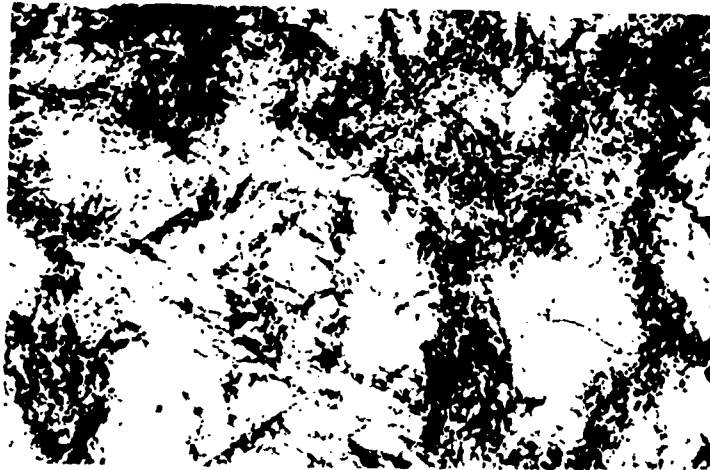
600X   Etchant: 2% Nital   R3131

(b)   Heat Affected Zone Structure

FIGURE 12. PHOTOMICROGRAPHS OF WELDMENT CONDITION
V-A2Z (Weldment No. 66)
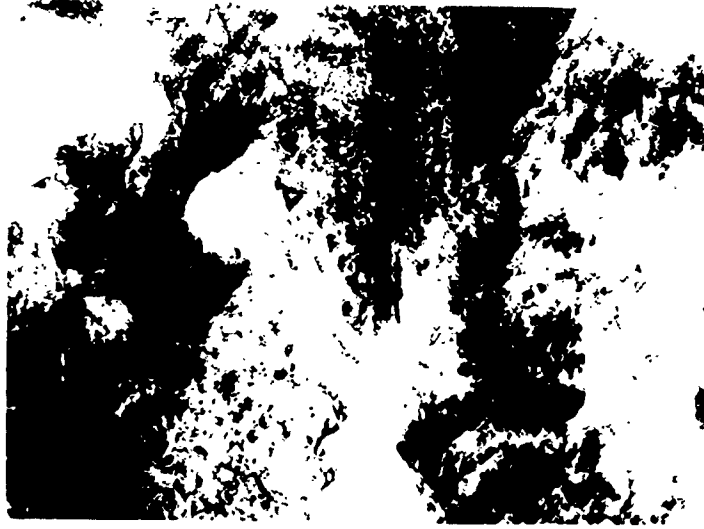
ರಿರಿOX   Etchant: 2% Nital   R3133

eld metal structure

FIGURE 13. PHOTOMICROGRAPHS OF ELDMENT CONDITION V-B3X
(Weldment No. 52)

Some microstructures were also examined in the hardened and tempered conditions, as is shown in Figure 14; the heavy carbon segregation in the region of the grain boundaries in the weld metal of specimen 42 (V-C1X) is not entirely removed by the hardening and tempering heat treatment. Figure 15, however, indicates that the fine-line carbon precipitate of weldment 68 (V-C3Y) was removed by hardening and tempering. The as-hardened and tempered microstructuresof weldments 69 (V-C2Y), 60 (V-H1Y), and 76 (V-A2Z) were tempered martensite similar to those of specimen 68, shown in Figure 15.

A special test was performed to determine wheth~r isothermal transformation from austenite to bainite occurred with the 600 F preheat treatment B described in Table 11. In this test a special weld was prepared and air cooled after the isothermal hold at 600 F for 24 hours. According to the isothermal transformation diagram for steel No. 3, transformation should begin after 15 minutes. Metallurgical examination indicated that untempered bainite was predominant, as shown in Figure 16. Microhardness measurements indicated that the average hardness of the weld metal was Rc 57.5. The hardness of the heat-affected zone was Rc 55, which was as expected from the heat treatment.

Tensile Tests

Sheet Specimens - Tensile data for unwelded test specimens in steel No. 3 are given in Table 13. Groups of four specimens were subjected to the three postheat treatments which the base metal of the weldments received prior to hardening and tempering. The results indicate that the postheat treatments did not significantly affect properties after hardening and tempering. Base metal average yield strength was 235,000 psi, while average tensile strength was 283,000 psi, and average elongation was 5.0 percent.

Transverse-weld tensile test data for 28 weldment conditions are given in Table 14 for sheet specimens of steel No. 3. Eighteen percent of the fractures occurred in the base metal, 25 percent occurred in the heat-affected zone, and 57 percent occurred in the weld metal. From these data of welded specimens there is no correlation between the plastic-flow angle, $\emptyset$, and elongation values.

On one occasion some difficulty was experienced in controlling the tempering temperature. Seven of the sheet weldment conditions were tempered at a slightly higher temperature than planned. To correct this, weldment conditions 50, 51, 52, 57, and 59 were given a full anneal and were rehardened and tempered. The annealing treatment consisted of holding the specimens for 1/2 hour at 1500-1600 F and air cooling. This anneal was reported by the steel producer to be necessary between hardening operations

41
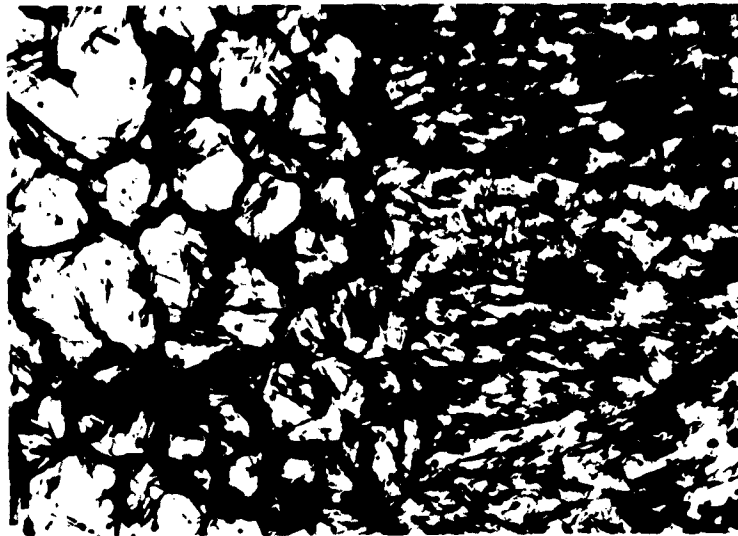
600X   Etchant: 2% Nital   R2049

(a)   After postheat treating; before hardening and tempering
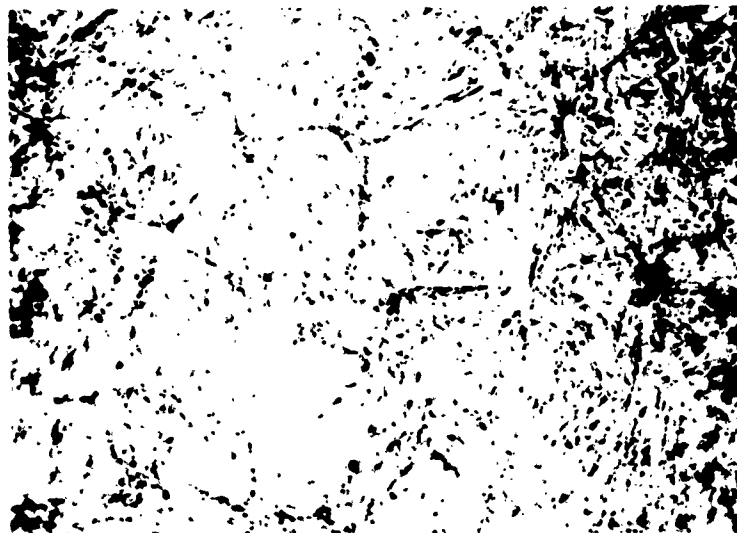
600X   Etchant: 2% Nital   R3034

(b)   After hardening and tempering

FIGURE 14. MICROSTRUCTURE OF SPECIMEN NO.42, WELDMENT CONDITION V-ClX
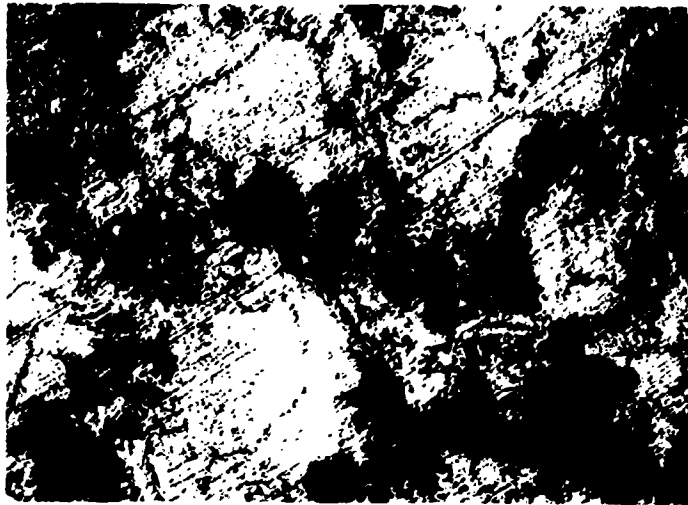
600X   Etchant: 2% Nital   R3134

(a)   After postheat treating; before hardening and tempering
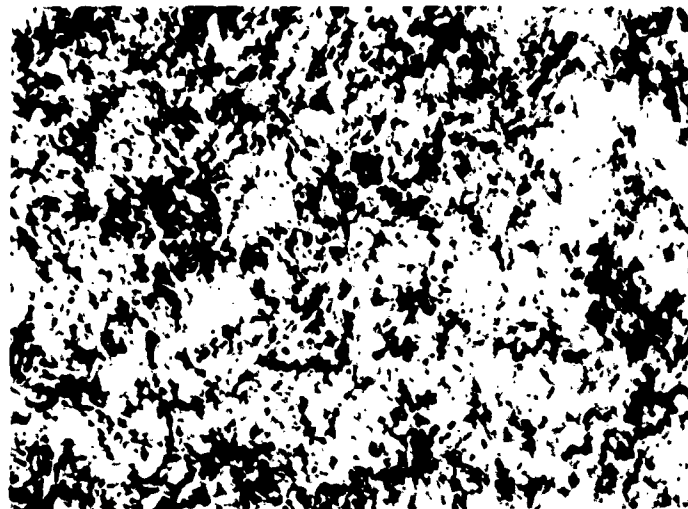
600X   Etchant: 2% Nital   R3135

(b)   After hardening and tempering

FIGURE 15. WELD METAL MICROSTRUCTURE OF SPECIMEN
            NO. 68, WELDMENT CONDITION V-C3Y

1000X   Etchant: Picral + HCl   R3076

FIGURE 16. BAINITIC STRUCTURE OF SPECIAL WELDMENT PREHEATED
AT 600 F, HELD ISOTHERMALLY AT 600 F FOR 24 HOURS
AND AIR COOLED

44

TABLE 13. TENSILE DATA FOR UNWELDED SHEET SPECIMENS OF STEEL NO. 3

Specimen No.	Postheat Condition(a)	Yield Strength, psi	Tensile Strength, psi	% Elongation in 2 in.	Hardness, Rc Avg.	Hardness, Rc Range	Extent of Shear Fracture(d)	Plastic Flow Angle, θ, Degrees
1	1	228,000	279,000	6.0	53.0	51-55	I	57.0
2	1	244,000	292,000	(b)	53.5	53-54	III	(c)
3	1	236,000	286,000	4.0	52.0	52-54	III	0
4	1	233,000	286,000	(b)	55.0	53-56	III	0
Average		235,000	285,000	5.0	53.5			
5	2	230,000	281,000	5.0	53.5	51-56	IV	56.0
6	2	234,000	285,000	5.5	55.0	53-56	IV	56.5
7	2	238,000	286,000	4.5	54.0	53-54	IV	58.0
8	2	236,000	281,000	(b)	54.0	53-56	III	51.5
Average		234,500	283,000	5.0	54.0			
9	3	234,000	285,000	4.5	53.0	51-55	III	58.5
10	3	240,000	283,000	4.5	55.0	54-56	III	62.0
11	3	230,000	279,000	6.5	55.0	54-59	III	57.0
12	3	236,000	272,000	6.0	53.5	53-54	III	55.5
Average		235,000	280,000	5.4	54.1			
Average of 12 Specimens		235,000	283,000	5.11				

(a) Unwelded tensile specimens were subjected to the postheat treatments given welded specimens so that more precise comparisons could be made.

(b) Specimen fractured outside of gage length.

(c) Two small wedge shaped pieces of the specimen broke away at fracture, making it impossible to determine the flow angle.

(d) Percent shear was classified in quadrants; quadrant I was 0-25 percent shear, III was 50-75 percent shear, and IV was 75-100 percent shear.

45

TABLE 14. TRANSVERSE-WELD TENSILE TEST DATA FOR SHEET SPECIMENS OF STEEL NO. 3

Weldment No. & Condition	Specimen No.	Yield Strength, psi	Tensile Strength, psi	% Elongation in 1/2 in	1 in	2 in	Base Metal Hardness, Rc(j) Avg.	Range	Location (k) of Fracture	Extent of Shear Fracture (n)	Plastic(h) Flow Angle, θ, degrees
41, V-D1X	1	246,000	287,000	12.5	6.0	4.5	54	-----	Fusion Line	II	62.0
	2	248,000	287,000	11.0	5.5	4.5	55	-----	Fusion Line	II	63.0
42, V-C1X	1	246,000	292,000	12.5	6.5	4.5	53	-----	WM	II	55.0
	2	247,500	296,000	3.0	2.5	4.0	54	-----	BM(d)	II	53 & 52(c)
44, V-C2X	1	248,500	288,500	6.0	6.5	4.0	54	-----	BM(e)	I	57.0
	2	256,000	283,000	6.5	1.5	1.5	55	-----	HAZ(g)	I	None
46, V-C3X	1	257,000(f)	286,000	12.5	8.0	4.5	54	-----	BM	II	61.0
	2	254,000	282,000	12.5	6.5	4.5	54	-----	HAZ	II	57.0
48, V-A1X	1	235,000	273,000	12.0	7.0	4.5	53	51.5-54	WM	II	63.0
	2	232,000	272,000	16.0	9.0	5.5	52.5	52.5-53	WM	III	57.5
47, V-A2X	1	222,000	263,000	4.0	3.0	6.0	52	51.5-52	BM	II	54.0
	2	214,500	262,000	4.0	3.0	6.5	52	51.5-52.5	BM	IV	57.5
49, V-A3X	1	219,000	274,000	14.0	9.0	5.0	53.5	53-54	--	--	----
	2	195,000	244,000	12.0	7.0	4.0	54.5	54-55	--	--	----
50, V-B1'X	1(i)	234,000	271,500	16.0	8.0	4.5	53	51-54	WM	III	54.0
	2(i)	230,000	270,000	16.0	9.0	5.5	53	53-53.5	HAZ	III	61.5

TABLE 14. TRANSVERSE-WELD TENSILE TEST DATA FOR SHEET SPECIMENS OF STEEL NO. 3

(Continued)

Weldment No. & Condition	Specimen No.	Yield Strength, psi	Tensile Strength, psi	% Elongation in 1/2 in.	1 in.	2 in.	Base Metal (j) Hardness, Rc Avg.	Range	Location (k) of Fracture	Extent of Shear Fracture (n)	Plasti(h) Flow Angle, β, degrees
51,V-B2'X	1	231,000	271,000	16.0	9.0	6.0	52	49.54	HAZ	III	45.0
	2	204,000	242,000	16.0	9.0	6.0	53	52-53	HAZ	III	62.5
52,V-B3'X	1	224,000	264,000	0	2.0	6.5	52	50-53	BM	III	60.5
	2	224,000	262,000	14.0	8.0	5.0	51.5	49.5-53	HAZ	III	61.5
56,V-A1Y	1	219,000	264,000	12.0	7.0	4.0	51	50.5-52	WM	--	57.0
	2	220,000	256,000	12.0	7.0	4.0	52	51.5-53	WM	--	52.0
73,V-A2Y	1	242,000	288,000	14.0	7.0	5.0	54	53-55	HAZ	III	56.5
	2	230,000	282,000	12.0	7.0	4.0	55	54-55	WM	II	54.0
57,V-A3'Y	1	222,000	257,000	14.0	8.0	4.0	52.5	51.5-53	WM	III	51.0
	2	202,500	255,000	0.0	3.0	6.5	51.5	51-52	BM	II	65.0
75,V-B1Y	1	242,000	293,000	14.0	8.0	4.4	55.5	55-56	HAZ	III	59.0
	2	233,000	276,500	12.0	7.0	3.5	55.5	55-56	WM	III	59.0
74,V-B2Y	1	232,000	268,000	14.0	6.0	4.0	54	53.5-54	WM	III	60.0
	2	226,000	268,000	14.0	7.0	2.5	52	51.5-52	BM	III	65.0
59,V-B3'Y	1	224,000	248,000	14.0	8.0	5.0	53	53-54	WM	IV	76.0
	2	220,000	259,000	16.0	9.0	5.0	53.5	53-54	WM	IV	68.0

47

TABLE 14. TRANSVERSE WELD TENSILE TEST DATA FOR SHEET SPECIMENS OF STEEL NO. 3

(Continued)

Weldment No. & Condition	Specimen No.	Yield Strength, psi	Tensile Strength, psi	% Elongation in 1/2 in.	1 in.	2 in.	Base Metal Hardness, Rc(j) Avg.	Range	Location of Fracture (k)	Extent of Shear Fracture (n)	Plastic Flow Angle, φ, degrees (h)
70,V-C1Y	1	221,000	272,000	14.0	8.0	5.0	53.5	52.5-54.5	WM	II	62.0
	2	226,500	270,000	18.0	10.0	5.5	53.5	53-54	WM	III	63.0
69,V-C2Y	1	215,000	257,500	6.0	5.0	3.0	53	52-53.5	WM	I	60.5
	2	220,000	282,000	14.0	8.0	5.0	53	52.5-54	WM	IV	60.0
68,V-C3Y	1	230,000	276,500	12.0	6.0	3.5	54	54-54	WM	I	52.5
	2	234,000	274,500	10.0	5.0	4.0	55	55-55	WM	I	60.0
63,V-A1Z	1	237,000	279,000	12.0	7.0	4.0	54	53-54.5	WM	III	52.0
	2	235,000	284,000	12.0	7.0	4.5	53.5	52-54.5	HAZ	III	52.5
76,V-A2Z	1	228,000	272,000	14.0	8.0	5.5	53	52-53	HAZ	IV	57.5
	2	226,000	274,000	16.0	8.0	5.0	54	54-54	HAZ	IV	54.0
66,V-A3Z	1	231,000	283,000	14.0	8.0	4.5	54	54-54	WM	III	53.0
	2	236,000	281,500	12.0	6.0	4.0	54.5	54-55	HAZ	III	61.0
65,V-B1Z	1	233,000	285,000	12.0(d)	8.0	4.5	54.5	53.5-55.5	HAZ	II	66.0
	2	234,500	282,000	0(e)	0(e)	5.5	54.5	53.5-55	BM	---	58.0
67,V-B2Z	1	220,000	266,000	16.0	10.0	5.5	52.5	50.5-53.5	WM	III	63.0
	2	225,000	268,000	10.0	7.0	6.0	52.5	52-53	WM	IV	63.5

TABLE 14. TRANSVERSE-WELD TENSILE TEST DATA FOR SHEET SPECIMENS OF STEEL NO. 3

(Continued)

Weldment No. & Condition	Specimen No.	Yield Strength, psi	Tensile Strength, psi	% Elongation in 1/2 in, 1 in, 2 in			Base Metal Hardness, Rc(j) Avg. Range		Location (k) of Fracture	Extent of Shear Fracture (n)	Plastic(h) Flow Angle, φ, degrees
64, V-B3Z	1	219,000	263,000	12.0	8.0	4.5	52.5	51.5-53.5	WM	---	60.5
	2	219,000	261,000	16.0	8.0	5.0	52.5	52.5-53	WM	II	62.5
71, V-C1Z	1	240,000	288,500	10.0	4.0	3.5	55.5	55-56	WM	II	None
	2	231,000	285,500	14.0	8.0	5.0	55	54-55.5	WM	III	54.0
77, V-C2Z	1	224,000	266,000	14.0	7.0	3.5	53.5	53-53.5	WM	III	59.0
	2	223,000	268,000	12.0	6.5	4.0	54	54-54	WM	IV	64.0
72, V-C3Z	1	220,000	262,000	16.0	6.0	5.0	53	53-54	WM	IV	54.0
	2	226,000	273,000	15.0	6.5	4.5	54	53.5-54	HAZ	III	65.0
60, V-H1Y	1	239,000	283,000	18.0	11.0	6.0	54.5	55-55	HAZ	IV	60.0
	2	238,000(m)	242,000	---	---	---	54.5	54-55	BM	II	None
61, V-H2Y	1	228,000	279,000	10.0	8.0	5.5	53.5	52.5-54.5	WM	III	58.0
	2	228,000	279,000	12.0	7.0	4.0	54	53-54.5	WM	III	60.5
62, V-H3Y	1	233,000	278,500	14.0	7.0	4.5	54	53.5-55	WM	III	52.0
	2	231,000	275,000	14.0	7.0	5.0	54	53-55	WM	III	57.0

(a) 0.2% offset
(b) Average of three readings
(c) Two bands diagonal to each other
(d) Fracture occurred outside the one-inch gage length
(e) Fracture occurred outside the 1/2-inch gage length
(f) Extrapolated value (extensometer was removed from specimen too soon)
(g) The heat-affected zone
(h) Plus or minus one degree

(i) Specimen 2 was annealed and rehardened while Specimen 1 was not. Annealing and rehardening are indicated by the "prime" symbol
(j) Hardness values were taken from three readings
(k) BM = Base Metal, WM = Weld Metal, HAZ = Heat Affected Zone
(l) Fracture occurred outside the 1/2- and 1-inch gage lengths
(m) Fracture occurred outside the 2-inch gage length due to a notch in the side of the specimen
(n) Percent shear was classified in quadrants: quadrant 1 was 0-25 percent shear, II was 25-50 percent shear, III was 50-75 percent shear, and IV was 75-100 percent shear

49

to prevent abnormal grain growth. The treatment is considered as a special postheat treatment and designated in symbol notation by a "prime" symbol following the postheat number.

Average hardness values of the tensile specimens varied from 50 Rc to 55 Rc; however, the data were normalized with respect to hardness by dividing tensile and yield strength by the average hardness value and by multiplying elongation and hardness values. The resulting values permit a comparison of properties independent of strength differences due solely to variation in hardness.

The following weldments had low yield strengths: 51 (V-B2'X), 57 (V-A3'Y), 69 (V-C2Y), 73 (V-A2Y), and 75 (V-B1Y), while weldment No. 51 also had low tensile strength. A predominance of the high energy input condition Y is associated with these low strength weldments.

It was found that some weld conditions resulted in a superior combination of both strength and ductility. These were conditions V-A1Z (No. 63), V-A2Z (No. 76), V-A3Z (No. 66), V-H1Y (No. 60), V-H2Y (No. 61), and V-H3Y (No. 62). This indicates that the AZ and the HY preheat and energy input conditions have the best properties, regardless of postheat. It should be noted that the H (200 F) preheat was used only with the Y energy input. It is expected, however, that a lower energy input would give even better results since AZ conditions are better than AX or AY conditions and the Y energy input appears to give generally lower properties. The low preheat and energy input conditions may be superior because of their effect of restricting the extent of the heat-affected zone.

Transverse-Notch Longitudinal-Weld Tests - Results of the transverse-notch longitudinal-weld tensile tests are given in Table 15. Originally, the specimen width was two inches; however, some of the specimens fractured at the pin-loading holes rather than at the notch. The problem was solved by reducing the specimen width to 1.5 inches.

It is evident that those specimens welded by the CX condition were abnormal in view of their low notch-strength and low percent shear. The transverse-weld tensile test indicated that these weldments possessed exceptional strength, but the elongation was not exceptionally low and did not reveal the extreme notch sensitivity of specimens from these weldments. Since these weldments were hardened and tempered in the same furnace load, it is suspected that a variance in the heat treatment may have caused these abnormal properties for this group of specimens.

It is interesting to note that of the five specimens in which failure did not initiate in the weld metal or heat-affected zone (welding conditions V-A2Y, V-A2Z, V-B2Y, V-B2Z, and V-B3'Y), four

TABLE 15. TRANSVERSE-NOTCH LONGITUDINAL-WELD SHEET TENSILE TEST DATA FOR STEEL NO. 3

Specimen No. & Condition	Nominal Width, in.	Thickness of Metal Beneath Notch, in.	Notch Radius, in.	Nominal Fracture Stress, psi	Source of Fracture Initiation	Notch Strength to Base Metal Strength Ratio[b]	Average Hardness, Rc	% Shear[a]
42,V-C1X	2	.0425	.005	240,000	HAZ	.85	55	I
44,V-C2X	2	.0510	.005	151,500	WM	.53	53	I
46,V-C3X	1.5	.0465	.005	146,000	WM	.52	--	I
48,V-A1X	--	.0446	.004	230,000	WM	.81	53	IV
47,V-A2X	2	.0415	.005	242,000	WM	.85	53	II
49,V-A3X	1.5	----	.004	310,000	WM	1.10	55	III
73,V-A2Y	1.5	.0431	.004	237,000	BM	.84	55	II
75,V-B1Y	1.5	.0426	.004	288,000	WM	1.02	54	III
74,V-B2Y	2.0	----	.004	264,000	BM[c]	----	--	---
59,V-B3Y	1.5	.0446	.005	286,000	BM	1.01	52	III
70,V-C1Y	2	.0450	.007	263,000	WM	.86	--	III
69,V-C2Y	1.5	.0456	.005	265,000	WM[b]	.94	53	II
68,V-C3Y	1.5	----	.004	270,000	WM[b]	.95	54	II
63,V-A1Z	1.5	.0415	.007	286,000	HAZ	1.01	54	III
76,V-A2Z	1.5	----	.004	313,000	BM[b]	1.11	53	IV
66,V-A3Z	1.5	----	.004	273,000	WM	.97	54	II
67,V-B2Z	1.5	----	.007	261,000	BM	.92	53	II
64,V-B3Z	1.5	----	.006	255,000	WM	.90	53	III

(a) Extent of shear fracture on fracture face: I - 0-10%
   II - 10-20%
   III - 20-30%
   IV - 30-40%

(b) Two sources of initiation, one in WM the other in BM.
(c) Source not well defined, no propagation.

51

of them received postheat treatment 2. It appears that weldment
conditions A2 and B2 are least likely to cause fracture initiation
in the weld or heat-affected zone.

Other welding conditions resulting in fracture strengths
greater than the average tensile strength of the unwelded material
were conditions V-A3X, V-A1Z, V-A2Z, V-B1Y, and V-B3Y.

Plate Specimens - Transverse-weld tensile data for plate specimens
of steel No. 3 are presented in Table 16. All fractures occurred
in the weld metal.

The average hardness values were generally within the Rc 51-32
range, which would be expected from the tempering temperature of
1050 F. The hardness range within one specimen is, however,
unexplainably large. Hardness readings were taken on opposite
sides of one end of the specimen.

The presence of slag in specimen V-E2V-B greatly decreased
both strength and ductility; however, this slag was not of suffi-
cient quantity to be detected by radiography.

The source of fracture in most plate tensile specimens was
observed to be porosity. All weldments were radiographed at two-
percent sensitivity after welding but the porosity and other flaws
were too small to be detected. In those fractures in which no
weld-metal defect could be found at the initiation source, the
fracture occurred at or near the center of the fracture face.
From these data, the presence of porosity did not appreciably
affect strength values, but it did lower the ductility. Specimen
which did not fail from weld defects had an average elongation in
two inches of 6.3 percent, while elongation for the others was
3.0 percent. Data for duplicate specimens of each weldment condi-
tion are in good agreement in spite of the presence of porosity.
The F2W condition apparently provides the highest yield strength
properties.

The presence of porosity may be attributed to unclean filler
wire. The wire was not copper-flash coated but was bright finished,
cleaned, and packed in plastic bags containing a desiccant. Some
oxidation occurred on some of the wires which were not properly
packed. The wire was cleaned by hand as well as possible, but it
is believed that the contamination contributed to the porosity.
A mechanical brush cleaning process was devised for use in subse-
quent cleaning operations to reduce the porosity.

Bend Tests

The bend test data are given in Table 17 for sheet weldments
of steel No. 3. Thirty-seven percent of the fractures initiated in

TABLE 16. TRANSVERSE-WELD TENSILE DATA FOR PLATE SPECIMEN OF STEEL NO. 3

Weldment No. and Condition	Specimen No.	Yield Strength, psi	Tensile Strength, psi	% Elongation in			Base Metal Hardness, Rc		Special Cause of Fracture	Location of Fracture Initiation Source (a)
				1/2 in.	1 in.	2 in.	Avg.	Range		
V-K1V	A	238,000	277,000	14.0	9.0	5.5	53	51-55	Porosity	45° I
	B	239,000	279,000	18.0	12.0	6.0	53	50.5-55.5	None	C
V-K2V	A	No Yield	281,500	6.0	4.0	3.0	52.5	52.5-53	Porosity	0° I
	B	No Yield	190,000	2.0	2.0	1.0	51	49-54	Slag Layer	45° I
V-P1V	A	237,000	239,500	2.0	2.0	1.0	53.5	52.5-54.5	Porosity	0° I
	B	234,000	275,500	16.0	9.0	6.0	52.5	51-55	None	C
V-P2V	A	237,000	276,000	18.0	12.0	7.0	52.5	52-53	None	45° I
	B	241,000	280,000	16.0	9.0	5.5	53.5	53-54	Porosity	0° I
V-E1W	A	239,000	241,000	2.0	2.0	1.0	53	52-54	Porosity	0° E
	B	239,000	241,000	2.0	2.0	1.0	53	51-54	Porosity	0° E
V-E2W	A	239,300	280,500	6.0	4.0	2.5	52.5	50.5-54.5	Porosity	45° E
	B	241,000	278,500	6.0	4.0	2.5	53	51.5-54	Porosity	45° E
V-P1W	A	238,000	275,000	10.0	6.0	4.0	52	50-54	Porosity	45° I
	B	239,200	275,500	14.0	8.0	4.5	53.5	52.5-54.5	Porosity	0° E
V-P2W	A	243,000	278,000	12.0	7.0	3.5	50.5	49.5-51.5	Porosity	45° I
	B	244,000	279,500	4.0	3.0	1.5	53	51.5-54	Porosity	90° I

(a) Code for source location on fracture faces; C = center; E = edge; I = intermediate; 0° = on major axis of rectangular cross section, 90° on minor axis, 45° on line bisecting axes.

TABLE 17. LONGITUDINAL-WELD BEND TEST DATA FOR SHEET SPECIMENS OF STEEL NO. 3

Weldment No. and Condition	Specimen No.	Minimum Bend Radius to Thickness Ratio	Bend Elongation, %	Base Metal Hardness, Rc(b) Avg.	Range	Region of Fracture Initiation	Plastic Deformation Pattern(c)
41, V-D1X	1	6.00	8.0	53.5	---	HAZ	B
	2	4.50	10.8	53.0	---	HAZ	B
42, V-C1X	1	6.50	6.9	55.0	---	HAZ	B
	2	3.00	13.0	53.5	---	HAZ	B
44, V-C2X	1	5.50	8.4	54.0	---	Indeterminate	A
	2	6.50	7.6	53.0	---	Indeterminate	A
46, V-C3X	1	2.50	16.2	53.5	---	HAZ	D
	2	4.0	11.1	52.0	---	Weld Metal	D
48, V-A1X	1	3.80	11.7	51	51	Weld & HAZ	B
	2	2.45	17.3	51.5	51-52	Weld & HAZ	B
47, V-A2X	1	3.00	14.2	52	52-53	Weld & HAZ	B
	2	1.65	23.0	51	50-51	HAZ	A
49, V-A3X	1(a)	2.80	15.2	51.5	51-52	HAZ	B
	2(a)	2.80	15.2	53.5	53-54	HAZ	A
50, V-B1'X	1	7.15	6.6	55	54.5-55.5	Base Metal	A
	2	6.70	6.9	54	53.5	Base Metal	A
51, V-B2'X	1	2.90	14.7	52	52-53	Base Metal (at both edges)	A
	2	2.95	14.4	53.5	53.5-54	Indeterminate	A
52, V-B3'X	1	5.40	8.5	54	54-55	HAZ	A
	2	5.05	9.0	56	55-57	Base Metal	A
56, V-A1'Y	1	4.00	11.1	54	53-55	Base Metal	A
	2	2.80	15.0	53	52.5-53.5	Base Metal	A
73, V-A2Y	1	3.57	12.3	52	50-54	HAZ	A
	2	3.97	11.1	54	53-54	Base Metal	A

(Continued)

Weldment No. and Condition	Specimen No.	Minimum Bend Radius to Thickness Ratio	Bend Elongation, %	Base Metal Hardness, Rc(b)		Region of Fracture Initiation	Plastic Deformation Pattern(c)
				Avg.	Range		
57,V-A3'Y	1	3.50	12.5	53.5	53-55	Base Metal	A
	2	3.70	11.8	54.5	53.5-55	Base Metal	C
75,V-B1Y	1	7.81	6.0	55	53-56	Weld Metal	B
	2	5.00	9.1	55	54-55	Weld Metal	B
74,V-B2Y	1	4.34	10.4	--	---	Weld Metal	A
	2	3.29	14.4	--	---	Weld Metal	B
59,V-B3'Y	1	2.00	19.9	53	51.5-54	Base Metal	A
	2	2.00	19.9	52	51-53	Base Metal	A
70,V-C1Y	1	2.50	16.7	53.5	53-54	HAZ	B
	2	4.02	11.1	54	53.5-54	Weld Metal	B
69,V-C2Y	1	6.67	7.0	52.5	51.5-53	Weld Metal	A
	2	3.57	12.3	54	54-54.5	Base Metal	A
68,V-C3Y	1	1.84	21.3	53	53-53.5	Weld Metal	D
	2	1.92	20.6	54.5	54-54.5	Weld (Porosity)	D
63,V-A1Z	1	2.68	15.7	54	53-55	HAZ	B
	2	1.92	20.6	54.5	54.5-54.5	HAZ	B
76,V-A2Z	1	2.04	19.6	54.5	54-54.5	Base Metal	A
	2	3.91	12.0	53	52.5-53.5	Base Metal	A
66,V-A3Z	1	1.81	21.6	54	52.5-54.5	Weld Metal	D
	2	2.57	16.3	54	54-54	Weld Metal	D
65,V-B1Z	1	2.98	14.4	54.5	54-55	HAZ	B
	2	4.88	9.3	54.5	54.5-54.5	Weld Metal	B
67,V-B2Z	1	9.06	5.2	52.5	52-53	Weld Metal	No appreciable flow
	2	3.68	12.2	53	52.5-53.5	Base Metal	A
64,V-B3Z	1	1.95	20.4	52	52-52.5	Weld Metal	D
	2	4.63	9.8	53	53-53	Weld Metal	D

TABLE 17. LONGITUDINAL WELD BEND TEST DATA FOR SHEET SPECIMENS OF STEEL NO. 3

(Continued)

Weldment No. and Condition	Specimen No.	Minimum Bend Radius to Thickness Ratio	Bend Elongation, %	Base Metal Hardness, Rc(b) Avg.	Range	Region of Fracture Initiation	Plastic Deformation Pattern(c)
71, V-C1Z	2	3.73	12.2	55	54-55	HAZ	B
77, V-C2Z	1	3.91	11.1	52	50-53	Weld Metal	D
	2	1.96	20.4	52	51-52.5	Weld Metal	A
72, V-C3Z	1	1.42	25.6	52.5	52-53	Weld Metal	A
	2	2.94	14.8	53	51.5-54	Weld Metal	D
60, V-H1Y	1	2.84	14.9	54	52.5-54.5	HAZ	B
	2	3.79	11.6	55	54-55	HAZ	B
61, V-H2Y	1	1.99	20.2	55.5	54.5-56	Base Metal	A
	2	1.81	21.6	54	53.5-54.5	HAZ	A
62, V-H3Y	1	2.04	19.3	53	52-53.5	Weld Metal	D
	2	1.51	24.8	52	51-53	HAZ	D

(a) Specimen 2 was annealed and rehardened while Specimen 1 was not. Annealing and rehardening is indicated by the "prime" symbol.

(b) Hardness values were taken from three readings.

(c) Plastic Deformation Pattern

Condition | Description

A | Slip lines were found on all surfaces except for two parallel lines in the HAZ.
B | Slip lines were found only in the weld metal and in the outer bands of the HAZ.
C | Slip lines were seen only in two parallel outer bands of the HAZ.
D | Slip lines were seen in weld metal only.

56

the weld metal, 27 percent in the heat-affected zone, 30 percent in the base metal, and six percent initiated in both weld metal and heat-affected zones.

The following weldments had exceptionally high bend ductility (20 to 25%) when normalized: weldment condition No. 61 (V-H2Y), 62 (V-H3Y), 68 (V-C3Y), and 63 (V-Al2). Weldment No. 67-1 fractured at the very low bend-elongation value of 5.2 percent.

Deformation bands were observed on the ground-finished surfaces of the bend specimens, as illustrated in Figure 17. The bands were present in the weld metal, being less prominent on the center line of the weld metal. In some cases (weldments No. 41 and 42) separate bands occurred on both sides of the weld in the heat-affected zone, separated by bands which did not contain deformation lines. In weldment No. 44, the two outer bands extended across the entire base metal so that essentially the entire surface contained deformation lines except for two narrow bands in the heat-affected zone. Weldment No. 46 exhibited a deformation band only in the weld metal region. These bands are significant in that they indicate a difference in the plastic behavior of the weld region with respect to the base metal. Fracture behavior was affected by the presence of the bands as shown by the discontinuous line of the fracture across these bands.

The distinct differences in the plastic-flow patterns of the bend specimens are of interest and are significant. Flow pattern B (defined in Table 17), in which flow occurred in the weld metal and the heat-affected zone only, is frequently associated with postheat condition No. 1; flow pattern A, in which flow occurred in the base metal as well, is associated with postheat treating condition No. 2. Flow pattern D, in which flow occurred only in the weld metal, is associated with postheat condition No. 3. No differences in microstructure of microhardness[1] could be associated with the flow behavior.

The fracture line was observed to be straight across the specimen when high elongation values were achieved but often appeared as a sinusoidal pattern for low elongation values.

Transverse-weld bend-test data for plate specimens are given in Table 18. Again, porosity was present which decreased bend-elongation values. All fractures occurred in the weld metal.

Charpy-Impact Tests

Charpy V-notch impact tests were performed on the weld metal and base metal of plate weldments of steel No. 3 at temperatures

1 Microhardness varied randomly from 580 to 640 Knoop values (Rc 52 to Rc 53.5) within the cross section of bend specimen No. 69.

FIGURE 17.   LONGITUDINAL-WELD BEND TEST SPECIMEN
             SHOWING LOCAL AREAS OF PLASTIC FLOW

TABLE 18. TRANSVERSE-WELD BEND TEST DATA FOR PLATE SPECIMENS OF STEEL NO. 3

Weldment No. and Condition	Specimen No.	Min. Bend Radius to Thickness Ratio	Bend Elongation, percent	Special Cause of Fracture	Location of Fracture Source(a)
V-51V	A	16.86	2.9	Porosity	C 3/4"
	B	15.68	3.1	Porosity	C 1/2"
V-52V	A	17.63	2.8	Porosity	C 3/4"
	B	19.00	2.6	Porosity	I 1/6"
V-71V	A	18.23	2.7	Porosity	I 3/8"
	B	19.21	2.5	Porosity	C 5/8"
V-72V	A	16.62	2.9	None	E 1/4"
	B	20.00	2.5	None	E 1/2"
V-51W	A	12.4	3.8	Porosity	E 1/4"
	B	20.6	2.4	Porosity	E 1"
V-52W	A	21.4	2.3	None	I 1"
	B	13.1	3.7	Porosity	E 1"
V-71W	A	11.6	4.2	Porosity	I 1/2"
	B	12.6	3.8	Porosity	I 7/8"
V-72W	A	∞	0.0	Porosity	I 1/8"
	B	11.7	4.1	None	E 1/8"

(a) Code for source location on fracture face. C, E, and I same as for Table 15. Distance from minor axis of 2" x 1/2" rectangular cross section is also given.

of 80, 212, 600, and 1000 F. The V-notch was placed in the weld metal with the root of the notch perpendicular to the plane of the weldment plate so that all the weld passes were traversed by the notch. For the base-plate, a similar notch-direction resulted in the fracture transversing the rolling direction.

The impact data are presented in Figure 18. The average weld metal impact values at room temperature were quite low (5.3-11.6 ft/lb). Since these steels are most promising for high-temperature applications, subsequent testing was performed at higher temperatures rather than at lower temperatures. No energy-transition temperature was observed.

Impact tests were performed on the base-plate materials which were subjected to the postheat treatments being evaluated in this weld parameter evaluation. The impact values for the base metal were only on the order of two to three foot-pounds higher than those for the weld metal.

The Charpy V-notch impact tests, based on the criteria of energy absorption, lateral contraction, and fracture appearance, did not indicate the relative merits of any welding condition. The values for any one welding condition appeared to fall in a random manner between the limits of the curves of Figure 18. It was therefore considered advisable to use the shallow-notch or large-radius impact test advocated for evaluating tool steels. In this test, a 1/2-inch radius notch approximately 5/64 inch deep is ground in a standard size Charpy specimen. The shallow notch is reported[1] to illustrate differences in materials not shown by the standard V-notched Charpy specimen.

Statistical Evaluation

The tensile-test and bend-test data from the variation of parameters study for sheet specimens were evaluated by statistical analysis of variance methods; computations were made by the 704 computer at Electric Boat Division. The findings imply that weld parameters of preheat, postheat, and energy input have an influence on the mechanical properties of weldments after hardening and tempering for sheet specimens but apparently not for plate specimens[2].

The results of the statistical analysis are presented in Table 19. A yes or no answer is given (using a 95% confidence level) to the question of whether the welding parameter had a significant influence on the mechanical property being considered, and if there were significant interactions between the welding

---

1   Reference 6

2   This may be a result of the smaller number of plate specimens tested in comparison with the sheet specimens.
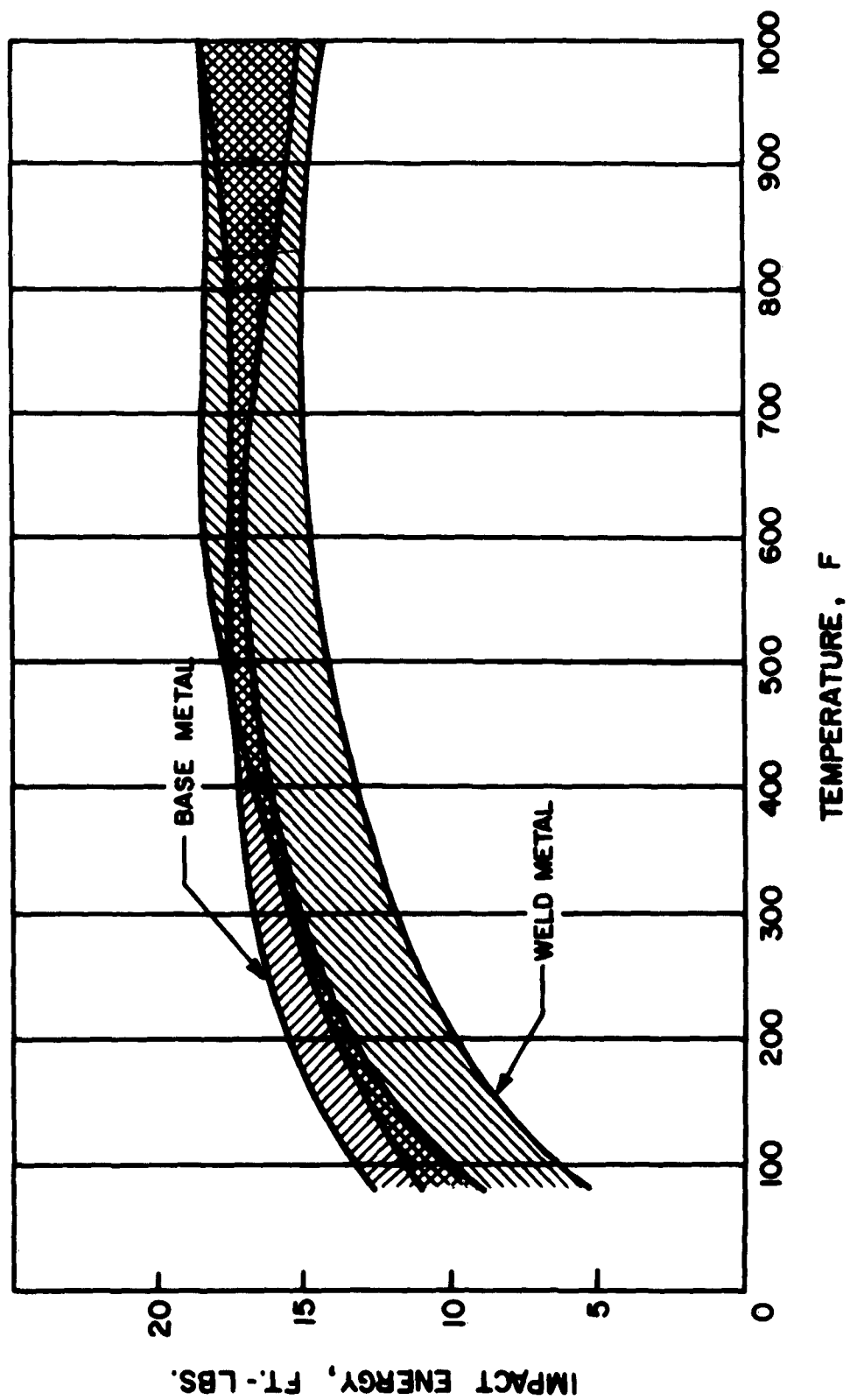
FIGURE 18 CHARPY V-NOTCH IMPACT DATA FOR STEEL NO. 3

TABLE 19. RESULTS OF STATISTICAL VARIATION OF PARAMETER STUDY FOR SHEET WELDMENTS OF STEEL NO. 3. Significance of Welding Parameters on Mechanical Properties

Mechanical Property	Correlation Coefficient	Preheat	Postheat	Energy Input	Preheat & Postheat	Preheat & Energy	Energy & Postheat	All Three Parameter Interactions
Sheet Specimens								
Tensile Strength	.7441	Yes C(AB)	Yes 1,2,3(a)	No	Yes	Yes	Yes	Yes
Yield Strength	.7284	Yes (BC)A	Yes (2,1)3	Yes (XX)Y	Yes	Yes	Yes	Yes
Tensile Elongation in Two Inches	.3991	Yes (BA)C	Yes (3,2,1)	No	No	No	No	No
Bend Elongation	.4195	No	Yes 3(1,2)	Yes(b) (XX)(YX)	No	No	No	No
Plate Specimens								
Tensile Strength	.7046	No	No	No	No	Yes	No	No
Yield Strength (c)	----	---	---	---	---	---	---	---
Tensile Elongation in Two Inches	.4535	No	No	Doubtful	No	No	No	Doubtful
Bend Elongation	.3509	No	No	No	No	No	No	No

(a) The weld condition symbols are listed in order of decreasing influence on the mechanical property. For this case, preheat Condition 1 is more desirable than Condition 2 and Condition 3 is the least desirable.

(b) Parentheses about BC indicate that preheat conditions B and C are of equal significance and are both more desirable than condition A.

(c) Values could not be determined since yield strength values are lacking for the two specimens of condition V-E2V.

parameters. For example, a significant interaction between preheat and energy input would indicate that the specific effects of energy input would be dependent on the particular level of preheat used. For those welding parameters found to be significant, the level found to give the highest values for each mechanical property was written first (by the use of the symbol notation of Table 11) with the other two levels written in the order of decreasing magnitude. Parentheses about two of the parameters indicate that neither was significantly better nor poorer than the other. Thus in considering the effect of preheat on tensile strength it was found that preheat C gave significantly higher tensile strength than either A or B and that the A and B preheats (in parentheses) were not significantly different.

A correlation coefficient indicates the degree of agreement between replicate mechnical specimens; two tensile specimens from a single weldment and two bend specimens from another weldment were tested for each welding condition. The higher the correlation coefficient number, the greater the agreement between replicate results. The tensile and yield strength correlation coefficients are acceptable; the elongation coefficients were much smaller. This is not surprising since it is conceded that elongation values for transverse-weld tensile specimens are not very meaningful values. This is illustrated by the spread in results given for the 1/2-inch, 1-inch, and 2-inch gage lengths in Tables 14 and 16. The bend elongation also showed poor correlation; however, it was realized that this test was performed primarily for qualitative rather than for quantitative results.

As was expected, interactions between the parameters are significant. The interaction between preheat and energy input is particularly strong. It should be noted that this significance can only be discerned through the use of a statistical analysis of variance experiment.

An inspection of Table 19 indicates that, considering strength alone, conditions C1X or C1Z would provide the highest strength. Considering ductility alone, conditions B3Z, B3Y, A3Z, or A3Y would be best.

Since the 200 F preheat (condition H) was used with only one energy input instead of three, it could not be evaluated by the computer.

Welding Parameters for the Other Steels

The remaining five steels listed in Table 1 were investigated by using the two or three most promising welding conditions determined from the investigation of steel No. 3, conditions C4X, A2Z, and H1X.

Effects of Energy Input, Preheat, and Postheat

The findings of both the statistical study and direct observation of mechanical data indicated that condition ClX produced the best strength, although the ductility was only average. The strength levels for the Cl conditions were higher than those of the other conditions, so that condition ClX warranted further investigation with the other steels. The postheat condition 1 was modified, however, to provide a longer isothermal holding time at 1350 F to insure total transformation from austenite, and to prevent the formation of untempered martensite. This modified postheat condition was subsequently referred to as postheat condition 4, i.e., C4X.

The AZ (AlZ, A2Z, A3Z) and the HY conditions produced the most favorable combination of both strength and ductility, as was stated in the presentation of tensile test results. The statistical results indicated that condition A3Z had superior ductility; however, the occurrence of carbide precipitation associated with postheat 3, even though it was observed to vanish upon hardening and tempering, precluded its inclusion as a good condition. The favorable as-welded microstructure associated with postheat 2 and the occurrence of untempered martensite associated with the Al conditions prompted the selection of condition A2Z.

Condition H1Y (weldment No. 60) had the best combination of properties among the HY group, discounting the results of tensile specimen No. 60-2 which failed because of an inadvertent notch in the base metal. Since the Y (highest) energy input was found to result in poorer mechanical properties, it was considered preferable to use the condition H1X for the other steels. The Z input condition was too low to make an effective weld in combination with the low 200 F (H) preheat.

Although welding conditions were not found to be significant for plate, the presence of porosity raised a question of the reliability of the results even though the correlation coefficient for tensile strength was quite good.

For plate welds, two promising weld conditions were selected for use with the other five steels. The results of the restraint tests indicated that a high preheat would reduce the tendency toward cracking of restrained plate; hence, only preheats above the Ms temperature were considered for plate. It was expected that condition B1W would produce martensite upon cooling from 800 F to 150 F which would be subsequently tempered by postheat 1; the welding procedure was also relatively simple. Condition F2W, although a more complicated welding procedure, subjected the weld to a 1700 F homogenization treatment before following the same treatment used for condition G1W. In neither case was austenite

slow-cooled or held isothermally, thus preventing the precipitation of carbides. The lower energy input condition W gave better yield strength values than energy input V for steel No. 3; this was consistent with the observation that lower energy input values were more favorable.

Metallographic Studies

The weld-zone microstructures of the five other sheet steels welded by condition A2 were compared prior to hardening and tempering. The microstructures for H-11 steel No. 3, H-12 steel No. 4, and steel No. 1 were nearly identical. The weld metal adjacent to the heat-affected zone (HAZ) and the interior weld metal of H-11 steel No. 2 shown in Figures 19a and 19b, respectively, are representative of these three materials. The elongated dendritic structure shown in Figure 19a was not as pronounced in the weld metals of the other two steels.

The heat-affected zone and weld metal microstructures of H-13 steel No. 6, shown in Figures 20a and 20b respectively, were more acicular. Comparable microstructures for H-13 steel No. 5, shown in Figures 21a and 21b, reveal the presence of a white phase, probably of untempered martensite in the darker regions of carbon concentration in the heat-affected zone. This phase is not present in the unaffected base metal microstructure of steel No. 5 shown in Figure 22a. The white phase is seen even more distinctly in Figure 22b in the 1/2-inch plate weldment of the same steel welded by welding condition G1W.

The microstructures obtained by welding condition C4X were different from welding condition A2Z. This is shown by comparing the heat-affected zone and weld metal microstructures of welding condition A-C4X, in Figures 23a and 23b for H-11 steel No. 2, with welding condition A-A2Z of Figure 19. The long isothermal hold at 1350 F for six hours resulted in regions of high carbon concentration and intergranular carbide precipitates in the weld metal. Nevertheless, the long isothermal hold permitted complete transformation of the austenite, thereby eliminating the untempered martensite regions (shown in Figure 14a) produced by the shorter-time isothermal hold of postheat 1.

The microstructures of 1/2-inch plate of the other five steels as welded with conditions G1W and F2W were fairly homogeneous with no evidence of carbide precipitates, untempered martensite, or other irregularity. The one exception, welding condition J-G1W, was previously discussed and shown in Figure 22b.

Tensile Tests

Sheet - Results of transverse-weld tensile tests of five sheet

65
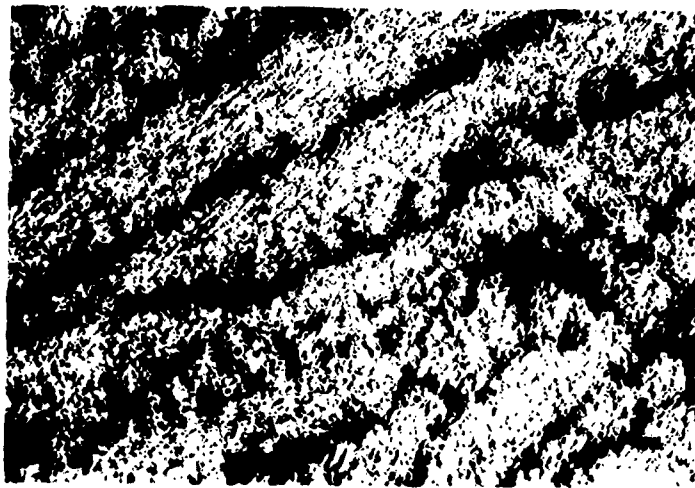
600X Etchant: 5% Nital R3168

a) Weld-Metal Microstructure Adjacent to the Heat-Affected Zone
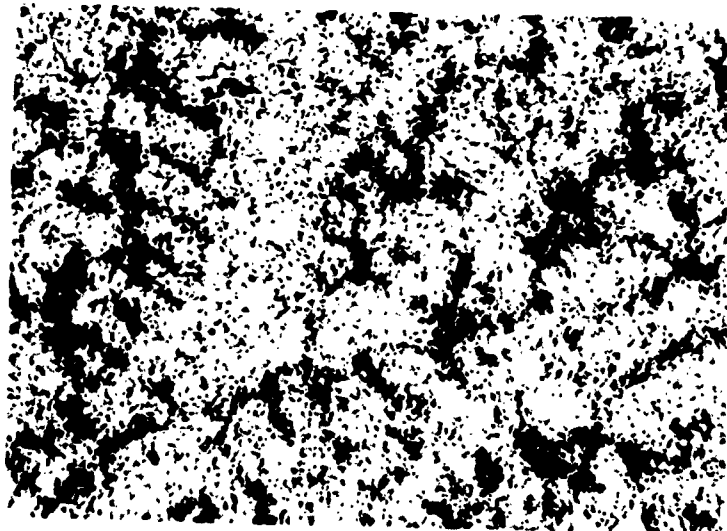
600X Etchant: 5% Nital R3169

b) Weld-Metal Microstructure

FIGURE 19. MICROSTRUCTURES OF WELDMENT CONDITION A-A2Z
(Weldment No. 91, Steel No. 2)
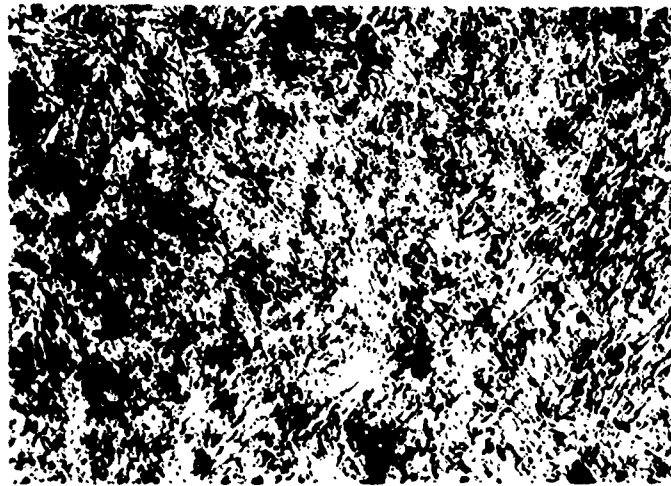
600X   Etchant: 5% Nital   R3165

a) Heat-Affected Zone Structure
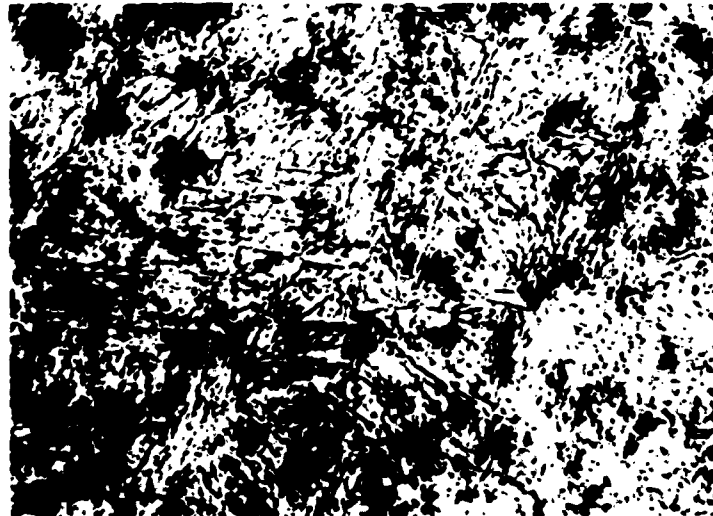
600X   Etchant: 5% Nital   R3166

b) Weld-Metal Structure

FIGURE 20. MICROSTRUCTURES OF WELDMENT CONDITION
M-A2Z (Weldment No. 93, Steel No. 6)
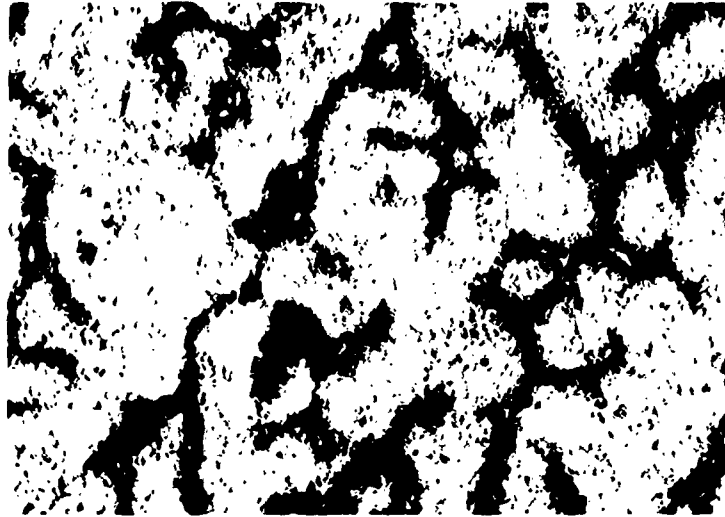
a) Heat-Affected Zone Structure
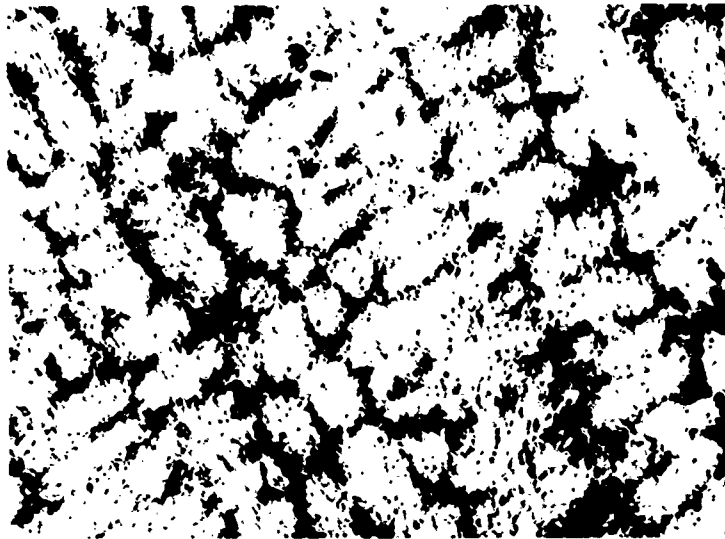
b) Weld-Metal Structure

FIGURE 21.   MICROSTRUCTURES OF WELDMENT CONDITION
             J-A2Z   (Weldment No. 94, Steel No. 5)
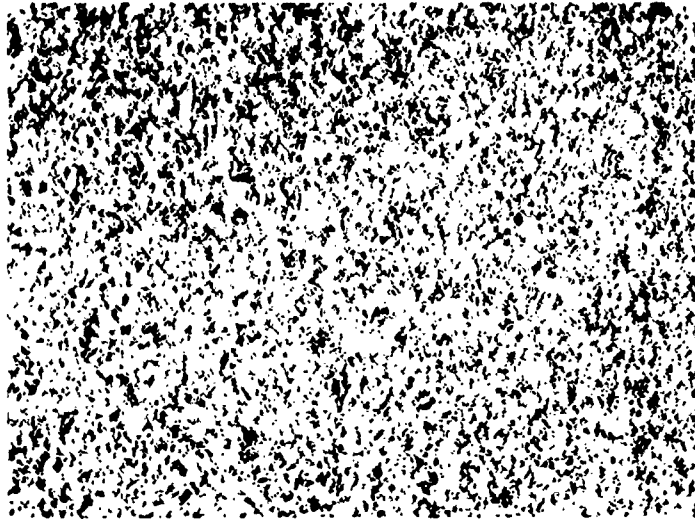
600X   Etchant: 5% Nital   R3161
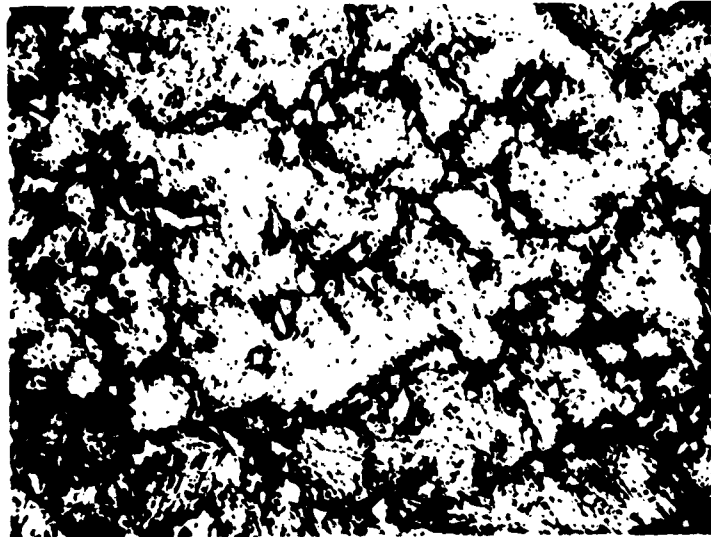
600X   Etchant: 5% Nital   R3192

b)   HAZ Microstructure of Weldment No. 10
Weld Condition GlW

FIGURE 22.   MICROSTRUCTURES OF WELDMENT IN H-13 STEEL NO. 5

600X   Etchant: 5% Nital   R3179
a) Heat-Affected Zone Structure
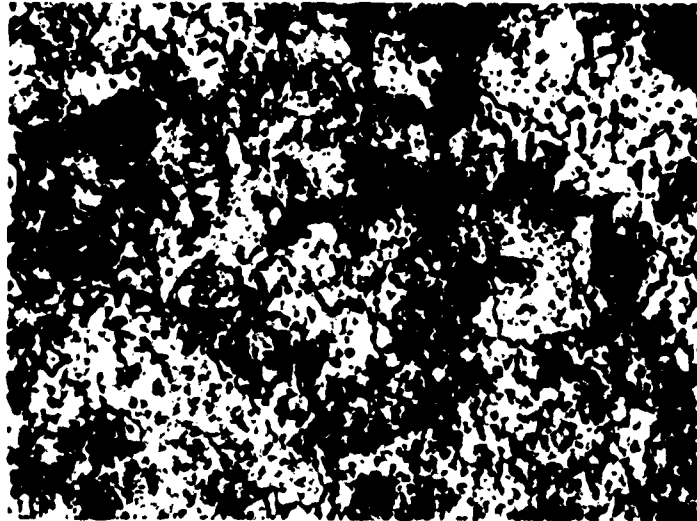
600X   Etchant: 5% Nital   R3181
b) Weld-Metal Structure

FIGURE 23.   MICROSTRUCTURES OF WELDMENT CONDITION
A-C4X (Weldment No. 103, Steel No. 2)

70

steels are presented in Table 20. The H-11 steel No. 2 and steel No. 1 are the strongest while H-13 steel No. 6 is the weakest. The H-13 steel No. 6, H-12 steel No. 4, and H-11 steel No. 2 have the better elongation properties than the other two steels. All steels were hardened and tempered by an identical treatment: austenizing at 1850 F and double tempering at 1050 F for 2 + 2 hours. Nothing was discovered in the literature to indicate that a different heat treatment would be preferable for any of the steels; however, the data for some steels were so meager that it should not be assumed that the optimum heat-treatment (with respect to maximum ductility at not too great a sacrifice in strength) was used. For example, the fact that H-13 steel No. 6 has the minimum strength and maximum ductility indicates that the steel was tempered at a higher relative value compared with the other steels. Perhaps steel No. 1, having a maximum strength and minimum ductility, should have been tempered at a higher temperature. Nevertheless, it can be seen that H-11 steel No.2 would probably retain the best combination of strength and ductility over a range of practical tempering temperatures. It should be remembered that the direct comparison of the properties of the steels given above compares the steels only at one heat treatment.

Sheet weldments were also welded by the TIG-manual welding process using welding condition A2X for comparison with the TIG automatic process. (It was necessary to increase the energy input for the manual process to condition X for the first pass and Y for the second pass). The tensile test results for these weldments are also presented in Table 20. Results are nearly identical to those obtained by the automatic TIG welding process for specimens of comparable hardness.

The average yield strength for sheet weldments in H-11 steel No. 2 welded by the TIG-automatic process was 211,500 psi while the average yield strength for the same steel welded by the TIG-manual process was 219,500 psi. Average tensile strength for the TIG-automatic process was 249,500 psi and for the TIG-manual process it was 252,500 psi. Average elongations in two inches were 4.25 percent for the automatic and 3.8 percent for the manual TIG process. The lack of adequate quantities of specimens for statistical reliability makes the comparison of subtle differences difficult.

Tensile properties for unwelded sheet base metal are given in Table 21. Again, it is apparent that the optimum tempering temperature was not achieved for all the steels. Steel No. 2, 4, and 6 have nearly identical elongation; however, the elongations for steel No. 1 and 5 are about the same as that of steel No. 3.

The average values for unwelded and welded specimens are compared in Table 22. It is evident that the weld properties were not as good as those of the base metal. This was particularly

TABLE 20. TRANSVERSE-WELD TENSILE DATA FOR SHEET SPECIMENS

Weldment No. & Condition	Steel No.	Specimen No.	Yield Strength, psi	Tensile Strength, psi	% Elongation 1/2"	1"	2"	Base Metal Hardness, Rc Avg.	Range	Location of Fracture	Extent of Shear Fracture
				Automatic TIG Weldments							
92, P-A2Z(b)	1	1	219,000	266,000	10.0	4.5	3.5	52.0	52.0-52.0	WM	I
		2	236,000	274,000	4.0	3.0	2.0	54.0	52.0-55.0	WM	I
86, P-H1X	1	1	233,000	272,000	8.0	4.0	2.5	53.0	50.5-54.0	WM	I
		2	228,000	279,000	8.0	5.5	3.0	54.5	54.0-55.0	WM	I
97, P-C4X	1	1	233,000	266,000	9.0	3.0	2.0	50.5	47.5-53.0	WM	I
		2	222,000	256,000	8.0	2.0	2.5	49.0	47.0-52.0	WM	I
Average			229,000	270,000	7.8		2.4				
91, A-A2Z	2	1	210,000	247,000	14.0	5.0	4.5	48.0	45.0-51.0	WM	III
		2	213,000	252,000	12.0	2.0	4.0	51.5	51.0-51.5	WM	III
85, A-H1X	2	1	228,000	271,000	13.0	7.0	3.0	49.0	47.0-52.0	HAZ	III
		2	240,000	275,000	12.0	5.0	4.0	53.5	52.5-54.0	WM	III
103, A-C4X	2	1	225,000	261,000	10.0	5.5	2.5	51.0	50.5-51.5	WM	II
		2	233,000	270,000	13.0	6.0	3.5	52.5	52.0-53.0	WM	II
Average			226,000	263,000	12.3		3.6				
95, C-A2ZX(d)	4	1	217,000	250,000	2.0	2.0	5.0	50.5	49.5-51.5	BM	III
		2	211,000	241,000	3.0	3.0	5.0	49.5	48.0-51.0	BM	III
89, C-H1X	4	1	227,000	259,000	13.0	4.0	2.5	52.0	49.5-54.0	HAZ	III
		2	215,000	256,000	12.0	3.0	3.0	53.0	52.0-53.5	WM	II
96, C-C4X	4	1	230,000	237,000	12.0	5.0	3.5	52.0	51.0-53.5	WM	II
		2	200,000	263,000	10.0	3.0	3.0	50.5	50.0-51.0	WM	I
Average			217,000	251,000	11.8(c)		3.7				

TABLE 20. TRANSVERSE-WELD TENSILE DATA FOR SHEET SPECIMENS

(Continued)

Weldment No. & Condition	Steel No.	Specimen No.	Yield Strength, psi	Tensile Strength, psi	% Elongation 1/2"	1"	2"	Base Metal Hardness, Rc Avg.	Range	Location of Fracture	Extent of Shear Fracture(f)
94,J-A2Z	5	1	228,000	252,000	8.0		2.0	52.0	51.5-52.0	WM	I
		2	226,000	257,000	6.0	2.0	1.8	52.0	51.5-53.0	WM	I
88,J-H1X	5	1	242,000	249,000	8.0	2.5	2.0	51.5	50.0-53.0	WM	I
		2	223,000	270,000	8.0	3.0	1.5	51.0	49.0-54.0	WM	I
98,J-C4X	5	1	241,000	236,000	10.0	4.0	2.0	54.0	54.0-54.5	WM	I
		2	219,000	265,000	4.0	1.0	1.0	52.0	51.5-52.5	HAZ	I
Average			230,000	255,000	7.3		1.7				
93,M-A2ZX(d)	6	1	212,000	248,000	14.0	9.0	5.0	47.0	46.0-48.0	WM	III
		2	208,000	247,000	15.0	11.0	5.0	46.5	4o.0-47.0	WM	III
87,M-H1X	6	1	203,000	238,000	2.0	2.0	5.0	50.0	50.0-50.0	BM	II
		2	208,000	247,000	2.0	2.0	5.0	50.0	48.5-52.0	BM	III
104,M-C4X	6	1	197,000	229,000	0.0	0.0	3.5	49.5	49.0-50.0	BM	I
		2	195,000	235,000	8.0	5.0	3.5	49.0	48.5-49.0	WM	I
Average			204,000	241,000	12.3(c)		4.5				
Manual TIG Weldments											
105C,A2X&Z(e)	2	1	219,000	249,000	4.0	2.0	2.0	51.0	50.5-51.0	WM	II
		2	218,000	253,000	13.0	7.5	5.5	50.0	49.5-50.5	WM	III
105C,A2X&Z(e)	2	1	222,000	257,000	12.0	9.0	4.0	51.5	51.0-52.0	WM	III
		2	219,000	251,000	10.0	6.0	3.0	52.0	52.0-52.0	WM	III
Average			219,500	252,500	9.7		3.8				

(a) All specimens were austenitized at 1850 F and double tempered at 1050 F for 2 plus 2 hours.
(b) The symbol notation is defined in Table 11.
(c) The 1/2-inch elongation values for base metal fractures were not included in computing the averages.
(d) Energy condition 2X is between energy Z and X in value.
(e) Energy condition X was used for the first pass and Z for the second pass.
(f) Percent shear was classified in quadrants: quadrant I was 0-25 percent shear, II was 25-50 percent shear, III was 50-75 percent shear.

73

TABLE 21. UNWELDED BASE-METAL TENSILE DATA FOR SHEET SPECIMENS(a)

Specimen No.	Steel No.	Yield Strength, psi	Tensile Strength, psi	% Elongation in 2 in.	Hardness, Rc Avg.	Hardness, Rc Range	Extent of Shear Fracture(c)
P-1	1	250,000	291,000	5.0	50.0	48.5-52.0	II
P-2	1	246,000	290,000	5.5	53.5	53.0-54.0	II
Average		248,000	290,500	5.2	52.0		
A-1	2	231,000	281,000	6.0	53.5	52.0-54.0	II
A-2	2	228,000	281,000	(b)	53.0	52.0-54.0	III
A-3	2	233,000	283,000	5.5	53.0	51.5-54.0	II
A-4	2	224,000	272,000	6.0	52.0	52.0-52.5	II
Average		229,000	279,500	5.8	53.0		
C-1	4	231,000	277,000	6.0	53.5	53.0-54.0	III
C-2	4	222,000	273,000	5.5	54.0	53.5-55.0	III
Average		226,000	275,000	5.8	54.0		
J-1	5	267,000	289,000	(b)	54.5	54.0-55.0	II
J-2	5	263,000	292,000	5.0	54.5	54.5-55.0	II
Average		255,000	290,500	5.0	54.5		
H-1	6	221,000	264,000	6.0	52.0	52.0-52.5	II
H-2	6	213,000	261,000	(b)	51.0	50.5-51.5	II
Average		217,000	262,500	6.0	51.5		

(a) Austenitized at 1850 F and double tempered at 1050 F for 2 plus 2 hours.
(b) Broke outside gage length.
(c) Percent shear was classified in quadrants: quadrant II was 25-50 percent shear, III was 50-75 percent shear.

74

TABLE 22. COMPARISON OF WELDED SHEET AND UNWELDED DATA FOR
THE OTHER SHEET STEELS (Welded by the TIG Auto-
matic Process)

	Steel No.	Yield Strength, psi	Tensile Strength, psi	% Elongation in 2 in.
Unwelded Average	1	248,000	290,000	5.2
Welded Average	1	229,000	270,000	2.4
Difference		-7.7%	-6.9%	-53%
Unwelded Average	2	229,000	279,500	5.8
Welded Average	2	226,000	263,000	3.6
Difference		-1.3%	-5.85%	-38%
Unwelded Average	4	226,000	275,000	5.8
Welded Average	4	217,000	251,000	3.7
Difference		-4.0%	-8.7%	-36%
Unwelded Average	5	255,000	290,000	5.0
Welded Average	5	231,000	250,000	1.7
Difference		-10.6%	-13.8%	-66%
Unwelded Average	6	217,000	262,000	6.0
Welded Average	6	204,000	241,000	4.5
Difference		-6.0%	-8.0%	-25%

the case for H-13 steel No. 5. The welded H-11 steel No. 2 was in closest agreement with its base metal properties.

The effects of welding parameters on the tensile properties of the sheet steels after hardening and tempering are listed in Table 23.

TABLE 23. THE EFFECTS OF WELDING CONDITIONS ON AVERAGE TENSILE PROPERTIES

	Welding Condition		
Property	H1X	A2Z	C4X
Yield Strength, psi[a]	229,000	219,000	201,000
Tensile strength, psi[a]	266,000	255,000	254,000
Elongation in 2 in. [a]	3.15	3.75	2.70
Elongation in 1/2 in.[a]	10.40	10.25	9.34

(a) Data from specimens which failed in the base metal were not used in computing these average values.

It is evident that condition C4X results in inferior strength and ductility. Condition H1X (no preheat) produces the best combination of strength and ductility but condition A2Z is nearly as good. Furthermore, the 400 F preheat of condition A2Z is not so likely to result in weld-cracking in a configuration involving restraint as the no-preheat conditon H.

It may be seen that there is a 15 percent difference in yield strength between the C4X and H1X conditions; however, less fference was noted for the other mechanical properties. These results

(although based on a few tests) supplement the more extensive study of the steel No. 3 in which it was found that welding parameters did not have a very appreciable influence on the mechanical properties after the hardening and tempering heat treatments.

Plate - The results of transverse-weld tensile tests for plate are presented in Table 24. It is evident that weldments of H-11 steel No. 2 and H-13 steel No. 6 generally had the best strength and ductility.

The weldments of H-13 steel No. 6 welded with condition G1W were the only ones in which the weld was stronger than the base metal. Excellent elongation for this steel was obtained. Weldments of steel No. 4 and No. 5 lacked ductility; however, elongation values might have been increased by using higher tempering temperatures.

TABLE 24. TRANSVERSE WELD TENSILE DATA FOR PLATE SPECIMENS

Weldment No. and Condition	Steel No.	Specimen No.	Width	Yield Strength, psi	Tensile Strength, psi	% Elongation in 1/2"	1"	2"	Base Metal Hardness, Rc Avg.	Range	Location of Fraction	Source of Fracture Initiation
11,A-G1W	2	1	0.499	(a)	264,000	24.0	13.0	7.5	52.5	52.0-53.0	WM	(d)
		2	0.252	251,000	271,000	18.0	11.0	5.5	53.0	53.0-53.0	WM	---
20,A-F2W	2	1	0.500	234,000	270,000	4.0	3.0	1.0	53.5	53.0-54.0	WM	Slight Porosity
		2	0.503	(a)	280,000	20.0	12.0	6.0	54.0	53.0-54.0	WM	---
13,C-G1W	4	1	0.252	248,000	280,000	6.0	3.5	1.0	53.0	52.0-55.0	HAZ	Lack of Penetration
		2	0.251	(b)	227,000	3.0	2.0	0.5	52.0	52.0-53.0	WM	---
14,C-F2W	4	1	0.252	(b)	246,000	4.0	2.0	1.0	53.0	53.0-53.5	HAZ	(c)
		2	0.251	(b)	230,000	4.0	2.5	1.0	53.0	52.5-53.0	HAZ	(c)
10,J-G1W	5	1	0.498	(b)	241,000	4.0	1.0	1.0	53.0	53.0-53.5	WM	---
		2	0.504	(b)	249,000							
21,J-F2W	5	1	0.254	254,000	271,000	6.0	3.5	1.0	52.0	51.0-53.0	WM	---
		2	0.252	243,000	270,000	6.0	3.5	1.5	53.0	53.0-53.0	WM	---
12,M-G1W	6	1	0.501	(a)	264,000	13.0	11.5	10.0	52.5	52.0-52.5	BM	Central Crack
		2	0.503	(a)	270,000	5.0	7.0	9.5	52.0	50.5-52.5	BM	---
23,M-F2W	6	1	0.251	241,000	264,000	7.0	4.5	2.0	52.0	52.0-52.0	WM	Slight Porosity
		2	0.252	(a)	254,000	20.0	11.5	5.0	51.0	51.0-51.0	WM	---

(a) Yield strength was not recorded due to difficulties in gripping the specimen in tensile testing machine.
(b) Fracture occurred at or before the yield point.
(c) An interface separating region of different fracture characteristics was seen.
(d) No defect visible.

77

It was found necessary to reduce the width of most of the plate tensile specimens from 0.50 inch to 0.25 inch because of difficulties in gripping some of the specimens.

Steel No. 1 was not tested because radiography at one percent sensitivity detected porosity in all plate welds. Attempts to eliminate porosity in welding this particular steel were futile. Small clusters of porosity in the order of 1/32-inch diameter were observed in specimens 20-1 and 23-2. The porosity reduced elongation values in the former but not in the latter specimens. The problem of consistent porosity encountered previously was eliminated (except for steel No. 1) by more rigid control of arc-voltage and improving the wire cleaning procedures.

The ductility of specimen 13-2 was impaired by a lack of penetration resulting in non-fusion at the lands.

Inclusions lying in the plane of the plate and sheet were frequently found in the base metals of these steels. A large central inclusion, shown in Figure 24a, extending across one-half the width of the base metal in a direction perpendicular to the fracture face, caused the fracture of specimen 12-1 but only after a ten percent elongation had been achieved. The presence of inclusions perpendicular to the fracture face was also found in specimens 11-2, 13-1, and 21-1 but it was apparent from the fracture markings that they were not the cause of fracture initiation. Inclusions were also found in sheet base-metal as is shown in Figure 24b. The evidence of an inclusion is shown in the top picture of Figure 24b, which is a cross-sectional view of the fracture face through the inclusion. The inclusion opened up near the fracture face upon fracture but remains closed and identifiable to the right of the fracture face.

Transverse-Notch Longitudinal-Weld Tests

These tests were performed with 1.5-inch wide specimens; the two-inch wide specimens were found unsatisfactory with steel No. 3. Notch radii were between .004 and .006 inch, as measured on a shadow comparator. The results are presented in Table 25. Specimens of H-11 steel No. 2 and H-12 steel No. 4, both welded with condition A2Z, did not fail in the weld metal or heat-affected zone. Specimens of the H-13 steel No. 6 welded with conditions A2Z and H1X had a notch-strength equal to or greater than the average base-metal tensile strength for the steel given in Table 21.

The percent shear observed on the fracture face does not correlate well with the notch-strength to base-metal strength ratio.

The H-13 steel No. 6 and H-11 steel No. 2 have superior notch strength to H-13 steel No. 5; all three steels had about the

78
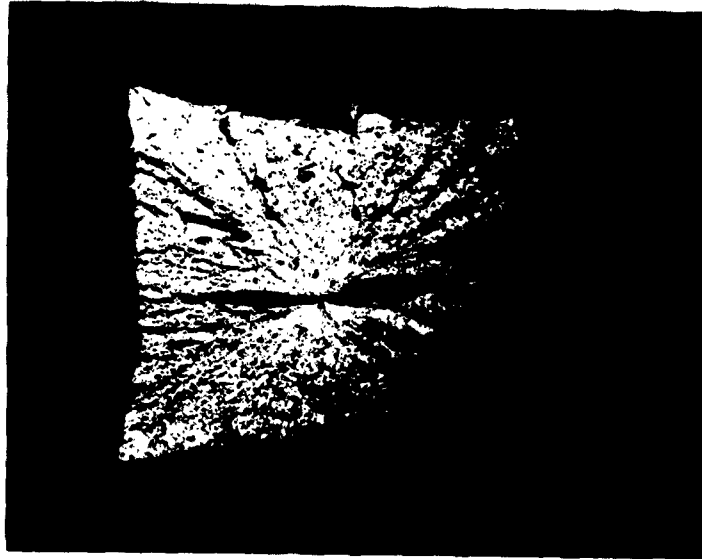
300X   Etchant: None   R3197
a)   Plate Tensile Specimen 12-1

Fracture Face, Bottom; Cross Section into Fracture Face, Top
20X   Etchant: None   R3212
b)   Sheet Tensile Specimen

FIGURE 24.   INCLUSIONS IN BASE METAL OF HOT-WORK TOOL
STEEL PLATE AND SHEET

79

TABLE 25. TRANSVERSE-NOTCH LONGITUDINAL-WELD TENSILE DATA FOR SHEET WELDMENTS

Specimen No. & Condition	Steel No.	Thickness of Metal Beneath Notch	Notch Radius, in.	Nominal Notch-Fracture Stress, psi	Source of Fracture Initiation	Notch Strength to Base Metal Strength Ratio(b)	Average Hardness, Rc	Percent(a) Shear
92,P-A2Z	1	.0474	.005	243,000	WM	.84		II
86,P-H1X	1	.0444	.005	270,000	WM	.93	55.0	III
97,P-C4X	1	.0465	.005	271,000	WM & HAZ	.93		II
Average				261,000		.90		
91,A-A2Z	2	.0447	.004	273,000	BM	.98	52.5	V
85,A-H1X	2	.0460	.005	263,000	HAZ	.95		IV
103,A-C4X	2	.0470	.004	264,000	WM & HAZ	.95	54.0	V
Average				267,000		.96		
95,C-A2Z	4	.0511	.004	248,000	BM	.90		III
89,C-H1X	4	.0470	.005	235,000	WM & HAZ	.85		IV
96,C-C4X	4	.0424	.005	236,000	WM	.86	52.0	IV
Average				240,000		.87		
94,J-A2Z	5	.0475	.005	206,000	HAZ	.71		II
88,J-H1X	5	.0633	.004	227,000	WM & HAZ	.78		I
98,J-C4X	5	.0449	.005	240,000	WM	.83	52.5	V
Average				224,000		.77		
94,M-A2Z	6	.0418	.005	284,000	WM	1.09	52.5	III
87,M-H1X	6	.0451	.006	262,000	WM	1.00	51.0	II
104,M-C4X	6	.0461	.004	257,000	WM & HAZ	.98	49.5	II
Average				268,000		1.02		

(a) Roman numerals indicate the following extent of shear fracture:

    I - 0-10%
   II - 10-20%
  III - 20-30%
   IV - 30-40%
    V - 40-50%

(b) The ratio of the nominal notch-fracture stress to the average base-metal tensile strength of that steel given in Table 21.

80

same elongation (about 5.8%). Steel No. 1 has superior notch strength to H-13 steel No. 5 even though their elongations were about the same (5%).

Welding conditions had no effect on the strengths of these specimens. The average strength for conditions A2Z, H1X, and C4X was 251, 252, and 253 ksi, respectively.

Bend Tests

Sheet - Longitudinal-weld bend test data are given for sheet specimens in Table 26.

The load on the specimen at fracture was recorded. The corresponding bending stress in the plastic range could not be easily determined; however, if it can be assumed that the extent of necking and geometry remain the same for all specimens, the fracture load values should provide an indication of the comparative fracture-strength of these specimens.

A crude parameter, the product of the elongation and the fracture load, was devised to indicate in a comparative manner the energy absorbed at fracture. The units of this parameter pounds per inch, are meaningless; nevertheless, since specimen size and conditions of testing were constant, the parameter should provide a valid indication of the relative energy-absorption of the test specimens.

The values of elongation, fracture-load, and energy for specimens welded by the automatic TIG process were compared for three welding conditions. Similarly, the respective values of the same properties for each steel provided an average value for each steel. These average values are presented in Table 27. In view of the appreciable scatter of data between replicate specimens encountered in seven of the fifteen pairs of specimens, it is evident that various welding conditions had no significant effect on bend elongation. However, fracture-load and energy appeared to be significantly influenced, with condition C4X providing the strongest and toughest weldments and A2Z providing the weakest and least tough. This observation is contrary to that of the tensile data. A comparison is also presented in Table 27 between the bend data of sheet specimens of H-11 steel No. 2 welded by the TIG manual process with welding condition A2X and TIG automatic process with condition A2Z. It appears that the manual welding process produces stronger and more ductile weldments in bending for the few number of tests made.

The average bend-elongation values for each steel indicate that H-11 steel No. 2 has the best elongation, fracture load, and energy ratios while H-13 steel No. 5 has the poorest values for

TABLE 26. LONGITUDINAL-WELD BEND DATA FOR SHEET SPECIMENS

Weldment No. and Condition	Steel No.	Specimen No.	Minimum Bend-Radius to Thickness Ratio	Bend Elongation, %	Base Metal Hardness, Rc		Fracture Load, lb	Energy Parameter, lb	Region of Fracture Initiation	Plastic Deformation Pattern(a)
					Avg.	Range				
Automatic TIG Welding										
92,P-A2Z	1	1	3.8	11.5	53.5	53.0-54.0	3920	451	WM & HAZ	A
		2	4.1	10.8	53.5	53.0-54.0	3360	363	BM	A
86,P-H1X	1	1	4.6	9.8	53.5	53.0-54.0	3200	214	HAZ	A
		2	16.4	3.0	54.0	54.0-54.0	960	29	WM	A
97,P-C4X	1	1	3.7	12.2	55.0	54.0-55.5	4080	498	WM	A
		2	5.2	8.8	51.5	51.0-52.0	3920	345	WM	A
Average				9.4			3240	316		
91,A-A2Z	2	1	4.1	10.8	53.0	52.5-53.0	3840	415	HAZ	A
		2	4.1	10.8	53.0	52.0-54.0	3920	423	WM	A
85,A-H1X	2	1	4.1	10.8	53.5	53.0-54.0	4160	450	BM	B
		2	2.1	19.5	52.5	51.0-53.0	3040	593	BM	B
103,A-C4X	2	1	1.9	20.5	52.0	52.0-52.5	4640	952	WM	A
		2	1.9	20.5	50.5	49.5-54.5	5400	1110	WM	A
Average				15.5			4170	657		
95,C-A2ZX	4	1	9.0	5.3	52.5	52.0-52.5	2480	131	WM & HAZ	A
		2	4.0	11.2	52.0	52.0-52.5	4160	466	BM	A
89,C-H1X	4	1	3.9	11.4	53.0	52.5-53.0	3600	411	WM & HAZ	B
		2	1.9	20.6	51.5	51.0-52.0	4480	925		B
96,C-C4X	4	1	4.0	11.2	50.5	50.0-51.0	2600	269	WM	B
		2	4.2	10.4	51.5	51.0-52.0	3920	408	WM	B
Average				11.7			3510	435		
94,J-A2Z	5	1	9.2	5.1	53.5	53.0-54.5	960	49	WM	A
		2	9.2	5.1	52.0	50.0-54.5	1440	73	WM	A
88,J-H1X	5	1	7.3	6.4	51.5	50.0-52.5	2080	133	WM & HAZ	A
		2	6.5	7.2	51.5	50.5-52.5	2320	167		A
98,J-C4X	5	1	9.3	5.1	50.5	50.5-51.0	960	49	WM	D
		2	16.5	2.9	53.0	52.5-53.0	1120	32	WM	D
Average				5.6			1480	82		

82

TABLE 26. LONGITUDINAL-WELD BEND DATA FOR SHEET SPECIMENS

(Continued)

Weldment No. and Condition	Steel No.	Specimen No.	Minimum Bend-Radius to Thickness Ratio	Bend Elongation, %	Base Metal Hardness, Rc Avg.	Base Metal Hardness, Rc Range	Fracture Load, lb	Energy Parameter, lb	Region of Fracture Initiation	Plastic Deformation Pattern(a)
Automatic TIG Welding										
93,M-A22X	6	1	3.1	14.0	51.0	50.0-52.0	2400	336	WM	D
		2	8.3	5.7	50.0	49.5-51.5	960	55	WM & HAZ	B
87,M-H1X	6	1	3.4	12.8	50.0	49.5-51.0	4800	615	WM	D
		2	2.8	15.3	50.5	50.0-51.0	4200	633	WM	D
104,M-C4X	6	1	6.0	7.7	49.5	48.5-50.0	7500	577	WM	-
		2	3.7	11.8	49.5	49.0-50.0	3800	448	WM	B
Average				11.2			3950	444		
Manual TIG Welding										
105B,A-A2X&Y	2	1	3.7	11.8	52.0	52.0-52.5	4500	531	WM	B
	2	2	3.1	14.0	51.5	50.5-52.5	4800	672	BM	B
105E,A-A2X&Y	2	1	2.7	15.7	51.5	51.5-52.0	4560	716	WM	B
	2	2	3.8	11.5	51.0	50.0-51.5	9000	575	WM	B
Average				13.2			4715	618		

(a) Each hardness value is an average of three readings.

83

the heat treatment used.

TABLE 27. AVERAGE VALUES FOR LONGITUDINAL-WELD
BEND TEST DATA FOR SHEET SPECIMENS

Welding Condition (Automatic)	Average Bend Elongation	Average Fracture Load, lb	Average Energy Parameter, lb
A2Z	9.0	2744	276
H1X	11.7	3284	417
C4X	11.1	3774	469
TIG Manual[a] [a]	13.2	4715	618
TIG Automatic[a]	10.6	3450	387
Steel No.			
1	9.4	3240	316
2	15.5	4170	657
4	11.7	3510	435
5	5.6	1480	82
6	11.2	3950	444

(a) H-11 steel No. 2 welded by condition A2Z for automatic process and A2X for manual process.

It is interesting to note that, contrary to tensile-test values in which elongation is increased only at the expense of strength, both values increased or decreased for the bend test.

The coarse and fine plastic flow patterns were still influenced by the post-heat treatment as was the case for steel No. 3. However, for those steels for which the tempering temperature of 1050 F produced a high strength and hardness (and less ductility) the coarse flow pattern often occurred in the base metal, pattern A, even when the specimen was hardened from the annealed condition (post heats 1 and 3).

Neither microstructural examination nor micro-hardness traverses of unstrained cross sections revealed any distinguishing characteristics between fine and coarse slip regions of the weldment. Observation of the tested bend specimens indicated that fracture initiated in the coarse slip rather than the fine slip regions.

It should be noted that the analysis of the bend test is inherently difficult and that reliable information cannot be obtained unless a sufficient number of specimens for statistical analysis are tested.

Plate - Transverse-weld bend-test data are given for plate speci-
mens in Table 28. All fractures occurred in the weld metal or
heat-affected zone. There is no significant difference in bend
elongation percent for the condition G1W as compared to the
condition F1W.

Average values cannot be computed for the fracture loads or
the energy parameter, because some of the specimens withstood the
maximum-capacity of the hydraulic jack and were not fractured.

The data indicate that welding condition F2W produced
stronger and tougher weldments for steels No. 4 and No. 5 which
had lower elongations than the other steels. This difference
is probably a result of the normalizing-type postheat 2, although
there are three points of Rockwell c hardness difference in the
base metal hardnesses between the specimens of steel No. 4 welded
by the two different conditions.

A study of the fracture faces indicated that porosity was the
source of fracture initiation in only two specimens. Porosity
was not observed in any other fracture faces. The porosity was
very small (about .012 inch in diameter) and evidently it did not
appreciably reduce elongation or fracture-load values.

The location of the fracture source provided an indication
of the influence of the fracture-initiating defect. The weakening
effects of a centrally located defect which caused fracture was
greater than that of a defect located at the edge where the
tensile stress was greater.

No defects were found at most of the sources of fracture
initiation; however, most of the fracture sources appeared to
have a coarse fracture pattern.

Plate Specimens Welded by TIG Process - Plate weldments were pre-
pared by the TIG welding process to provide a comparison with
those prepared with the MIG welding process. Lack of fusion
occurred in these welds; however, it was expected that the bend-
test results would not be greatly influenced by a lack of
penetration as long as it was at the centroidal axis (center) of
the bend specimen. Bend-test results for TIG plate weldments are
presented in Table 28. A comparison of the data available for the
same steel indicates that the MIG process produced better bend
properties than the TIG process for plate weldments.

Charpy Impact Tests

The results of the large (1/2-inch) radius Charpy impact
tests for 1/2-inch plate weldments are shown in Figure 25. The
energy-transition temperature range, based on a pronounced change in

85

TABLE 28. TRANSVERSE-WELD BEND-TEST DATA FOR PLATE SPECIMENS
(All fractures occurred in the weld metal)

Weldment No. and Condition	Steel No.	Specimen No.	Minimum Bend Radius Thickness Ratio	Bend Elongation, %	Fracture Load No.	Energy Parameter, lb	Base Metal Hardness, Rc Avg.	Range	Special Cause of Fracture	Location of Fracture Sources(e)
Automatic MIG Welding										
11,A-G1W	2	1	12.6	>3.8	>50,000(a)	>1900	54.5	54.0-55.0	---	---
		2	13.1	>3.7	>50,000(a)	>1850	55.0	55.0-55.0	---	---
13,C-G1W	4	1	∞	0.0	18,000	0	54.5	53.0-55.0	None(b)	Indeterminate
		2	38.0	1.3	28,000	364	55.0	53.5-55.5	None(b)	E 1/4
10,J-G1W	5	1	69.0	0.7	28,000	196	53.0	51.0-54.0	None(b)	E 1
		2	32.7	1.5	29,000	435	54.5	54.0-55.0	None(b)	I 7/8
12,M-G1W	6	1	15.4	3.2	44,000	1410	52.5	52.0-53.0	Porosity(d)	E 0
		2	12.3	>3.9	>50,000	>1920	53.5	53.0-54.0	---	---
20,A-F2W	2	1	10.2	>4.7	>50,000(a)	>2350	55.0	55.0-55.0	---	---
		2	33.0	1.5	26,000	390	52.5	50.0-54.0	None(b)	E 1
14,C-F2W	4	1	24.6	2.0	35,000	700	51.5	51.0-52.0	None(b)	C 7/8
		2	28.8	1.7	43,000	730	51.5	51.0-52.0	Porosity(d)	E 1/48
21,J-F2W	5	1	35.5	1.4	32,000	448	54.0	52.0-55.0	None(b)	E 7/8
		2	29.0	1.7	38,000	646	53.0	51.0-54.0	None(b)	E 1
23,M-F2W	6	1	15.3	3.1	42,000	1300	52.5	50.5-53.5	None(c)(b)	E 1
		2	32.0	1.5	38,000	570	52.5	52.0-53.0	None(b)	C 1/2
Automatic TIG Welding										
AP1	2	1	17.2	2.8	38,000	1060	52.5	52.0-53.0	Lack of penetration	Indeterminate
AP3	2	2	10.2	4.7	45,000	2120	54.0	54.0-54.0	Lack of penetration	C 1/8
AP3	2	3	15.6	3.1	26,000	744	53.5	53.0-54.0	None(b)	E 7/8

(a) Did not fracture, load reached was full capacity of hydraulic jack.
(b) Fracture face appeared to have a convex pattern at source of initiation.
(c) Specimen shattered into many pieces near middle of specimen.
(d) A single porosity defect of .001-inch diameter.
(e) Code for source location on fracture face. C, E, and I same as for Table 6. Distance from minor axis of 2" x ½" rectangular cross section is also given.
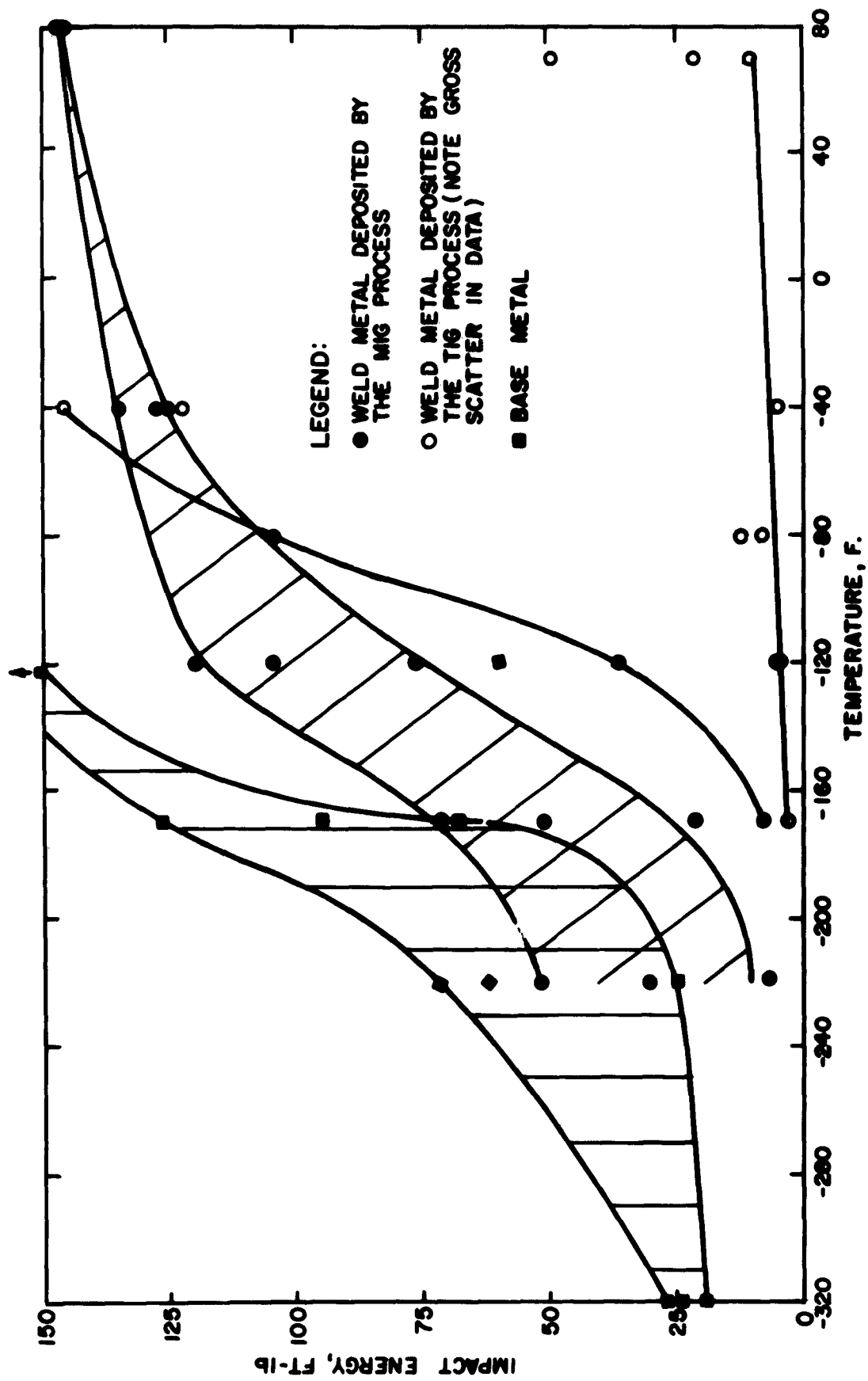
86

FIGURE 25   LARGE-RADIUS NOTCH CHARPY IMPACT DATA FOR STEEL NO.2

87

slope of curve at maximum and minimum energy levels for the weld metal of H-11 steel No. 2 welded by condition F2W, is about -90F to -190F, while that for the base metal of this steel is about -130F to -230 F.

There was considerable scatter in the results for weld metal deposited by the TIG welding process. This scatter of data may be attributed to an internal metallurgical notch effect at the fusion line. This notch, visible in Figure 26a, greatly lowered impact energy values. It was suspected that lack of penetration caused the defect; however, if lack of penetration existed, it would have extended across the entire width of the Charpy specimen. The curve of the maximum energy values obtained from flawless TIG welded specimens indicated that the energy-transition temperature was in the range of -40 to -160 F.

The results from the large-radius specimens showed differences in the performance of steel No. 3 that were not shown by the standard V-notch Charpy specimens. The influence of the sharp V-notch was so great for these tool steels that all the energy values for both weld metal and base metal fell within a narrow range of 5 to 20 ft-lb. The large-radius notch of the specimens used subsequently, however, did not provide a stress concentration but rather insured that fracture would occur across the most narrow region. Any notch-effect which occurred from metallurgical defects was not overshadowed by a sharp mechanical notch, hence the scattering of the data was meaningful.

The effects of test temperature on the bend angle of the impact specimens are shown in Figure 27. Less plastic deformation was encountered at lower temperatures.

Elevated-Temperature Tensile Tests

Transverse-weld tensile tests of welds in H-11 steel No. 2 were conducted at 400, 800, and 1000 F. The results are listed in Table 29. The elongation at fracture is not appreciably affected by test temperature. Both yield and ultimate tensile strength decreased with increasing test temperature.

Aging for 24 hours at test temperature prior to tensile testing showed an effect only at 1000 F. The aging at 1000 F resulted in a decrease in yield and ultimate tensile strengths with no appreciable change in elongation.

The high-temperature tensile strength of these weldments was reduced by 23 percent, and yield strength was reduced by 16 percent by heating to 1000 F for a short time. The 24-hour hold at 1000 F before testing resulted in a 36-percent decrease in tensile strength and a 31-percent decrease in yield strength. The difference between a short-time and 24-hour hold at 1000 F was a 17-

88
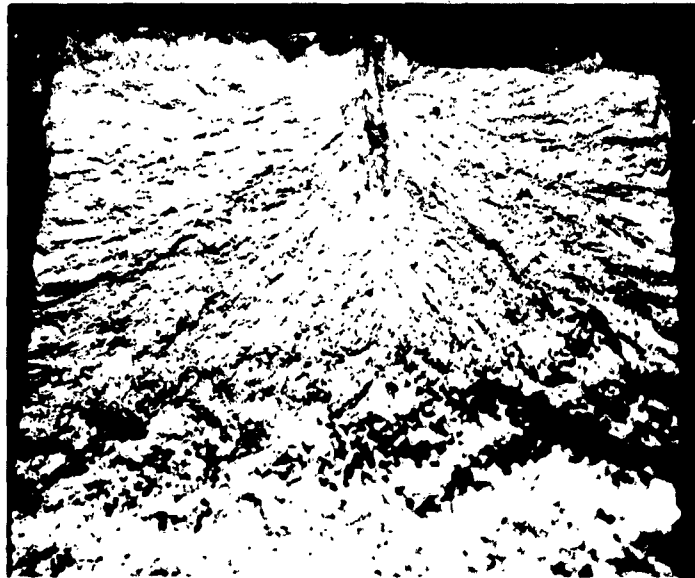
10X   Etchant: None   R3211

a) Region of Metallurgical Defect a Source of Initiation
    (-0 F Test Temperature, 10.4 ft-lb Fracture Energy)
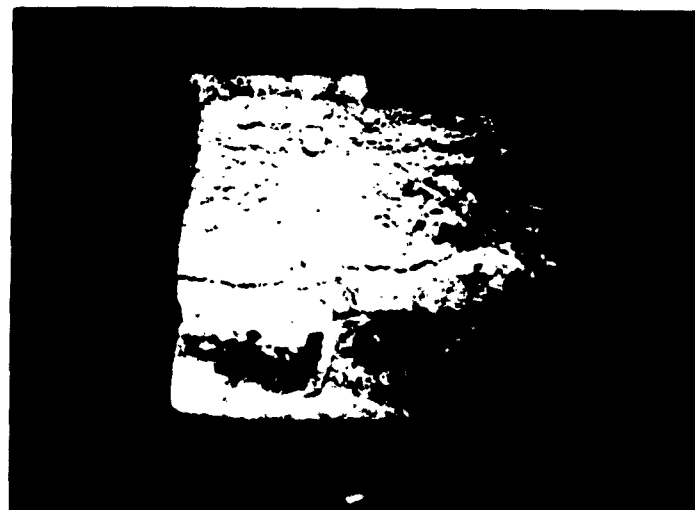
6X   Etchant: None   R3199

b) Porosity as Source of Initiation
(-120 F Test Temperature, 6 ft-lb Fracture Energy)

FIGURE 26. FRACTURE FACE IN THE WELD METAL OF LARGE-RADIUS CHARPY
            SPECIMENS SHOWING REGIONS AT WHICH FRACTURE INITIATED
            (Tensile region and large radius notch at top of
            specimen, compression region at bottom)

89
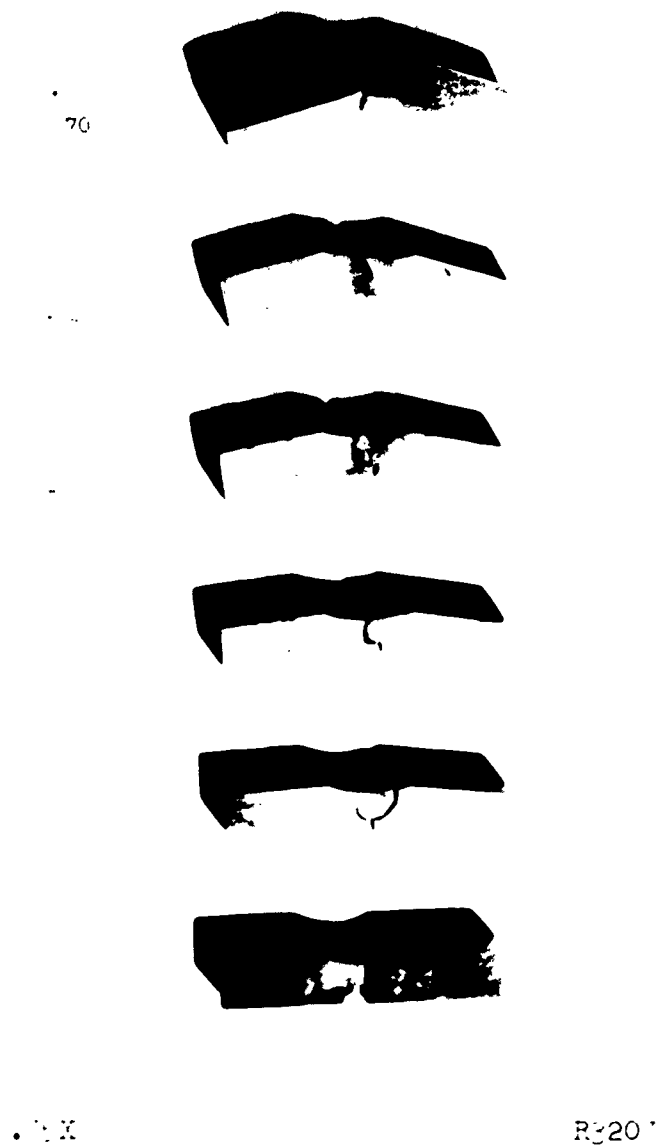
FIGURE 2. EFFECT OF TEST TEMPERATURE ON BEND-ANGLE OF LARGE-RADIUS CHARPY IMPACT SPECIMENS (Steel No. 2)

90

TABLE 29. TRANSVERSE-WELD TENSILE PROPERTIES AT ELEVATED TEMPERATURES FOR SHEET SPECIMENS OF STEEL NO. 2[a]

(Welded with Condition A2Z)

Specimen No.	Pretest Treatment	Test Temp. (°F)	Yield Strength, psi	Tensile Strength, psi	Elongation 1/2"	Elongation 1"	Elongation 2"	Base Metal Hardness Average, Rc Initial	Base Metal Hardness Average, Rc Average After Testing or Aging and Testing	Location of Fracture
1	A[b]	400	238,000	248,000	12.0	8.0	4.0	53.5	----	WM
2	A	400	230,000	248,000	16.0	9.5	6.0	52.5	53.0	HAZ
3	B	400	246,000	259,000	16.0	10.0	6.0	53.5	53.5	WM
4	A	800	204,000	220,000	19.0	12.0	6.5	53.0	53.0	HAZ
5	A	800	205,000	212,000	13.0	7.0	3.0	52.0	52.0	WM
6	B	800	212,000	221,000	17.0	19.5	5.0	52.5	54.0	WM
7	B	800	205,000	215,000	16.0	9.5	5.0	51.0	51.5	WM
8	A	1000	188,000	192,000	----	13.0	7.0	52.5	51.5	BM
9	A	1000	193,000	195,000	20.0	11.0	5.5	52.5	52.5	WM
10	B	1000	157,000	164,000	18.0	10.0	5.5	52.0	49.5	WM
11	B	1000	155,000	158,000	18.0	10.0	5.5	52.5	49.0	WM

(a) All specimens tested were welded by condition A2Z.
(b) A, None; B, Aged 24 hours at the test temperature under no-load before testing.

percent decrease in tensile strength, an 18-percent decrease in yield strength, and a decrease in base metal hardness of three points Rockwell c hardness.

Although 1000 F is below the tempering temperature of 1050 F for this steel, long time exposure results in a strength reduction. All of the specimens fractured in the weld metal with the exception of one base metal and two heat-affected zone fractures.

Bulge Tests

Sheet-bulge specimens of steels No. 1, 2, and 6 were welded by the A2X welding condition, hardened, and double tempered. Two specimens were made for each steel; however, a repair weld required for one of the specimens of steel No. 1 could not be made without changing the weld parameters under investigation. It was therefore decided not to test this specimen, since a change in welding parameters would not permit a comparison of the results of all test specimens.

Results of the tests are given in Table 30. Specimens No. 1 and 2 of H-11 steel No. 2 withstood a maximum pressure of 6200 and 6000 psi, respectively, without fracturing. When it was found that only a dynamic pressure (from dropping the weight) of about 4500 psi could be achieved by the test device, an initial static pressure was applied prior to dropping the weight. Specimens 3 and 4 failed, however, during the application of the static pressure at 1800 and 1400 psi, respectively. Specimen 5 failed upon the application of 2000 psi static, plus 1300 psi dynamic pressure. The variation of dynamic pressure with time is shown for the sixth cycle of bulge specimen No. 2 in Figure 28. (The drawing was traced from the actual oscilloscope photograph). The initial increase in pressure from 1500 to 5500 psi occurred within 310 microseconds at a rate of 12.9 psi per microsecond. The initial surge was followed by a maximum peak (at 6000 psi) occurring within 1000 microseconds. The other pressure-time curves were similar.

Bulge-test specimens 3 and 4 are shown in Figures 29a and 29b, respectively. The fractures of specimens No. 3, 4, and 5 all initiated in the weld metal. In vessels No. 4 and 5 the crack traveled transverse to the weld direction; in specimen No. 3 the crack traveled along the weld for a short distance and then bifurcated (branched).

In those specimens that failed, the source was attributed to porosity in the weld deposit. This porosity was small enough to escape detection by two percent sensitivity radiographic standards. The fracture sources are shown for bulge specimens 3 and 5 in Figures 30a and 30b, respectively. Very small porosity defects

TABLE 30. BULGE TEST RESULTS

Specimen No.	Steel No.	No. Pressure Cycles	Pressure, psi Static (Initial)	Pressure, psi Dynamic (Subsequent)	Total	Failure	Cause	Strain in Center of (b) Specimen, in.	Principal Strains in/in	% Elongation in ½ inch, in/in	Approximate Maximum Stress, psi
1	2	1st	2000	3000	5000	No		-----(a)			<319,000(f)
		2nd	2000	3400	5400	No					
		3rd	2000	4200	6200	No					
2	2	1st		4000	4000	No		.0120 .0146 .0060(e) -----(a)	ϵ_1=.0157 ϵ_2=-.0013(e)		<388,000(f)
		2nd		4500	4500	No					
		3rd		4000	4000	No					
		4th		4500	4500	No					
		5th	1000	4700	5700	No					
		6th	1500	4500	6000	No					
3	1	1st	1800	0	1800	Yes	Weld Porosity	-----(c)			
4	6	1st	1400	0	1400	Yes	Weld Porosity	.0032(e) .0055 .0045	ϵ_1=.0057 ϵ_2=-.0021(e)	22.8(g)	157,400(g)
5	6	1st	2000	1300	3300	Yes	Weld Porosity	.0056(d) .0053 .0052	ϵ_1=.0053(d) ϵ_2=.0053	21.2	>234,000(d)

(a) Strain gage unbonded.
(b) Strain readings from each leg of the rosette.
(c) Failure occurred before strain was recorded.
(d) Strain and stress from 2000 psi static load only.
(e) Strain gage malfunctioned. ϵ_1, ϵ_2 at all points of a circular membrane (this is true at the center even when bending is present).
(f) This value was determined from maximum bulge-deflection after load was removed. Actual stress was less.
(g) From principal strain values, considering maximum principal strain value (.0057) as the theoretical equiaxial strain.
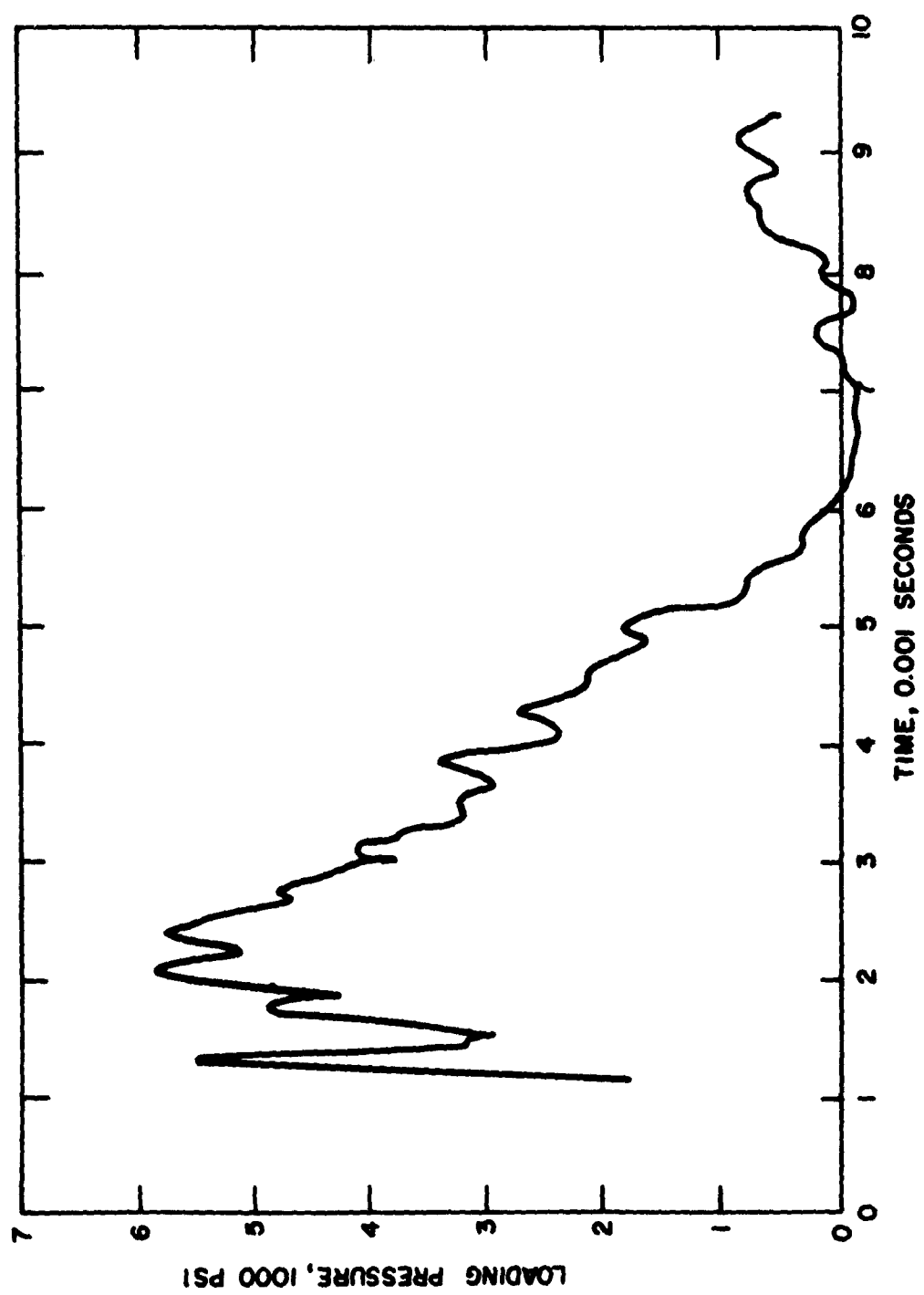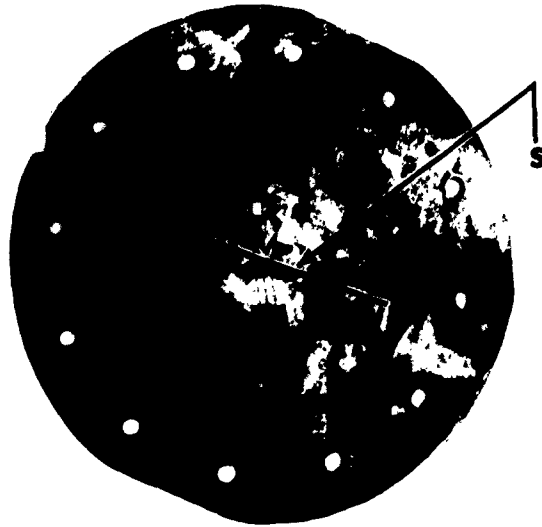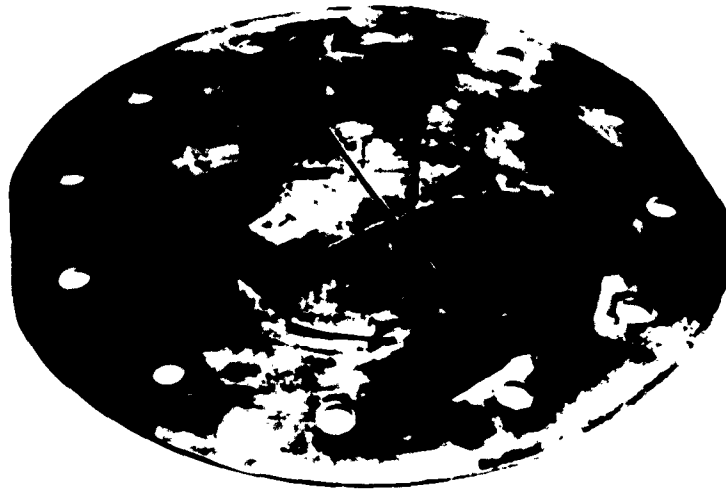
FIGURE 28 VARIATION OF DYNAMIC PRESSURE WITH TIME FOR BULGE SPECIMEN 2

94

.24X   R3177
a)   Specimen No. 3
Symbol "S" Indicates Source of Fracture Initiation
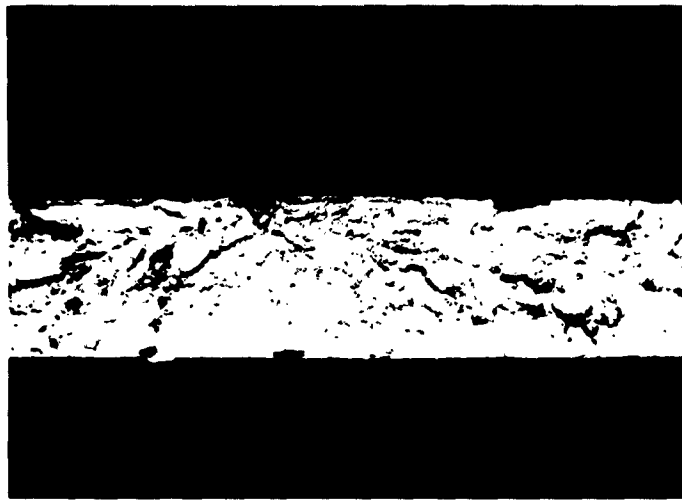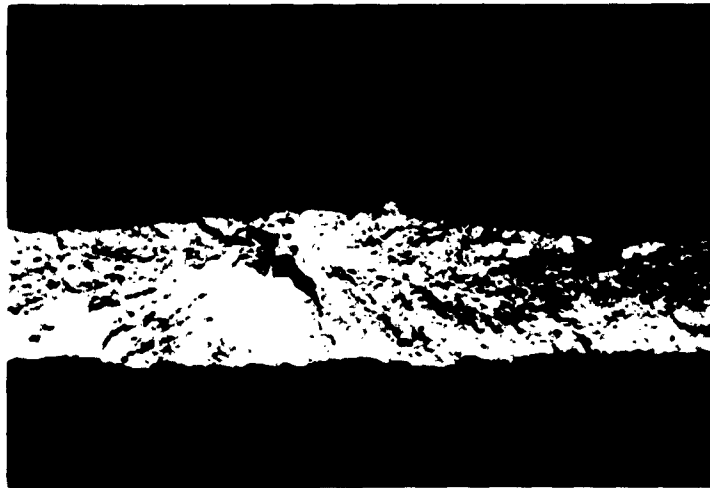

.35X   R3176
b)   Specimen No. 4
Source of Fracture Initiation is at Intersection of
Crack with Weld Center Line

FIGURE 29.   FRACTURED BULGE-TEST SPECIMENS

95

5.5X   Etchant: None   R3183
    a)   Bulge-Test Specimen 3

5.5X   Etchant: None   R3184
    b)   Bulge-Test Specimen 5

FIGURE 30.   FRACTURE FACES OF BULGE-TEST SPECIMENS SHOWING
             POROSITY AS SOURCE OF FRACTURE INITIATION

were seen at the source although the fracture markings mask the porosity to some extent in the photographs.

It is not known whether the superior performance of the specimens from steel No. 2 can be attributed to better ductility and strength properties or to the fact that the weld did not contain any porosity.

The maximum stress produced in specimen No. 1 and 2 was less than 319,000 and 388,000 psi, respectively. These stress values were calculated from the depth of bulge remaining in the specimen after the load was removed. The maximum deflection of the unfailed specimen under the loading pressure was greater than the measured deflection under no load, hence the actual stress was less than 319,000 psi and 388,000 psi. Nevertheless, the stress must have been of a high magnitude. Sample calculations are given in the Appendix. It should be noted that the weld-joints in these two specimens withstood considerable plastic deformation, yet did not fail. The other three bulge specimens fractured into several pieces, thus making it impossible to get an accurate measurement of bulge depth.

Strain at fracture was not recorded for some specimens because the strain gages separated from the specimen upon dynamic loading. Fracture stress can be computed from strain for specimens 4 and 5, for which strain was recorded. At the static failure pressure of 1400 psi, the maximum stress for specimen 4 was 157,400 psi. For specimen 5 the stress at the initial static load of 2000 psi was 234,000 psi. Sample calculations of the determinations of stress from membrane strain are given in the Appendix.

Pressure Vessel Tests

Results

The results of the dynamic and static pressure-vessel tests are given in Table 31. Pressure vessel No. 1 was tested repeatedly in an attempt to develop sufficient pressure in the drop-weight test to fracture the vessels. The structure supporting the vessel during dynamic testing was initially constructed of solid wooden blocks, which did not furnish sufficient support. When replaced with a welded steel structure the system was more rigid permitting a high enough pressure to fracture the vessel. Unfortunately, failure-pressure was not recorded for some of the tests because of a malfunctioning of the pressure-time recording oscilloscope.

Circumferential strains were measured on the weld and on the base metal 90 degrees from the weld. The strains would be expected to be the same since the yield strength of neither weld nor base

TABLE 31. PRESSURE-VESSEL TEST RESULTS

Pressure Vessel No.	Sheet Thickness and Average Hardness	No. of Cycles	Pressure, psi Static	Dynamic	Total	Failure	Measured Circumferential Strain, in./in Weld	Base Metal	% Elongation in 1/2 in. in/in	Circumferential Strain Rate, sec⁻¹ Weld	Base Metal	Time to Reach Peak Pressure, sec
1 Dynamically Loaded	.097 in. 52.0 Rc	1	0	3000	3000	No	.0024[c]	.0034		3.43	4.85	.0007
		2	2000	(a)	(a)	No	.0038	.0047		2.72	3.36	.0014
		3	2000	3250	5250	No	.0043	.0052		2.69	3.25	.0016
		4	2000	(a)	(a)	No	(b)	.0044		(b)	3.67	.0012
		5	2000	(a)	(a)	Yes	.0074	.0088	14.8	6.74	8.00	.0011
2 Dynamically Loaded	.095 in. 53.5 Rc	1	0	2700	2700	No	.0022	.0033		2.75	4.12	.0008
		2	2000	3500	5500	Yes	.0040	.0053	8.0	4.0	5.3	.0010
3 Statically Loaded	.092 in. 49.0 Rc	1	4800	0	4800	Yes	.0042	.0035	8.4	----	----	----
4 Statically Loaded	.095 in. 49.0 Rc	1	3300	0	3300	Yes	(e)	.0022	---	----	----	----

(a) Dynamic pressure load was not recorded due to malfunctioning of electronic apparatus.

(b) Strain gage became unbonded by impact.

(c) The difference in strain between weld and base-metal locations 90 degrees apart was due to an out-of-round condition in the vessel.

(d) Strain gage was cut by fracture of vessel.

(e) Strain gage did not function properly.

98

metal was reached and the elasticity of both is essentially the same. The welding of the vessel, however, produced an out-of-round region in the vessel. The internal pressure developed bending stresses about the weld as the vessel became round, which accounts for the discrepancy between the two strain values. The longitudinal weld of vessel No. 3 was initially flat; the bending moment increased the curvature and thereby the tensile strain. The other vessels initially had a peaked configuration at the weld joint which required bending moments to decrease the curvature to obtain roundness. This type of moment decreased the tensile strain below that in the round base-metal body.

The greatest strain-rate of eight inches per inch per second was achieved with vessel No. 1.

The fractured vessels are shown in Figure 31. The fractures of the dynamically loaded vessels No. 1 and 2 did not bifurcate as in the static tests. The main crack in both static vessels bifurcated symmetrically into two cracks 30 degrees to either side of the longitudinal direction (except in the heads of the the vessel). The crack initiated in the circumferential head-weld of vessel No. 1 and propagated in a straight line longitudinally through the base metal. The crack which originated in the weld metal of vessel No. 2 propagated in the weld toward the head for 2-1/2 inches and then moved laterally 1/8 inch into the heat-affected zone. A secondary source of fracture initiation located in Figure 31 caused this transition.

In the statically tested vessel No. 3 the crack initiated in the circumferential head-weld, propagated both along the circumferential weld and in a longitudinal direction through the base metal for about 1-1/2 inches, then moved laterally 1/4 inch to the weld to continue its propagation through the weld metal. The main crack initiated in the weld metal of pressure vessel No. 4 and bifurcated after it had traveled 2-1/2 inches from the source in both directions. Surprisingly, a large length of the fracture face to the right of the fracture initiation source of vessel No. 4 was about a 90 percent shear fracture.

Cracks propagated along the longitudinal welds of vessels No. 2, 3, and 4. In vessels No. 2 and 3, a special characteristic of the fracture was observed when the fracture propagated through regions in which the weld was repaired. The center of the fracture-face was flat and of a granular texture; no chevrons or other fracture markings were present. The chevrons emanated from this flat central region until they intersected the shear lip at the edges of the fracture face, probably the result of almost instantaneous fracture propagation through the repair-weld metal. This type of fracture was not observed in the longitudinal weld of vessel No. 4 in which no repair-welds were made in the
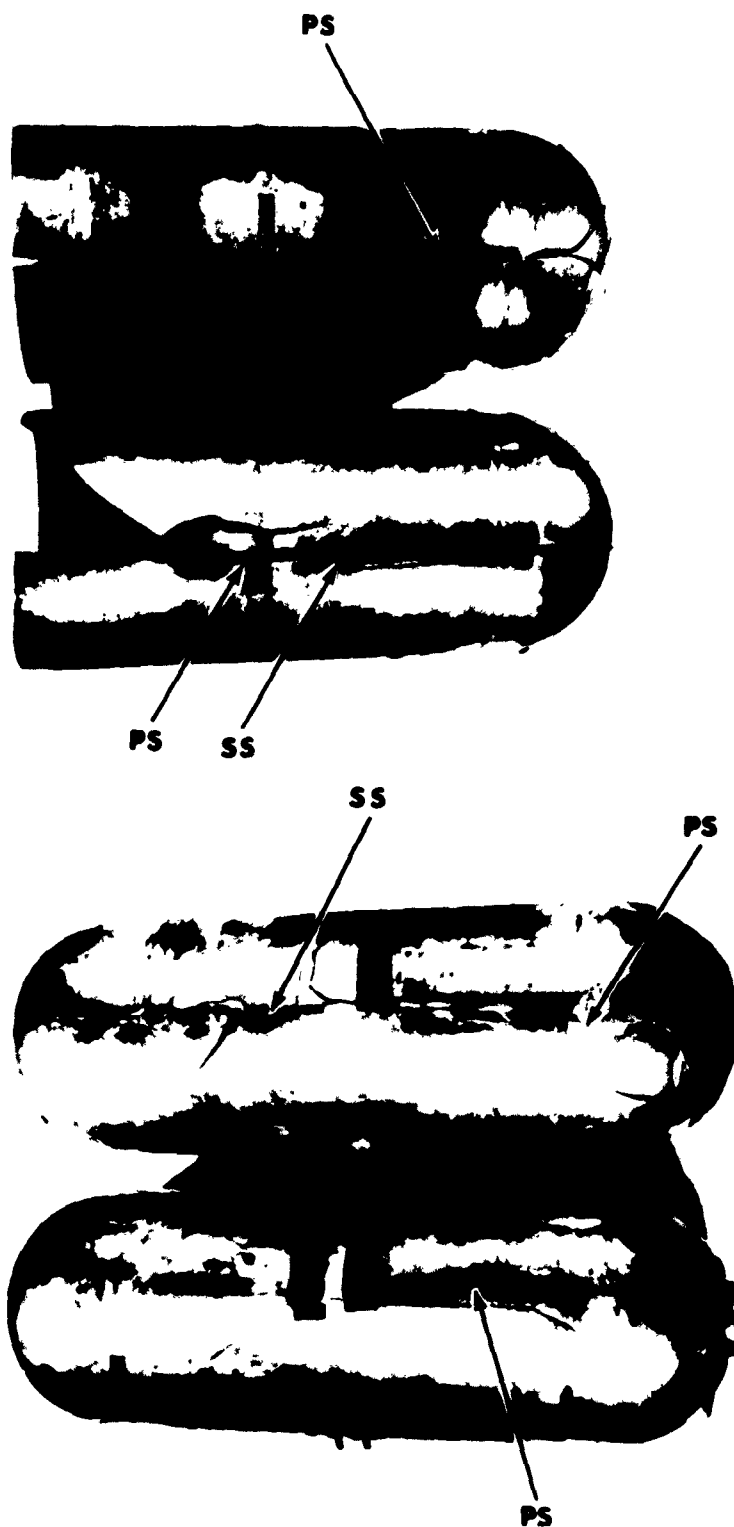
FIGURE 31. PRESSURE VESSELS FRACTURES BY DYNAMIC AND STATIC
TESTS (Vessels 1, 2, 3, and 4 shown in that order,
top to bottom)(PS and SS stand for primary and
secondary fracture sources, respectively)

longitudinal weld. The longitudinal weld of vessel No. 1 was repair-welded, although failure initiated in the girth-weld in which no repair-welds were made and propagated through the base metal about 90 degrees radially away from the longitudinal weld. The only vessel in which a failure initiated at the location of a weld-repair was vessel No. 2.

The values of the plastic properties n and K of the plastic strain-stress equation $\sigma = K\epsilon^n$ were measured from the stress-strain curves for unwelded base-metal specimens. These 0.090-inch thick specimens were hardened and tempered with the pressure vessels to provide an indication of the base-metal properties of the pressure vessel. These properties will include any effects from the very slight decarburization encountered. The tensile properties are for the longitudinal direction since the direction of the hoop stress in the pressure vessel is also in the direction of rolling. These values are given in Table 32.

TABLE 32. LONGITUDINAL TENSILE PROPERTIES FOR BASE-METAL SHEET SPECIMENS OF STEEL NO. 2 HARDENED AND TEMPERED WITH THE PRESSURE VESSELS

Specimen No. and Vessel No.	Yield Strength, psi	Tensile Strength, psi	% Elongation, in.	Average Hardness, Rc	Plastic Parameters[1] n	K
1 (PV-1)	222,000	269,000	5.0	50.5	0.457	196,400
2 (PV-2)	224,000	274,000	5.0	50.5	0.368	203,700
3 (PV-4)	211,000	254,000	5.0	----	0.480	172,900
				Average	0.435	191,000

Analysis of the Failures

There are two ways in which the pressure vessels might have failed: one is a ductile failure in which the vessel was strained in the plastic range until failure occurred; the other is one in which a crack may have initiated (often at a metallurgical defect) and propagated without gross plastic strain. Both methods of failure may be analyzed to some extent by theoretical considerations.

Failure from Plastic Flow - The simplified design equation for determining the bursting pressure of a thin-walled vessel considering plastic flow is [2]:

$$P = 2(3)^{-(\frac{n+1}{2})} \cdot (\frac{\sigma_{uT}}{R})$$ (1)

1 These values are different from those given in the literature for steels, probably because the strains were low and the parabolic plastic stress-strain relation is not applicable for either very small or very large strains.

2. Reference 7.

where $\bar{P}$ = bursting pressure

  n = strain hardening coefficient

  σ_u = nominal ultimate tensile strength

  T = initial thickness

  R = initial radius

The unwelded tensile specimens of H-11 steel No. 2 which were heat treated with the pressure vessel No. 1 had an average ultimate strength of 269,000 psi, a yield strength of 222,000 psi, and a strain hardening coefficient of 0.457 in the longitudinal direction. For the vessel No. 1

  T = 0.097 in. and R = 3.107 in.

hence,

$$\bar{P} = \frac{2}{3}(0.728) \cdot \frac{269,000(0.0970)}{3.107}$$

$$\bar{P} = .887(8230) = 7300 \text{ psi}$$

The failure pressure (at yielding) from the classic pressure-stress equation is:

$$\bar{P} = \frac{\sigma_y T}{R} \qquad (2)$$

where σ_y = the nominal yield strength

$$\bar{P} = \frac{222,000(0.090)}{3.107} = 6430 \text{ psi}$$

The simplified design equation for determining failure strain, considering plastic flow, predicts that the circumferential strain at maximum pressure at failure will be[1]

$$\bar{\epsilon} = \epsilon' (e^{\frac{n}{2}}-1) \cdot (e^n-1)^{-1} \qquad (3)$$

  $\bar{\epsilon}$ = circumferential strain at maximum pressure

  ϵ' = tensile necking strain

  e = base of the natural logarithm

---

1 Reference 7.

The unwelded tensile specimens processed with the pressure vessel had an average strain at the beginning of necking in the tensile test of $\epsilon' = .02$ in/in, hence

$$\bar{\epsilon} = .02 \left(e^{\frac{0.218}{2}} - 1 \right) \cdot \left(e^{0.435} - 1 \right)^{-1}$$

$$\bar{\epsilon} = (.02)\ \frac{.243}{.545} = 0.0089 \text{ in/in}$$

The circumferential strain, ϵ_c, as a function of stresses within the elastic range of the material is

$$\epsilon_c = \frac{1}{E} (\sigma_h - \mu \sigma_t) \tag{4}$$

where E = the elastic modulus
  μ = Poisson's ratio
  σ_c = circumferential hoop stress
  σ_t = tangential stress

at yielding of the material σ_c = 222,000 psi and σ_t = 222,000/2 or 111,000 psi. Hence,

$$\epsilon_c = \left[222,000 - .29(111,000) \right] / 29.5 \times 10^6$$
$$\epsilon_c = .00646 \text{ in/in at yielding}$$

This strain was exceeded only for pressure vessel No. 1. Furthermore, pressure vessel No. 1 attained the theoretical failure strain of .0089 in/in predicted by plastic failure; therefore, the failure pressure was in the order of 7950 psi[1].

The stress in the pressure vessels was determined both from pressure measurements using equation 2 and from strain measurements using equation 4. The 10 to 20 percent discrepancy in stress values was attributed to local deviation from roundness of the vessel at the weld. The analysis of results is presented in Table 33.

Previous studies have shown that subscale chambers (pressure vessels) of Vascojet 1000 failed in hydrotest at one-half the yield strength when heat treated to 230,000 psi yield strength[2].

1 The actual failure pressure of this vessel was not recorded because the oscilloscope failed to function properly.
2 Reference 8.

TABLE 33. ANALYSIS OF PRESSURE VESSEL TESTS

Pressure Vessel No.	Special Cause of Fracture and Location	Maximum Hoop Stress,(a) psi (from pressure)	Tensile Strength of Vessel,(i) psi	Maximum Stress,(b) psi in Base Metal (from strain)	Maximum Hoop Stress in Weld,(b) psi (from strain)	Approximate Critical Crack Length (from observation), in.	Approximate Strain-Energy Release Rate, in-lb/in² G_c
1	None, Head to Cylinder Weld	235,000(c)	269,000	(d)		.05	
2	Porosity(g) .015" dia., Longitudinal Weld. (Repair Weld)	180,500	198,000	158,300	140,900	.125	165(e)
3	None, Junction of Longitudinal & Circumferential Weld	166,000	182,000	120,000	141,700	.25	336(e)
4	Porosity(g) .007" dia., Longitudinal Weld	108,000	119,000	75,000	(h)	.50	158(f)

(a) As determined from pressure from Equation 2.
(b) As determined from strain in base metal or weld metal from Equation 4.
(c) Pressure not recorded. Since observed strain agreed with predicted failure strain considering plastic flow (Equation 3), actual failure pressure was assumed equal to the predicted failure pressure considering plastic flow. The pressure of 7150 psi was then used to determine the hoop stress.
(d) Equation 4 is not applicable in plastic range.
(e) G_c for welds using a fracture stress value determined from measured weld metal strain and Equation 6.
(f) G_c is for base metal using fracture stress value determined from base metal strain and Equation 6.
(g) Porosity was found in region of fracture initiation; however, fracture face markings did not emanate directly from porosity. Fracture initiated in a repair-weld.
(h) Weld strain was not recorded.
(i) Actual tensile strength of vessel material which is equivalent to the observed failure pressure. Determined from Equation 1.

104

This strength range approximates that of the vessels tested in this program. It was not reported whether the chambers contained a longitudinal weld or just a girth weld. In either event, vessels No. 1, 2, and 3 failed at nominal fracture stress values exceeding one-half the yield strength. The high fracture stress recorded for vessel No. 1 demonstrated that high performance welded vessels may be fabricated; however, the program also demonstrated that metallurgical discontinuities have a profound influence on the fracture stress when these steels are heat treated in the 211,000 to 224,000 psi yield strength and 254,000 to 274,000 tensile strength ranges.

A recent investigation[1] of small-scale pressure vessels of H-11 hot-work tool steels containing longitudinal welds revealed that of the vessels (containing no metallurgical defects) which were tempered to a tensile strength above 260,000 psi, five vessels had a circumferential stress at bursting equal to or greater than their tensile strength, while five vessels failed below the tensile strength. Three vessels failed at 130,000-150,000 psi levels. On the other hand, when the vessels were tempered at tensile strength levels between 230,000 and 260,000 psi the incidence of low strength failures (222,000 psi minimum) was greatly reduced.

Failure from Crack Propagation - The stress required to propagate a crack varies as the square-root of the reciprocal of the crack length. It is also dependent upon the inherent toughness of the material, its elastic properties, the geometry of the specimen, the environment, and rate of loading.

A close approximation to the crack-propagation stress can be made by the use of the center-notch tension test. In this test, a sheet tensile-specimen containing an internal crack is loaded until the crack propagates rapidly and fractures the specimen. Both the crack length and the stress at the moment of rapid propagation are recorded to determine the strain-energy release rate term, G_c, in the following equation.

$$G_c = \frac{\sigma^2}{E} w \tan \frac{\pi}{w} (c + \frac{E G_c}{2 \pi \sigma_y^2})$$

(5)

where c = one-half the crack length at the onset of rapid crack propagation
       E = Young's modulus
       σ = the fracture stress normal to the crack at the onset of rapid propagation

[1] Reference 9

σ_y = the yield strength of the material under test

w = the width of the sheet tensile specimen

The central crack in the tension specimen may be introduced by various techniques, such as the hydrogen embrittlement technique developed by Srawley and Beachem[1], or the method used by Kies where an internal notch of 0.001-inch radius is machined into the specimen by the "Elox" electrostatic machining process.

To date, G_c values have been used to compare the notch sensitivities of various materials, but it is also desirable to use G_c values for design purposes; for example, as yield strength is used for design purposes. Consider the use of G_c values for design purposes. Consider the use of G_c values for the design of pressure vessels. The G_c value for the pressure vessel material may be obtained from equation 5 by the use of center-notch tensile specimens of thicknesses and under conditions of temperature and strain rate approximating those which would be encountered by the pressure vessel. Knowing the G_c value, the yield strength σ_y, the elastic modulus, and the maximum stress in the pressure vessel as a result of the maximum pressure (or the working stress), the limit crack length 2c at which rapid propagation will occur can be calculated.

A large internally pressurized vessel may be treated for purposes of stress analysis as though it were under an infinite stress field. For this case the equivalent form of equation 5 is[2]:

$$G_c = \frac{\pi \sigma^2 \, \sigma_y^2 (2c)}{E(2\sigma_y^2 - \sigma^2)} \tag{6}$$

Solving for 2c:

$$2c = \frac{E \, G_c \, (2\sigma_y^2 - \sigma^2)}{\pi \, \sigma^2 \, \sigma_y^2} = \frac{E \, G_c \left(\frac{2\sigma_y^2}{\sigma^2} - 1\right)}{\pi \sigma_y^2} \tag{7}$$

The value of 2c is the critical crack length[3] at the onset of rapid crack propagation under the applied maximum stress σ. It was often assumed that, as long as the vessel did not contain cracks of initial length greater than this value, the catastrophic fracture would not occur. It was found, however, that although

---

[1] Reference 10
[2] Reference 11. See Appendix for derivation of Equation 6.
[3] c is one-half the crack length by division.

cracks might be initially smaller than the critical crack length, they would often grow slowly until they reached the critical length, then they would propagate rapidly to cause catastrophic failure.

The extent to which an initial crack of length c_0 will grow slowly in a pressure vessel must be determined. For example, if it were known that initial cracks could grow only to a limit of 60 percent of their original length, then the critical crack half-length, c, at propagation could be replaced by the value $1.6 c_0$. All cracks of initial half-length c_0 greater than $\frac{c}{1.6}$ could be detected in a structure by nondestructive testing and removed. In a general sense, $c = m c_0$, where m is a constant designating the extent of slow-crack growth anticipated. The term $m c_0$ can be substituted for c in equation 7.

In equation 7 the working stress σ was known and the maximum crack length c, or more realistically $m c_0$, which could be tolerated was determined. However, it is often the case that the maximum initial crack length which cannot be avoided will be known, then the safe working stress σ can be determined by solving equation 7 for the working stress.

$$\sigma = \left[\frac{E\, G_c (2\sigma_y{}^2 - \sigma^2)}{2\pi m\, c_0\, \sigma_y{}^2}\right]^{\frac{1}{2}} \quad \text{or} \quad \sigma = \sqrt{\frac{2\,\sigma_y\, E\, G_c}{2\pi m\, c_0\, \sigma_y{}^2 + E\, G_c}} \quad (8)$$

This latter procedure is likely to be used more frequently than the former.

If one were to ignore the condition of slow-crack growth, m would be equal to one in equation 8, which would result in a high allowable working stress. If slow-crack growth is considered, m would be greater than one, which would give a lower stress from the above equation; therefore, slow crack growth cannot be ignored.

For center-notch tensile specimens, the Naval Research Laboratory[1] has found the value of m to vary between 1.07 and 2.1 with an average value m = 1.6, for several different materials over a range of $\frac{G_c}{\sigma_y}$ values. For the present, the average value of $1.6 c_0$ has been substituted for c in equation 8 for pressure vessels. However, slow-crack extension data has not been obtained for pressure vessels and it is not known whether slow-crack-extension data from tensile specimens can be used for pressure vessels.

---

[1] Reference 11.

Only pressure vessel No. 1 was stressed beyond its yield strength; the others failed below the yield strength. All vessels showed evidence of failure by propagation of a crack. From the observation of the fracture face, the source of fracture initiation was determined since the chevron-like fracture markings pointed toward the source. An estimate was made of the critical crack length at the onset of rapid crack propagation. This approximate critical crack length, 2c, the average yield stress of 223,000 psi of the weldments of H-11 steel No. 2, and the failure stress σ in the weld of the vessel, were used in equation 5 to obtain an approximate strain-energy release-rate value G_c for the weldments. The G_c values presented in Table 33, ranging from 156 to 336 in-lb per square inch, agrees fairly well with reported values of 240 to 284 pounds per inch for .060"-thick unwelded Vascojet 1000 steel having a nominal yield strength of 239,000 psi[1]. It is misleading to compare G_c values of steels of different thickness since G_c values vary with thickness.

GENERAL DISCUSSION

The investigation to determine the cracking susceptibility of the weld metals showed that both low and high temperature cracking could occur in plate specimens under high (maximum Lehigh) restraint. Cracking was not observed in the non-restrained butt-weld plate weldments from which the mechanical specimens were taken. Preheats as low as 400 F were used for these tests. For higher amounts of restraint, the preheat temperature should be increased to reduce the cooling rate and prevent an acicular microstructure upon the formation of martensite after welding.

Sheet specimens were welded by the manual TIG process as readily as by the automatic TIG process. Mechanical properties of weldments prepared by the manual process were comparable to those prepared by the automatic process.

The welding of plate with the TIG process resulted in several unusual effects. Those weldments from which the tensile specimens were to be taken contained lack of penetration even though the energy-input of the TIG process was higher than that of the MIG process. Voltage and amperage were lower for the TIG process but the slower travel speed of the TIG process resulted in a higher energy. The Charpy impact specimens did not show any lack of fusion; but upon testing, a narrow region of unusual appearance (shown in Figure 26) was observed in the center of the fracture face in the region of maximum tensile-bending-stress. The narrow region was the fusion line which acted as a metallurgical notch resulting in low fracture-energy values.

---
[1] Reference 8

Various cleaning procedures were evaluated early in the program for steel No. 3 using radiography of a two percent penetrameter sensitivity to determine the presence of porosity. This level of sensitivity was not adequate to locate porosity which initiated fractures of the plate tensile specimens of steel No. 3. Subsequently, for the other steels, weld wire was cleaned by a power-wire brush process and the arc voltage was maintained within a very narrow range which prevented aspiration of air into the weld. Variation of the voltage was accompanied by variation of the amperage to maintain the prescribed energy input. These procedures reduced the incidence of porosity by about 50 percent in weldments of the other steels which were inspected by radiography of one percent penetrameter sensitivity. Very fine porosity was found occasionally in the fracture faces (not having been detected by the one percent radiography sensitivity), but it usually did not appear to have contributed to the initiation of the fracture.

Large lamallar inclusions were sometimes found (lying in the plane of the plate) in these steels. It did not appear that these inclusions contributed to failure; however, they caused a temporary diversion of the direction of a propagating crack.

Microstructure studies of weldments before hardening and tempering revealed that certain welding conditions produced questionable microstructures; however, the objectional features of these microstructures generally disappeared upon hardening and tempering. It was found, for example, that when a weld was not allowed to cool to form martensite but was heated from the preheat temperature to the postheat temperature of 1350 F and held for two hours, the austenite was not held isothermally a sufficient time to produce high temperature transformation products. As a result, large regions of as-quenched martensite were formed upon air cooling. This process is commonly used in industry but it is believed not to be a safe stress-relief process.

Subsequently, a process (C4X) was used in which the weld was postheated at 1350 F for four hours rather than two hours to transform all the austenite. The longer isothermal hold, however, resulted in segregated regions of higher carbon concentration and slight chain-like carbide precipitation.

Carbide segregation and precipitation occurs in these steels if they are held isothermally or are cooled very slowly in the temperature region of the nose of the isothermal transformation diagram. Most of the chain-like precipitation was light and disappeared upon hardening and tempering; however, such precipitates would weaken structures in the as-welded condition. Postheat condition 3, which utilized a slow cool from 1700 F to 1350 F, produced grain-boundary precipitates which disappeared upon hardening and tempering and did not cause a reduction in mechanical

properties after the hardening heat treatments. Nevertheless, the use of a heat treatment producing a carbide network involves some risk.

Several new mechanical-property tests which have not been often used to date were used in this program. The transverse-notch longitudinal-weld test indicated that most failures initiated in the weld or HAZ region rather than in the base metal, as well as providing notched to un-notched strength ratios. The A2 and B2 welding conditions had a higher incidence of base metal initiations than the other conditions. Notches of .005-inch radius did not appreciably reduce the strength of many of the specimens. The notch tensile test was found to reveal an abnormal condition more readily than the un-notched test.

The V-notch Charpy test provided very low impact values which did not vary appreciably over a range of temperatures. When a 1/2-inch radius was used, however, the energy values had a more meaningful range and considerable scatter with temperature. Any metallurgical defects in the weld are quickly revealed since the notch-effects of the defects are not overshadowed by a sharp V-notch. The large-radius Charpy test appears to be quite favorable for weldability studies of tool steels.

Longitudinal-weld bend tests are not new; however, it is significant that when the specimen surfaces are gound, different plastic flow patterns of the weld, HAZ, and base metal can be observed which reveal the heterogeneous plastic flow characteristics of the weldment. Such patterns merit further study since the attainment of a uniform flow pattern across the weldment would indicate an ideally homogeneous weldment.

The sheet impulse-bulge test permitted the evaluation of a sheet weldment under a sudden impulse-load on a relatively inexpensive specimen as compared with a pressure vessel. The maximum principal stresses (in the center of the vessel) are equal in all directions and provide a comparison with the 2:1 ratio of principal stresses of the pressure vessel.

The dynamic testing of pressure vessels provides data on the effects of high loading rates on actual vessels which are not generally available. The dynamically-tested vessels were the stronger. The fracture of vessels No. 1 (dynamic) and No. 3 (static) both initiated in a girth (cylinder to head) weld and the sources were similar in appearance. The statically-loaded vessel failed at 4800 psi while the dynamically-loaded vessel failed at a much higher pressure (estimated to be about 7950 psi). Similarly, the fractures of vessels No. 2 (dynamic) and No. 4 (static) were similar, initiating in the longitudinal weld (possibly from porosity); however, the failure pressure of the static vessel

was 3300 psi as compared with 5500 psi for the dynamically loaded vessel. It is postulated that, in the statically loaded vessels, fracture-initiating cracks were able to grow as the load was slowly increased. Since fracture stress is inversely proportional to the square root of the crack length, the strength of the vessel was reduced by the slow-crack growth. For the dynamic tests, the load increased so rapidly that no crack growth could occur before the stress reached the (higher) critical stress corresponding to the shorter crack length.

Weld repairs were made on the pressure vessels and bulge specimens. Cracks appeared to propagate more rapidly through the repaired regions of the weld, than through the unrepaired weld metal. However, failure initiated at a repair weld in only one pressure vessel. The effects on mechanical properties of repairing welds of these steels should be investigated further.

The statistically designed investigation for steel No. 3 was considered necessary to determine effects of welding parameters on properties after hardening and tempering. The statistical experiment suffers the disadvantage that data for each condition must be obtained in order to perform a complete analysis. If, for some reason, several specimens do not provide valid data, then the statistical analysis becomes impossible. Nevertheless, a maximum of information is provided for a given number of tests with a measurable degree of accuracy by this method. Furthermore, it is the only means of determining the effects of interactions of one variable upon another which was proven to be important in this study. The interaction between preheat and energy input is quite strong. Effects of weld conditions on mechanical properties were discerned. A low preheat and energy input increased properties, possibly by limiting the extent of the heat-affected zone; however, the effects were quite small and for all practical purposes, insignificant. The hardening and tempering operations appeared to wipe out the effects of welding conditions. Far more critical was the tempering temperature. The hardness (and strength) for these steels is quite sensitive to small changes in tempering temperature.

The six steels can be compared (provided the limitations of using a common tempering temperature are kept in mind) by reference to Table 34 in which the average values of mechanical properties for the six steels are presented. The H-11 steel No. 3 as well as H-13 steel No. 6, suffered the least loss of properties from welding. The tempering of steel No. 6 at 1050 F resulted in good ductility and notch strength. The H-13 steel No. 5 would have been improved by tempering at a higher temperature, while steel No. 1 had low weld elongation. Steel No. 1 was found to be the most susceptible to the formation of weld porosity, and since weld porosity was found to reduce elongation, porosity may have been

111

TABLE 34. A COMPARISON OF AVERAGE VALUES OF MECHANICAL PROPERTIES OF UNWELDED AND WELDED SHEET AND PLATE

Steel No.	Condition	Yield Strength, ksi		Tensile Strength, ksi		% Elongation in 2 in.		Bend Elongation, %		Notch Tensile Tests of Sheet Fracture Stress, ksi	Notch to Base Metal Strength Ratio
		Sheet	Plate	Sheet	Plate	Sheet	Plate	Sheet	Plate		
1	Unwelded Average	248	---	290	---	5.2	---	---	---	---	---
	Welded Average	229	---	270	---	2.4	---	9.4	---	261	.90
	Difference	-7.7%	---	-6%	---	-53%	---	---	---	---	---
2	Unwelded Average	229	---	279	---	5.8	---	---	---	---	---
	Welded Average	226	242	263	271	3.6	5.0	15.5	>9.43(a)	267	.96
	Difference	-1.3%	5.7%	-5.85%	-2.9%	-38%	-1.4%	---	---	---	---
3	Unwelded Average	235	---	283	---	5.0	---	---	---	---	---
	Welded Average	228.5	---	272.5	---	4.6	---	14.7	---	259	.89
	Difference	-2.8%	---	-3.7%	---	-8%	---	---	---	---	---
4	Unwelded Average	226	---	275	---	5.8	---	---	---	---	---
	Welded Average	217	241	251	246	3.7	0.87	11.7	1.25	240	.87
	Difference	-4.0%	6.6%	-8.7%	-10.5%	-36%	-83%	---	---	---	---
5	Unwelded Average	255	---	290	---	5.0	---	---	---	---	---
	Welded Average	231	245	250	258	1.7	1.17	5.6	1.32	222	.77
	Difference	-10.5%	-3.9%	-13.8%	-11%	-66%	76.5%	---	---	---	---
6	Unwelded Average	217	---	262	---	6.0	---	---	---	---	---
	Welded Average	204	241	241	263	4.5	6.6	11.2	>2.92(a)	268	1.02
	Difference	-6.0%	1.1%	-8.0%	0.4%	-25%	10%	---	---	---	---

(a) Some of the plate bend specimens did not fracture at the full-load capacity of the bending device; hence, actual bend elongation of the weld was greater than that which could be obtained.

112

the cause of the observed lower weld-elongation values. The high notch-strength of this steel perhaps reflects its potential toughness in the absence of porosity.

Since base metal properties of sheet and plate would be expected to be identical (having been obtained from the same heat treatment), base metal properties of plate were not determined. The tensile strengths of plate weldments of steels No. 2 and 6 equal those of the sheet base metal while yield strengths of all plate weldments are higher than those of sheet base metal. They were obtained by the deflectometer rather than an extensometer; however, they should be accurate considering the refinements from the equivalent-gage-length method used for these specimens.

Table 35 presents a summary of the mechanical properties of H-11 steel No. 2 as determined from tensile, bend, bulge, and pressure-vessel tests. Bend elongation (of the outer-fiber) is higher than tensile elongation, as is the usual case. The elongations (22%) at failure of the bulge specimens were larger than those of the pressure vessels (8-15%) which were in turn larger than those of the transverse weld tensile specimens (5.0%), and unwelded base-metal tensile-specimens (5.8%). It is not known why the elongations of the biaxially loaded bulge specimens whould be so high unless bending stresses are greater than membrane tensile stresses. This is unlikely (especially in the center of the specimen).

Transverse-weld strengths of weldments of H-11 steel No. 2 were reduced in the order of 20 percent by a short-time heating to 1000 F, and by 34 percent as a result of a hold at 1000 F for 24 hours prior to testing. No decrease in strength was observed at 800 F, however. A comparison of hardness values before and after testing indicates that secondary hardening occurred at 800 F while a 24-hour hold at 1000 F decreased the hardness.

SUMMARY AND CONCLUSIONS

1. Statistical analysis of variance study by an electronic computer revealed that the preheat, postheat, and energy input do not appreciably influence the mechanical properties of modified H-11, H-12, and H-13 steels after hardening and tempering treatments.

2. The mechanical properties and welding characteristics of the six hot-work tool steels investigated were not identical. Even the two H-11 steels had different tempering character- istics, as did the two H-13 steels.

3. It is evident that the 1050 F tempering temperature for H-13 steel No. 6 resulted in weldment-elongation nearly equal to

TABLE 35. MECHANICAL PROPERTIES OF H-11 STEEL NO. 2 SHEET SPECIMENS

Type of Test	Yield Strength, psi	Tensile Strength, psi	Failure Hoop Stress, psi (from failure pressure)	% Elongation
Unwelded Base Metal Tensile Strength	229,000	279,500	------	5.8
Transverse-Weld Tensile	226,000	263,000	------	5.0[a]
Transverse-Notch Longitudinal-Weld Tensile	------	267,000[d]	------	---
Longitudinal-Weld Bend	------	------	------	15.5
Bulge Test, Specimen No. 1 (dynamic)	------	------	<319,000	---
Specimen No. 2 (dynamic)	------	------	<388,000	---
Specimen No. 4 (static)	------	------	157,400	22.8[b]
Specimen No. 5 (dynamic)	------	------	<234,000	21.2[b]
Pressure Vessel No. 1 (dynamic)	------	------	254,000	14.8[a]
Pressure Vessel No. 2 (dynamic)	------	------	180,500	8.0[c]
Pressure Vessel No. 3 (static)	------	------	166,000	8.4[c]
Pressure Vessel No. 4 (static)	------	------	108,000	---

(a) Elongation in a two-inch gage length.
(b) Elongation in a 1/4-inch gage length, as determined by strain gages.
(c) Elongation in a 1/2-inch gage length, as determined by strain gages.
(d) Nominal fracture strength.

114

that of the base metal and a notch strength in the order of base metal strength. However, this same 1050 F tempering temperature did not give such good properties for all weldments. For example, the weld elongation of H-13 steel No. 5 was 66 percent below that of the base metal and the notch strength was only 77 percent of the tensile strength of the base metal. It might be concluded that weld elongation and notch sensitivity of the other steels could be made to approach that of unwelded base metal by tempering at temperatures slightly higher than 1050 F. However, the strength would be reduced by the higher tempering temperature.

4. The strength properties of the welded sheet steels were within 14 percent of the base material for the heat treatment used, while the elongation of the welded specimens ranged between 25 and 66 percent of the unwelded sheet. The greatest difference between welded and unwelded properties was shown for the modified H-13, steel No. 5, probably because it contained 0.50 percent carbon, 0.10 percent higher than the other steels.

5. Most of the mechanical-test failures initiated in the weld metal even though no metallurgical welding defects were present. Hardening and tempering did not eliminate the columnar pattern of the weld microstructure.

6. Certain welding conditions caused the formation of microstructures such as untempered martensite and carbide networks; these might contribute to low mechanical properties if the welds were not subsequently hardened and tempered, as is the case for many final closure-welds and large-structural welds.

7. The 1/2-inch radius of the impact specimens was not acute enough to cause stress concentration. Any notch effects present stemmed from metallurgical weld defects. The impact-energy transition temperature range was -90 F to -190 F for weld metal and -130 F to -230 F for base metal of plate weldments; in considering these temperatures it must be realized that a very generous radius was used. This large radius, Charpy-impact-test specimen appeared to be more suitable than the standard V-notch test for comparing the toughness of ultra-high strength steels and weld metals.

8. Bend deformation patterns in the weld and metallographic micro-examination illustrated the existence of heterogeneity between base and weld metal after hardening and tempering.

9. The high-strength pressure vessel, tested dynamically, failed in the base metal at 90 degrees from the weld. Dynamically tested vessels were of higher strength than the statically tested vessels. The two pressure vessels tested at strain rates

in the order of five to eight inches per inch per second were a minimum of 8.8 percent and a maximum of 57.5 percent stronger than the two vessels tested statically.

10. Modified H-11 steel No. 2 maintained transverse tensile weld strength of 205,000 psi to 800 F but decreased to 190,000 psi at 1000 F; a further decrease in strength to 156,000 psi at 1000 F was noted after holding at 1000 F for 24 hours.

11. Lehigh restraint test studies indicated that both hot and cold cracking can occur, with the occurrence of the latter more likely. Low temperature cracking can be prevented by increasing the preheat for most of the steels studied in this program.

12. Small defects which were not detected by the two percent penetrameter radiographic sensitivity were the source of fracture initiation in weldments of these steels. Very high radiographic standards should be used for the inspection of welds in these steels.

13. Weld metal porosity was the most commonly encountered metallurgical defect for the consumable-electrode welding process. It was found that arc-voltage must be maintained within a narrow tolerance to prevent porosity in the weld metal. Steel No. 1 was more susceptible than the others to the formation of porosity in the weld metal. Porosity in the welds reduced tensile and bend-elongation values but did not affect the yield or ultimate tensile strength appreciably.

14. Tensile properties of weldments prepared by the TIG-manual process were comparable with those prepared by the TIG-automatic process. However, the bend properties of the TIG-manual welds were better than those prepared with the TIG-automatic process.

15. Impact properties of TIG plate-weldments were erratic. Satisfactory tensile data were not obtained for the TIG plate-weldments because lack of penetration was encountered.

RECOMMENDATIONS

1. The effects of various repair welding techniques on mechanical properties should be investigated for these steels.

2. The effects of welding conditions on the mechanical properties of as-welded (unhardened and tempered) weldments would be pronounced and should be studied.

3. The advantages of using vacuum-melted steels and filler metals should be investigated.

4. A hardening and tempering study should be conducted for the six steels to determine optimum heat treatment.

5. Various external methods such as vibrations should be considered as a method of eliminating the columnar weld structures that exist even after hardening and tempering.

6. Homogenizing treatments should also be considered as a method of reducing chemical segregation in the weld deposit.

7. The influence of cooling rates on solidification, which in turn effect the dendritic spacing and microsegregation of weld deposits, should be studied.

BIBLIOGRAPHY

1. Nulk, D. E., "Fuel Containers for Rockets", Metal Progress, March 1959, p. 66-72.

2. Private Communication from Materials Information Center, Battelle Memorial Institute.

3. Private Communication with Vanadium Alloys Steel Company.

4. Parker, E. R., "Brittle Behavior of Engineering Structures", New York, John Wiley & Sons, 1957.

5. Pulse of the Nation's Welding, Metal Progress, June 1958.

6. Steven, G., "Impact Test for Evaluating Tool Steels", Metal Progress, Vol. 75, No. 5, May 1959.

7. Cooper, W. E., "The Significance of the Tensile Test to Pressure Vessel Design", Welding Journal, Vol. 36, No. 1, Jan. 1957.

8. Warga, J. J., "Use of the Center Notch-Tensile Test to Evaluate Rocket Chamber Materials", Welding Journal, 40(3), Research Supplement, March 1961, p. 130S-134S.

9. Haynes, C. W. and Valdez, P. J., "Rocket Motor Case Material Evaluation by Pressure Vessel Testing", Aerospace Engineering, December 1960.

10. Srawley, J. E., and Beachem, C. D., "Crack Propagation Tests of High-Strength Sheet Steels Using Small Specimens", NRL Report 5127, April 9, 1958.

11. Kies, J. A., Romine, H., Smith, H. L., and Bernstein, H., "Minimum Toughness Requirements for High-Strength Sheet Steel", Naval Research Laboratory (not yet published).

12. Adams, C. M., "Cooling Rates and Peak Temperatures in Fusion Welding", Welding Journal, Vol. 37, No. 5, May 1958.

13. Den Hartog, J. P., "Advanced Strength of Materials", McGraw Hill, 1952.

APPENDIX I

CALCULATIONS

DETERMINATION OF WELD COOLING RATES

The equation for the cooling rate at the center of a weld for two-dimensional heat flow is as follows[1]:

$$\frac{dT}{dX} V = 2 \pi K_p c_p \left(\frac{Vt}{q}\right)^2 (T-T_o)^3 \tag{9}$$

Where: T = steady temperature in the solid at a point on the center line

T_o = initial (preheat) temperature of plate
V = velocity of the source
K = thermal conductivity of plate
P = density of plate
c_p = specific heat of plate
q = rate of heat flow from source
t = plate thickness

Using the following values for the restraint tests performed in this program we may obtain the cooling rate at 1000 F for a 400 F preheat.

T = 1000 F
T_o = 400 F
V = .233 in/sec
K = 3.8 X 10^{-4} $\frac{BTU\text{-}in}{in^2\text{-}sec\text{-}^oF}$

p = .28 lb/in^3

c_p = .16 $\frac{BTU}{lb\text{-}F}$

t = 1/2 in
Welding Volts v = 29
Welding Amp a = 355
q = v a joules/sec

q = $\frac{29(355)}{1052}$ = 9.77 BTU/sec

$\frac{dT}{dX} V = 2 \pi 3.8 \times 10^{-4} (.28)(.16)\left(\frac{.233(.5)}{9.77}\right)^2 (1000-400)^3$

$\frac{dT}{dX} V = (1.12 \times 10^{-4})(1.42 \times 10^{-4})(216 \times 10^6)$

$\frac{dT}{dX} V = 3.43 \frac{^oF}{sec}$

---

[1] Reference 12.

CALCULATION OF BEND ELONGATION

The percent elongation of the outer tensile fiber of a bend specimen is given by the equation[1]:

$$e = \frac{t}{2r + t} \, (100) \tag{10}$$

where: t = specimen thickness
r = minimum inside bend radius of specimen at fracture

For the .0749-inch thick specimen of Weldment No. 42 which had a minimum bend radius of .5 inch, the percent elongation is:

$$e = \frac{(.0749)}{(1.0749)} \, (100) = 7 \text{ percent}$$

CALCULATION OF EQUIVALENT LENGTH FOR HIGH
TEMPERATURE TENSILE SPECIMENS

Symbol Notation

l_1 Length of the portion of tensile specimen having width W_1 = .5 inch.

l_2 Length of the portion of tensile specimen having width W_2 = .75 inch extending beyond top grip.

l_3 Length of the portion of tensile specimen having width W_3 = .75 inch extending beyond bottom grip.

l_4 Length of the portion of tensile specimen in region where width reduces from .75 to .5 inch having an equivalent constant width of w_4.

e   Elongation, in.
ϵ Unit lateral strain, in/in
S   Stress, lbs/in^2
A   Cross sectional area, in^2
t   Thickness, in.
P   Load, lbs
E   Young's Modulus, psi

Total elongation is equal to the sum of the component elongations. Total strain,

---

[1] Reference 13, p.104-105

$$e_T = e_1 + e_2 + e_3 + 2e_4$$

$$e_T = \epsilon_1 l_1 + \epsilon_2 l_2 + \epsilon_3 l_3 + 2\epsilon_4 l_4$$

$$\frac{S}{\epsilon} = E \text{ or } \epsilon = \frac{P}{AE}$$

P and E are the same for every value of ϵ, hence

$$\epsilon_1 = \frac{P}{A_1 E} \qquad \epsilon_2 = \frac{P}{A_2 E}, \text{ etc.}$$

Substituting in the equation for e_T above

$$e_T = \frac{P}{E} \left(\frac{l_1}{A_1} + \frac{l_2}{A_2} + \frac{l_3}{A_3} + \frac{2\, l_4}{A_4} \right)$$

$$e_T = \epsilon_T l_T = \frac{P}{E} \left(\frac{l_1}{w_1 t_1} + \frac{l_2}{w_2 t_2} + \frac{l_3}{w_3 t_3} + \frac{2\, l_4}{w_4 t_4} \right)$$

However, the thickness t is constant for the entire length of the specimen, hence

$$\epsilon_T = \frac{P}{E l_T t} \left(\frac{l_1}{w_1} + \frac{l_2}{w_2} + \frac{l_3}{w_3} + \frac{2\, l_4}{w_4} \right) \tag{11}$$

Assume a uniform specimen of the same thickness and of width w_1 (w_1 = .5 in.), having an equivalent length l_{eq} so that the elongation, e_u, for the uniform specimen is the same as e_T for the actual test specimen; $e_u = e_T$.

$$e_u = \frac{P l_{eq}}{E w_1 t}$$

$$\frac{P l_{eq}}{E w_1 t} = \frac{P}{E t} \left(\frac{l_1}{w_1} + \frac{l_2}{w_2} + \frac{l_3}{w_3} + \frac{2\, l_4}{w_4} \right)$$

$$l_{eq} = w_1 \left(\frac{l_1}{w_1} \quad \frac{l_2}{w_2} \quad \frac{l_3}{w_3} \quad \frac{2\, l_4}{w_4} \right)$$

For one of the specimens (l_2 and l_3 varied for different specimens)

$$l_1 = 2.25'' \qquad\qquad w_1 = 0.50''$$

$$l_2 = 1.06" \qquad w_2 = 0.75"$$
$$l_3 = 1.24" \qquad w_3 = 0.75"$$
$$l_4 = 0.45" \qquad w_4 = 0.62"$$
$$l_T = 5.45$$

$$l_{eq} = 0.50 \left[\frac{2.25}{0.50} + \frac{1.06}{0.75} + \frac{1.24}{0.75} + 2 \left(\frac{0.45}{0.62} \right) \right]$$

$$l_{eq} = 0.50 \ (4.5 + 1.41 + 1.65 + 1.45)$$

$$l_{eq} = 0.5 \ (9.01)$$

$$l_{eq} = 4.5" \ \text{(gage length)}$$

Although the total length of the variable width specimen between grips was 5.45 inches, its strain behavior was the same as a specimen of a constant width of .5 inch of length 4.5 inches.

CALCULATION OF THE BULGE SPECIMEN STRESS FROM MAXIMUM DELFECTION

The maximum membrane stress is given as a function of the maximum deflection for a clumped circular membrane from the equation[1]:

$$\sigma = \frac{PR^2}{4tw} \qquad\qquad (12)$$

where P = the pressure, psi
t = the thickness, in.
R = the radius of the membrane, in.
w = the maximum deflection, in.
σ = the maximum stress, psi

Since maximum deflection was not measured during the test, only the no load plastic deflection remaining after the test could be measured. This deflection, after spring-back, was 0.81 inch, hence

$$\sigma = \frac{6200 \ (4)^2}{4(.096)(.81)} = 319,000 \ \text{psi}$$

From geometric considerations stress can be determined from strain by the equation[2]:

---

[1] Reference 13, p. 138-139
[2] Reference 13, p. 138-139

$$\sigma^2 = \frac{P^2 R^2}{24 t^2 \epsilon} \quad \text{or} \quad \sigma = (24\epsilon)^{-\frac{1}{2}} \left(\frac{PR}{t}\right) \tag{13}$$

The principal strains are equal at any point on a circular membrane. For bulge specimen 5 the maximum strain e = .0053 at 2000 psi.

$$\sigma = \frac{1}{\sqrt{24(.0053)}} \cdot \frac{(2000)4}{.096}$$

$$\sigma = 234,000 \text{ psi}$$

CALCULATION OF STRAIN ENERGY RELEASE RATE EQUATIONS

The derivations of equations 5 and 6 are as follows.

The original equation for crack propagation in brittle fracture in an infinite stress field as derived by Griffith is[1]:

$$\sigma^2 = \frac{2 E \gamma}{\pi c} \quad \text{or} \quad E = \frac{\pi \sigma^2 c}{2} \tag{14}$$

Irwin replaced the surface tension term γ with the term G_c to include both surface tension and local plastic flow at the crack faces. The Griffith equation then becomes:

$$E G_c = \pi \sigma^2 c \tag{15}$$

which is applicable to very wide tensile specimens and pressure vessels which can be considered as having an infinite stress field.

For center-notch specimens of finite width, Irwin developed a correction factor for equation (15) as follows:

$$E G_c = \sigma^2 w \tan \frac{\pi c}{w} \tag{16}$$

Irwin attempted to separate the influence upon the G_c term of local stress relaxation due to crack extension as distinguished from plastic strain at the crack front by substituting the factor $(c + \Delta c)$ for the crack length c in the previous equations.

It was deduced that:

---
[1] Symbol notation given on page 125

124

$$\Delta c = p \frac{E\,G_c}{2\pi\sigma_y^2} \tag{17}$$

where σ_y is the yield strength and p is a numerical factor assumed to be 1.

Equations 16 for the center-notch tensile specimens and 15 for the pressure vessel become, upon substitution of $(c + \Delta c)$ for c:

Equations (16) $\quad E\,G_c = \sigma^2 w \tan \dfrac{\pi}{w}\left(c + \dfrac{E\,G_c}{2\pi\sigma_y^2}\right) \tag{18}$

Equation (15) $\quad E\,G_c = \pi\,\sigma^2\,(c + \Delta c)$

$$E\,G_c = \pi\,\sigma^2 c + \frac{E\,G_c\,\sigma^2}{2\,\sigma_y^2}$$

$$E\,G_c \left(1 - \frac{\sigma^2}{2\,\sigma_y^2}\right) = \pi\,\sigma^2 c$$

or finally

$$E\,G_c = \frac{2\pi c\,\sigma^2\,\sigma_y^2}{(2\,\sigma_y^2 - \sigma^2)} \tag{19}$$

The symbol notations for the preceding equations are:

c = one-half the crack length at the onset of rapid crack propagation
E = Young's modulus
σ = the fracture stress normal to the crack at the onset of rapid propagation
σ_y = the yield strength of the material under test
w = the width of the sheet tensile specimen
G_c = strain energy release rate
γ = surface tension

GENERAL DYNAMICS CORPORATION, ELECTRIC BOAT
DIVISION, Groton, Conn. INVESTIGATION OF
WELDABILITY OF HY-80N TOOL STEELS, by E. A.
Sinclair, J. G. Hudson, and R. P. Sopher.
December 1961. 129p. incl. figs. and tables.
(Project 730; Task 73001) (AD TR 61-166)
(Contract AF 33(616)-6519)
Unclassified report

The weldability of six hot-work tool steels
was investigated. Welds were made in sheet
and plate with the inert-gas tungsten-arc and
inert-gas consumable electrode processes under
various welding conditions. Variation in
preheat, postheat, and energy input were in-
vestigated and a statistical analysis of the
effects on mechanical properties after harden-
ing and tempering was determined.

Tendencies toward hot and cold cracking were
investigated using Lehigh restraint tests.
The effect of preheat temperature on low-
temperature cracking was also studied. Impact
data were presented on various weldments in
addition to the determination of tensile prop-
erties at room and elevated temperatures.
High temperature weld strength was found to
be 190,000 psi for an HY-80 steel and de-
creased to 135,000 psi after holding at 1100°F
for 24 hours. Welds made dynamically and statically
were tested both dynamically and statically
and shear hole tests were conducted.